# Ecophysiology of carrageenophytes (Gigartinales) and kelps (Laminariales) in the western Pacific Ocean

**（太平洋西部におけるカラギーナン原藻（スギノリ目）およびコンブ類（コンブ目）の生理生態）**

**Iris Ann Borlongan**

**2019**

TABLE OF CONTENTS

## List of Figures

## List of Tables

**ABSTRACT**

Knowledge concerning the effects of abiotic factors on the physiology of carrageenophytes and kelps is essential from the perspective of massive expansion of seaweed-based industries, as well as the conservation of natural communities in the face of climate change. Photosynthetic measurements are good tools to assess the effects of numerous stressors in macroalgae, which could provide insights into the causes and consequences of shifts in macroalgal productivity. The study presents the photosynthetic characteristics of economically important carrageenophytes (*Eucheuma denticulatum* and *Kappaphycus* spp.) and kelps (*Costaria costata* and *Alaria crassifolia*) distributed in the western Pacific Ocean, as determined by examining their photosynthetic response to a gradient of temperature and photosynthetically active radiation (PAR) using dissolved oxygen measurements and the pulse amplitude modulated (PAM)-chlorophyll fluorometer. Information such as these in the present study are considerably important as researches in carrageenophyte or kelp cultivation are directed towards the development of effective management protocols, as well as production of improved seaweed species and/ or strains with respect to growth, product yield/ quality, abiotic stress tolerance and disease resistance.

Photosynthesis–PAR ($P$–$E$) experiments on *E. denticulatum*, *K. striatus*, and *K. alvarezii* from Indonesia at 26°C revealed that net photosynthetic rates of the three seaweeds increased until the estimated saturation PAR ($E_k$) of 130–157 μmol photons $m^{-2}$ $s^{-1}$; and that no photoinhibition was observed at the highest PAR of 1000 μmol photons $m^{-2}$ $s^{-1}$. *K. alvarezii* also exhibited photosynthetic tolerance to high PAR as shown by their recovery in maximum quantum yields ($F_v/F_m$) following chronic exposures. Temperature responses of all carrageenophyte samples revealed their tolerance over a broad range of temperature, which is from 18.2 to 31.0°C for *E. denticulatum*, 15.7–31.6°C for *K. striatus*, 19.7–28.5°C for brown *K. alvarezii*, and 17.4–32.4°C

for green *K. alvarezii*. These characteristics indicate that they are well-adapted to the annual seawater temperatures observed at the cultivation site; however, they are also likely close to threshold levels for thermal inhibition, given the decline in $F_v/F_m$ above 30°C. Higher photosynthetic parameter values of *E. denticulatum* also suggest that this species will probably be more superior in productivity under optimal conditions in commercial seaweed cultures.

The *P–E* curve of the Japanese *Kappaphycus* sp. (*K. striatus* auctorum japonicorum) from Okinawa, Japan at 24°C revealed that the compensation ($E_c$) and saturation ($E_k$) PAR were 26 μmol photons $m^{-2}$ $s^{-1}$ and 140 μmol photons $m^{-2}$ $s^{-1}$, respectively. No inhibition in oxygenic evolution and quantum yield was observed at the highest PAR of 1000 μmol photons $m^{-2}$ $s^{-1}$. However, the ability of the seaweed to recover from photoinhibition was complicated following 6-h PAR exposures at 18°C but not at 28°C. The native alga showed temperature tolerance for photosynthesis at 17.4–29.1°C. These characteristic results were closely related to the depth of its habitat and its northern limit of distribution in Okinawa, as influenced primarily by seawater temperature. Mariculture of this native carrageenophyte in subtropical waters of Okinawa, Japan is feasible, and may be conducted throughout the year under natural seawater temperatures.

*P–E* curves of the two life history stages of *C. costata* and *A. crassifolia* revealed the higher $E_c$ (4–9 μmol photons $m^{-2}$ $s^{-1}$) and $E_k$ (53–243 μmol photons $m^{-2}$ $s^{-1}$) of the sporophyte as compared to the gametophyte ($E_c$ = 0–7 μmol photons $m^{-2}$ $s^{-1}$; $E_k$ = 7–44 μmol photons $m^{-2}$ $s^{-1}$). This reflects the low-PAR adaptation of the microscopic stage that is commonly found on the underside of rocks or in crevices where light exposure is limited. Both stages exhibited chronic photoinhibition, as shown by the failure of recovery in their $F_v/F_m$ following high PAR stress, with greater possibility of photodamage at low temperature. As for the temperature response, gross photosynthesis (*GP*) and $F_v/F_m$ characteristics were similar for both developmental stages; their temperature optima range from 14 to 23°C, which correspond to the growth and maturation periods of these kelp species in Japan. They are also likely to suffer from thermal inhibition as both *GP* rates and $F_v/F_m$ declined above 24°C. These physiological performances provide a basis for understanding the persistence of these kelp species near its southern boundary in the western Pacific.

## CHAPTER 1: General Introduction

Photosynthesis is an anabolic process by which biomass is produced from carbon dioxide, and this process is driven by sunlight. It is responsible for the energy supply in the formation of organic compounds and for the metabolism in primary producers. The photosynthetic process is divided into light and dark reactions. In the light reactions, light energy absorbed by the photosynthetic machinery (chlorophyll a) is used to withdraw hydrogen from water to generate electrons to liberate $O_2$. At the same time, chemical energy (NADPH and ATP) is produced, which is used in the dark reactions to reduce carbon dioxide to the level of carbohydrates.

Photosynthesis is an easily measured process that has routinely been used to assess the effects of environmental conditions on algae. Measurement of the photosynthetic responses in macroalgae is dominated by two techniques: measurements of oxygen production within sealed or flow-through chambers (photorespirometry) and variable chlorophyll a fluorescence (commonly measured by Pulse Amplitude Modulated [PAM] fluorometry). Each of these methods has its advantages and disadvantages, but both allows for a powerful determination of integrated community metabolism and the relative contributions of community components to photosynthetic output (Tait *et al.* 2017). Measured across a range of irradiances, photorespirometry allows the effects of irradiance on efficiency of light harvesting, light saturation and compensation to be determined at the whole-community level. On one hand, PAM fluorometry has become one of the most powerful and widely used techniques for ecophysiological studies (Beer *et al.* 2014; Enriquez and Borowitzka 2011). Chlorophyll fluorescence provides information about the efficiency of photosystem II (*PSII*) photochemistry, as most chlorophyll *a* fluorescence originates in the antenna complexes of *PSII*. It can tell the extent to which *PSII* is using the energy absorbed by chlorophyll and the extent to which it is damaged by excess light or other stress factors. The status of the photosynthetic apparatus, as determined by variable chlorophyll a fluorescence, is defined by several parameters including yield (a measure of the efficiency of converting photons into electron transport), which may be the maximum ($F_v/F_m$ – determined in the dark) or effective ($\Phi_{PSII}$ – under ambient PAR) photochemical efficiency of *PSII*; photochemical ($q_P$) and non-photochemical ($q_N$) quenching coefficients; and the photoprotective capacity of the tissue to dissipate excess energy absorbed (non-photochemical quenching, *NPQ*).

To some extent, algae can adjust their photosynthetic machinery to changing PAR conditions; this is called photoacclimation. Photoacclimation of macroalgae does not only refer to their ability to maintain photosynthetic capacity despite the ambient light conditions, but also maximizes the photosynthetic response at an optimum light level (Gantt, 1990). In high PAR conditions, photo-inactivation and photooxidative damage are avoided by down-regulation of excitation pressure on *PSII* and quenching of potentially harmful long-living excitation states of chlorophyll (Nishiyama *et al.* 2006; Allakhverdiev *et al.* 2008). Other ways in which macroalgae can achieve photoacclimation include adjustment of the photosynthetic apparatus itself via changes of the reaction center ratio, changes of the relative size of the light harvesting complex, or changes in the relative content of light protective pigments; all of these mechanisms influence primarily pigment ratios of the algae (Marquardt *et al.* 2010).

The light and dark reactions of photosynthesis can be expressed in a photosynthesis versus PAR (*P–E*) curve (Lobban and Harrison 1994). This curve shows the oxygen production rate of algae as a function of PAR. It is prepared by illuminating specimens with a sequence of PAR levels up to and beyond the point at which a further increase in PAR does not cause a measurable change in photosynthetic rate. The basic description of *P–E* curve requires a nonlinear mathematical function to account for the light-saturation effect (Webb *et al.* 1974; Jassby and Platt

1976; Platt *et al.* 1980; Henley 1993). In the mid-1970's, Jassby and Platt introduced the hyperbolic tangent function. This mathematical formula, which was based on two parameters: the initial slope of the light saturation curve ($\alpha$) and the photosynthetic rate at light saturation ($P_{max}$), appeared to fit experimental data with a high degree of fidelity, especially if a coefficient for photoinhibition is included (Jassby and Platt, 1976). At low PAR, some photosynthesis occurs; however, respiratory process of $O_2$ consumption exceed quantities produced by photosynthesis. The PAR level at which photosynthesis equals respiration is the compensation PAR ($E_c$). At levels greater than $E_c$, plants exhibit net photosynthetic production. The slope ($\alpha$) of the initial part of the curve shows the rate of the light reaction with increasing PAR. The slope indicates quantum yield of oxygen evolution, which is the amount (mol) of oxygen which can be produced per amount (mol) of PAR absorbed. It measures the efficiency with which a plant harvests light. Steep slopes, or high values of $\alpha$, indicate high quantum yield, while more gradual slopes indicate lower activity. The rate of photosynthesis increases until the level of PAR is saturating, where it becomes limited by the dark reactions of photosynthesis. Over this interval, the curve tends toward a horizontal asymptote. The horizontal part of the curve represents the maximum rate of the enzymatic processes ($P_{max}$) involved in the dark reaction of photosynthesis at the prevailing temperature. The saturation PAR ($E_k$) represents the optimum irradiance for photosynthesis (Falkowski and Raven 2007). At the saturation level, the rate of light absorption greatly exceeds the rate of steady-state electron transport from water to $CO_2$. The efficiency of photosynthesis is high; hence the larger part of the light energy absorbed by the algae can be allocated to biomass growth. At irradiances lower than $E_k$, there is photolimitation – the available light is insufficient to support the maximal potential rate of the light-dependent reactions, and thus limits the overall rate of photosynthesis. At higher PAR, photosynthetic efficiency (i.e., the quantum yield of oxygen evolution) drops because the rate of light absorption increases linearly with light intensity; while the rate of photosynthesis saturates. Such drop in photosynthetic efficiency, dependent on both PAR and the duration of exposure, is referred to as photoinhibition (Murata *et al.* 2007). Photoinhibition may either be dynamic or chronic. Dynamic photoinhibition takes place under moderate excess light; characterized by a temporary decline in photosynthetic efficiency even before reaching the saturation level ($P_{max}$); or if reached, $P_{max}$ remains unchanged (Hanelt *et al.* 1992). In this way, the excess light energy absorbed is dissipated as heat (i.e., non-photochemical quenching, NPQ). Such protective mechanism enables the photosynthetic system of macroalgae to cope with short-term light stress (Hanelt *et al.* 2003). On the other hand, chronic photoinhibition results from exposure to high levels of PAR that cause irreversible damage to $D_1$ protein of *PSII* by photooxidation (Allakhverdiev *et al.* 2008; Colvard *et al.* 2014). Photodamage is manifested by a decrease in both quantum yield ($\alpha$) and $P_{max}$.

Aside from PAR, temperature affects the photosynthetic activity of algae. Photosynthetic rates of algae are stimulated by increases in temperature, within a certain range, depending on species and acclimation. Macroalgae are able to adapt and to acclimate to varying temperatures to a different degree. Temperature adaptation is the result of evolutionary processes over long time periods, short-term acclimation is achieved within days or weeks (Davison 1991). High temperatures are deleterious to plant survival, and often occur in combination with high PAR (Lobban and Harrison, 1994). The possible causes of algal death at high temperatures include processes such as denaturation of proteins, and damage to heat-labile enzymes or membranes. Similarly, at low temperatures, the turnover of enzymes is reduced and the metabolic activity of the algae becomes lower. The temperature response of photosynthesis is often drawn as a bell-shaped curve centered somewhere between 20 and 30°C; this type of temperature response can be modeled with the generalized Arrhenius function (Thornley and Johnson 2000; Alexandrov and Yamagata 2007), which include the effect of temperature on enzyme activity. This function offers certain advantage over polynomial, Gaussian, or other ad hoc functions applied to modeling temperature response of plant productivity, as it relates the width of the "bell" to thermodynamic concepts, such as activation energy of chemical reactions converting carbon dioxide and water to carbohydrates (Jørgensen and Svirezhev 2004).

Several studies using a pulse amplitude modulated (PAM)-chlorophyll fluorometer, coupled with dissolved oxygen measurements, revealed the photosynthetic responses of macroalgae to photosynthetically active radiation (PAR) and temperature (Vo *et al.* 2014, 2015; Fujimoto *et al.* 2015; Kokubu *et al.* 2015; Terada *et al.* 2016a, b, c, 2018). Indeed, their photosynthetic characteristics vary, as primarily influenced by these environmental variables in their respective habitats. For instance, the deep- and shallow-water ecotypes of the red alga *Solieria pacifica* (Yamada) Yoshida showed different temperature optima for photosynthesis (19.5–19.9°C, deep-water vs. 18.6–27.0°C, shallow-water *S. pacifica*) that reflect the temperature ranges in the 35- and 5-m depths of the sublittoral zone, respectively (Borlongan *et al.* 2017d). The shallow-water *S. pacifica* also had higher saturation PAR ($E_k$ =131 μmol photons m$^{-2}$ s$^{-1}$) than the deep-water ecotype ($E_k$ = 15 μmol photons m$^{-2}$ s$^{-1}$), which can be attributed to the higher PAR levels experienced by the seaweeds occurring at depths of 5 m. Watanabe *et al.* (2014a, 2016) likewise revealed differences in environmental requirements for optimum photosynthesis between the two life history stages of *Pyropia tenera* (Kjellman) Kikuchi *et al.* and *Pyropia yezoensis* (Ueda) Hwang *et* Choi; the different temperature optima observed were related to their respective seasonal occurrences. The optimal temperature for $F_v/F_m$ (22.7°C) was much higher for the microscopic sporophyte, which occurs during the summer season when mean water temperatures range from 18 to 28°C (i.e., May to August). Whereas, the optimal temperature for gross photosynthesis and $F_v/F_m$ for the macroscopic gametophytes were 9.3°C and 12.6°C, respectively, which is close to the mean water temperatures during November to March (e.g., 12–22°C). The difference in critical temperatures of the subtropical *Cladosiphon okamuranus* Tokida (Fukumoto *et al.* 2018a) from those of the temperate *Cladosiphon umezakii* Ajisaka (Fukumoto *et al.* 2018b) provided a physiological explanation for the latitudinal distribution of these two species in Japan; *C. okamuranus* is distributed in the southern and middle part of Ryukyu Islands, while *C. umezakii* is distributed in the temperate waters of Honshu, Shikoku, and Kyushu islands. Low temperature-induced photoinhibition was observed at 16°C for *C. okamuranus*, and at 8°C for *C. umezakii*, which were close to the lowest winter temperatures at the respective northern limits of distribution of these species.

*Eucheuma* and *Kappaphycus* (Solieriaceae, Gigartinales) are economically important red seaweeds, serving primarily as raw materials for the production of iota and kappa-carrageenan, respectively. Because of their unique gelling properties, carrageenan is widely used in the food, cosmetic, and medical and pharmaceutical industries. Aside from being used as raw materials for extraction of carrageenan, these seaweeds are also considered promising sources of bioethanol (Khambhaty *et al.* 2012; Meinita *et al.* 2013). Hence, the high demand for such raw materials encourages tropical and subtropical mariculture sites to increase production of established species, further diversification to other carrageenophyte species available in local ecosystems, and eventually the establishment of cultivation systems for new species (McHugh 2003).

On one hand, kelp forests are highly productive components of cold-water rocky marine coastlines (Steneck *et al.* 2002). They include large perennial brown algae in the order Laminariales, such as *Macrocystis pyrifera* (Linnaeus) C. Agardh; *Saccharina japonica*

(Areschoug) Lane *et al*., *Laminaria digitata* (Hudson) Lamouroux, *Undaria pinnatifida* (Harvey) Suringar, *Costaria costata* (C. Agardh) Saunders, and *Alaria crassifolia* Kjellman. These underwater forests are of great ecological importance within coastal ecosystems, serving as feed, habitat, and a nursery for many associated organisms. Several studies have focused on kelp species, not only from the standpoint of their ecological importance, but also of their commercial value as a source for extraction of bioactive compounds and fresh food (Zemke-White and Ohno 1999; Bixler and Porse 2011; Vásquez *et al.* 2014).

Overall, the study focused on the ecophysiological aspect of certain economically important carrageenophyte and kelp species distributed in the western Pacific Ocean. It involved the determination of their photosynthetic responses to temperature and PAR gradients, based on PAM-chlorophyll fluorometry and oxygen evolution measurements. The effects of temperature and PAR on the photosynthesis of *Eucheuma denticulatum, Kappaphycus striatus,* and *K. alvarezii* from Indonesia were examined in chapter 2. The temperature and PAR requirements for photosynthesis of the native alga *Kappaphycus* sp. from Okinawa, Japan were determined in chapter 3. The photosynthetic performance in the two life history stages of *Costaria costata* and *Alaria crassifolia* were investigated in chapter 4. The photosynthetic characteristics of these seaweeds were related to their adaptation to the current environment in their respective habitats, as well as to their limit of distribution in the western Pacific Ocean. This information will enhance our understanding of the potential causes of decline and even local extinction of some of these species that occur across latitudinal temperature gradients.

## CHAPTER 2: Effects of temperature and PAR on the photosynthesis of *Eucheuma denticulatum, Kappaphycus striatus,* and *K. alvarezii* from Indonesia

### Introduction

*Eucheuma denticulatum* (Burman) Collins et Hervey (known as '*spinosum'*), *Kappaphycus alvarezii* (Doty) Doty ex Silva (known as '*cottonii'*), and *Kappaphycus striatus* (Doty) Doty ex Silva (Solieriaceae) are extensively cultivated across Southeast Asia, particularly in Indonesia, Philippines, and Malaysia (Neish 2013; Hurtado *et al.* 2014a; 2015), as well as in tropical and subtropical waters of India (Krishnan and Narayanakumar 2013), Tanzania (Msuya *et al.* 2014), and countries in Latin America (Hayashi *et al.* 2013) and the Caribbean (Hurtado *et al.* 2014b). These seaweeds are observed abundant in growth from shallow to deep-water farming areas, employing different cultivation techniques. The off-bottom monoline, single floating-raft and hanging long-line are popular methods adopted in Indonesia (Adnan and Porse 1987, Luxton 1993).

Due to their economic value, these carrageenophytes have been subjects of numerous investigations, including studies on the ecophysiology of these species, particularly on determining their photobiology under intense PAR and ultraviolet (UV) radiation (Aguirre von Wobeser *et al.* 2001; Granbom *et al.* 2001; Schubert *et al.* 2004, 2006; Schmidt *et al.* 2010a, b), as well as on clarifying optimum farming conditions for maximum production and control of epiphytic filamentous algae (EFA; Borlongan *et al.* 2011, 2016). Pulse amplitude modulated (PAM)-chlorophyll fluorometry has long been used as a rapid method to quantify the effects of changing environmental conditions on macroalgal photobiology (Renger and Schreiber 1986; Gévaert *et al.* 2002; Enriquez and Borowitzka 2011), providing greater detail, especially on their photosynthetic activity in response to temperature (Lideman *et al.* 2013; Fujimoto *et al.* 2015; Kokubu *et al.* 2015;

Vo *et al.* 2015; Terada *et al.* 2016a, b). For instance, the rapid light curves (RLCs) of the electron transport rate (ETR) of *E. denticulatum* and *Kappaphycus* sp. (Sumba strain) from South Sulawesi, Indonesia were strongly affected by temperature, with optimum temperatures for photosynthesis ranging from 23 to 32°C and 22 to 33°C, respectively (Lideman *et al.* 2013). Whereas the highest maximum quantum yield [maximum photochemical efficiency of photosystem II (*PSII*), $F_v/F_m$; Cosgrove and Borowitzka 2011] of *K. alvarezii* from Vietnam occurred at 22.2°C, with relatively high growth rates between 28 and 32°C (Terada *et al.* 2016b). These species were well-adapted to the natural temperature environment of their corresponding cultivation sites. A characteristic midday decline in effective quantum yield ($\Phi_{PSII}$), and a subsequent recovery by late afternoon was also observed in Vietnamese-cultivated *K. alvarezii*, suggesting that optimum PAR for gross photosynthesis with the minimum decline of $\Phi_{PSII}$ would be lower.

It is of our great interest to evaluate and clarify site- and species-specific response to environmental conditions. However, our former study on the Indonesian entities (Lideman *et al.* 2013) was limited to relative ETRs (*rETR*s) from PAM measurements, and lacked results from dissolved oxygen measurements. These species are also cultivated differently; the choice of farming system often depends on the environmental conditions of the culture site (e.g., seasonality, temperature, weather condition, and water quality). Knowledge on the temperature and PAR optima of these species are valuable for proper selection of carrageenophyte species and/ or strains, relative to the cultivation site and method employed, for maximum crop yield and production.

This study was conducted to determine the photosynthetic responses of *E. denticulatum, K. striatus* (Sacol strain), and *K. alvarezii* (brown and green color morphotypes) from Indonesia to various temperature and PAR conditions, by PAM-chlorophyll fluorometry and use of dissolved oxygen sensors. Changes in the *PSII* photochemical efficiency ($F_v/F_m$ and $\Phi_{PSII}$) of *K. alvarezii* in response to continuous PAR exposures that are typically encountered in the cultivation site were also evaluated.

## Materials and Methods

### *Sample collection and stock maintenance*

*E. denticulatum* and *K. striatus* were collected from a farming area along Geger Beach, Nusa Dua, Bali, Indonesia (08°48.915' S, 115°13.580' E) on 28 August 2015. These seaweeds are cultivated by fixed off-bottom method, a farming technique practiced in shallow reef areas like the coastline, with the lowest mean tide level ranging from 25 to 100 cm (Doty 1973; Trono 2000). On one hand, *K. alvarezii* [brown and green color morphotypes] were collected from a carrageenophyte farm at Arakan, Sulawesi Utara, Indonesia (1°22'40.43" N, 124°33'12.58" E) on 2 December 2015. These seaweeds are cultivated by the hanging long-line method (Hurtado *et al.* 2014a).

Approximately 1 kg of each seaweed sample was collected; wrapped with a wet paper towel that was moistened with seawater; and separately stored in plastic bags. All samples were transported to Japan via an overnight airline trip.

They were maintained for 1 to 3 days before examination at the Faculty of Fisheries, Kagoshima University, Japan in an aquarium tank (1500 L) containing seawater at a salinity of 33, pH of 8.0, seawater temperature of 26°C (i.e., actual seawater temperature during collection), and at PAR of 200 μmol photons $m^{-2}$ $s^{-1}$ (14:10 light: dark cycle). Aeration (approximately 2.0 L $min^{-1}$) was also provided to maintain saturated conditions of dissolved oxygen. Voucher herbarium specimens of the two taxa were deposited in the Herbarium of Kagoshima University Museum, Kagoshima.

*Effect of temperature on photosynthesis and respiration*

Methods for the photosynthesis–temperature (*P*–*T*) experiment were described in previous studies (Fujimoto *et al.* 2015; Kokubu *et al.* 2015; Vo *et al.* 2015; Terada *et al.* 2016a, b). Seaweed samples were examined under eight temperature treatments (10, 14, 18, 22, 26, 30, 34, and 38°C) with five replicates, at PAR of 200 μmol photons $m^{-2}$ $s^{-1}$. Light was provided by a metal halide lamp, and adjusted with neutral density screens. Water temperature in the reaction vessel was controlled using a water bath (Coolnit CL-600R, Taitec, Inc., Tokyo, Japan). Oxygen production or consumption was measured with DO meters equipped with optical DO sensors (ProODO-BOD; YSI Incorporated, Yellow Springs, USA).

Prior to the experiments, randomly cut segments (apical, mid, or basal) of *E. denticulatum* [0.98 ± 0.13 g fresh weight ($g_{fw}$; mean ± standard deviation, SD)], *K. striatus* (1.37 ± 0.65 $g_{fw}$), and brown and green *K. alvarezii* (1.08 ± 0.16 $g_{fw}$) were acclimated overnight with sterile natural seawater in the incubator. At the onset of the experiment, three to four explants were randomly selected and placed in biological oxygen demand (BOD) bottles ($n$ = 5) containing approximately 100 mL sterile natural seawater. (Note: Exact volume varies from each BOD bottle, which was accounted for in the analysis). The DO sensors were placed in sterile natural seawater carefully so that no visible bubbles would be trapped.

Net photosynthesis (*NP*) rates were determined by measuring the dissolved oxygen concentrations (mg $L^{-1}$) every 5 min for 30 min after a 30-min preincubation to acclimate the samples to each experimental condition. Respiration rates (i.e., "post-illumination respiration"; Colombo-Pallota *et al.* 2010; Vásquez-Elizondo and Enríquez 2016) were determined following net photosynthesis measurements, by wrapping the BOD bottles with aluminum foil. Water in the bottles was continuously stirred during the measurement. Sterile natural seawater was renewed after every measurement to avoid any effects that can be attributed to the depletion of nutrients and dissolved carbon dioxide.

A least-squares linear regression model was fit to each of the concentrations with respect to time; and the slope estimated from the model was used as the photosynthetic or respiration rate, expressed in μg $O_2$ $g_{fw}^{-1}$ $min^{-1}$. All rates were normalized to the water volume of each BOD bottle and fresh weight of the sample.

### *Effect of PAR on oxygenic photosynthesis*

Methods for the photosynthesis–PAR (*P–E*) experiment followed those of previous studies (Fujimoto *et al.* 2015; Kokubu *et al.* 2015; Terada *et al.* 2016a, b). Photosynthesis rates were determined at nine PAR levels (0, 30, 60, 100, 150, 200, 250, 500 and 1000 μmol photons $m^{-2}$ $s^{-1}$), with five replicates at 26°C. Various PAR levels were obtained by appropriately layering neutral density screens between the reaction vessel and the light source (metal halide lamp). Temperature was controlled using a water bath (Coolnit CL-600R, Taitec, Inc., Tokyo, Japan).

Approximately 1.08 ± 0.18 $g_{fw}$ of *E. denticulatum*, 1.27 ± 0.09 $g_{fw}$ of *K. striatus*, and 1.14 ± 0.2 $g_{fw}$ of brown and green *K. alvarezii* segments, respectively, were placed into each BOD bottle (*n* = 5) containing sterile natural seawater. They were allowed to acclimate in the dark for 10 min. After acclimation, the magnitude of dissolved oxygen concentration (mg $L^{-1}$) was recorded every 5 min over a 30-min interval for each bottle, with the incubation water continuously stirred to avoid boundary layer effects. Seaweed segments were subsequently subjected to eight PAR levels, from 30 to 1000 μmol photons $m^{-2}$ $s^{-1}$. The incubation water was renewed with sterile natural seawater and a 10-min light acclimation period was provided prior to DO measurements before commencing each PAR treatment. Similar to temperature experiment, the slope of the linear regression of the DO concentrations over a 30-min period was determined to estimate photosynthetic or respiration rates.

***Effect of temperature on chlorophyll fluorescence***

The $F_v/F_m$ of the alga were measured from 8 to 38°C in 2°C increments, with a Maxi Imaging-PAM (Heinz Walz GmbH, Effeltrich, Germany), as described in previous studies (Fujimoto *et al.* 2015; Kokubu *et al.* 2015; Vo *et al.* 2015; Terada *et al.* 2016a, b). Initially, 6–8 cm-long sections of the thalli of each species were cut and dark-acclimated overnight in the incubator at 26°C. Sections were then placed in a stainless-steel tray (12 cm × 10 cm × 3 cm) with sterilized natural seawater, providing 10 replicates for each temperature condition. Seawater temperature in the tray was controlled with an aluminum block incubator (BI-535A; Astec, Fukuoka, Japan), and monitored with a thermocouple (model 925; Testo AG, Lenzkirch, Germany). Each increment in temperature occurred over a 30-min period, with an additional 30 min for temperature and dark acclimation. Thus, one set of experiments typically took more than 8 h to complete.

***Photoinhibition-recovery experiments***

To evaluate the effects of continuous PAR exposure on quantum yields of brown and green *K. alvarezii*, twenty randomly selected >8 cm-long segments of each seaweed sample were incubated overnight (12 h) under dark conditions until the experiment. $F_v/F_m$ at 0 μmol photons $m^{-2}$ $s^{-1}$ were measured to provide initial values. The sections were then divided into two PAR treatment groups (i.e., 300 and 1000 μmol photons $m^{-2}$ $s^{-1}$). Samples were placed in separate beakers (1000 mL) containing sterile natural seawater maintained at 26°C (Coolnit CL-600R, Taitec, Inc.), and were exposed to either 300 or 1000 μmol photons $m^{-2}$ $s^{-1}$ (metal halide lamp). $\Phi_{PSII}$ (10 replicates) were measured every hour for 6 h of continuous exposure to each PAR level. Water in the beakers was continuously stirred throughout the exposure. Following the experiment, samples were once more dark-acclimated for 12 h at 26°C; and the $F_v/F_m$ for each section were measured to assess recovery. Laboratory measurements of quantum yields ($F_v/F_m$, $\Phi_{PSII}$) were carried out with a Maxi Imaging-PAM (Kokubu *et al.* 2015; Terada *et al.* 2016a).

### *Modelling the photosynthetic response to temperature and PAR*

The responses of gross photosynthetic (*GP*) rates and maximum quantum yield ($F_v/F_m$) to temperature were analyzed using a Bayesian approach. The model was based on a thermodynamic non-linear equation (Thornley and Johnson 2000; Alexandrov and Yamagata 2007; Eq. 1), where $y$ is the response variable, which can either be the *GP* rate, or $F_v/F_m$; and $K$ is temperature expressed in Kelvin. The thermodynamic non-linear model (Eq. 1) assumes that photosynthesis enters a less active state beyond some optimal temperature. There are four parameters in this model: $y_{max}$ is a scaling parameter to fit the model to the range of $y$; $K_{opt}$ is the absolute temperature where $y$ is maximized; $H_a$ is the activation energy in kJ mol$^{-1}$; and $H_d$ is the deactivation energy in kJ mol$^{-1}$. $R$ in this model is the ideal gas constant, and has a value of 8.314 J mol$^{-1}$. The optimal value of $y_{opt}$ at $K_{opt}$ can be determined by substituting $K_{opt}$ into the equation.

$$y = \frac{y_{max} \cdot H_d \cdot exp\left(\frac{H_a \cdot (K - K_{opt})}{K \cdot R \cdot K_{opt}}\right)}{\left(H_d - H_a \cdot \left(1 - exp\left(H_d \cdot \frac{(K - K_{opt})}{(K \cdot R \cdot K_{opt})}\right)\right)\right)} \tag{1}$$

The gross photosynthesis rate, which is the sum of net photosynthesis rate and respiration rate, was estimated by simultaneously fitting the measured respiration rates to the Arrhenius equation (Eq. 2), and the net photosynthesis rates to the difference in Eq. 1 and Eq. 2. Gross photosynthesis rates were estimated by assuming that respiration rates after light pre-incubation were a good proxy for "kinetically-limited" mitochondrial respiration, wherein oxygen is not a limiting factor in the process (Colombo-Pallota *et al.* 2010). $R_m$ is the respiration rate at the median temperature (i.e., at 24°C, $K_m$ = 297.15) and $E_a$ is the activation energy. Simultaneous model fittings and determination of model parameters for Eq. 1 and 2 were done using a Bayesian approach, with appropriate prior probability distributions assigned to the parameters:

$$R_d = R_m exp\left(-\frac{E_a}{R}\left(\frac{1}{K - K_m}\right)\right) \quad (2)$$

In the case of $F_v/F_m$, the expected values were assumed to be beta distributed, given that $F_v/F_m$ is a ratio that is bounded by 0 and 1.

The response of net photosynthesis to PAR was examined by modelling the data using an exponential equation (Webb *et al.* 1974; Jassby and Platt 1976; Platt *et al.* 1980; Henley 1993), which included a respiration term ($R_d$) that had the form

$$P_{net} = NP_{max}\left(1 - exp\left(\frac{-\alpha}{NP_{max}}E\right)\right) - R_d \quad (3)$$

where $P_{net}$ is the net photosynthetic rate, $NP_{max}$ is the maximum net photosynthetic rate, $\alpha$ is the initial slope of the $P$–$E$ curve, $R_d$ is the dark respiration rate, and $E$ is the incident PAR. From this model, the saturation PAR ($E_k$) was calculated as $NP_{max} / \alpha$ and the compensation PAR ($E_c$) was $NP_{max} ln\left(\frac{NP_{max}}{(NP_{max} - R_d)}\right)/\alpha$.

***Statistical analyses***

Statistical analyses were done using *R* version 3.3.3 (R Development Core Team 2017) and Bayesian model fitting was done using rstan version 2.17.3 (Stan Development Team 2017).

RStan primarily uses a variant of a Hamiltonian Monte Carlo sampler to construct the posterior distributions of the parameters; and four chains of at least 500,000 samples per chain were generated and assessed for convergence, which provided at least 1,000 effective samples of each of the parameters of interest.

A one-way ANOVA was used to examine if continuous PAR exposures affected $\Phi_{PSII}$ of brown and green *K. alvarezii* for each PAR level. Time was considered a factor with levels: 0, 6, and 18 h after the start of the experiment (i.e., initial $F_v/F_m$, $\Phi_{PSII}$ after 6 h of PAR exposure, and the final $F_v/F_m$ after 12 h of darkness).

## Results

### *Effect of temperature on photosynthesis and dark respiration rates*

The *NP* rates of *E. denticulatum, K. striatus,* and *K. alvarezii* increased with rise in temperature from 10 to 30°C, and then declined up to 38°C (Fig. 1a–d). Peak *NP* rates of *E. denticulatum* and *K. striatus* at 30°C were 10.2 and 2.1 µg $O_2$ $g_{fw}^{-1}$ $min^{-1}$ [7.7–12.6 and 0.5–3.8, 95% Bayesian prediction interval (BPI)], respectively. *NP* rates were highest at 26°C for brown *K. alvarezii* [1.8 µg $O_2$ $g_{fw}^{-1}$ $min^{-1}$ (1.0–2.5, 95% BPI)], and at 30°C for green *K. alvarezii* [3.4 µg $O_2$ $g_{fw}^{-1}$ $min^{-1}$ (2.8–4.1, 95% BPI)].

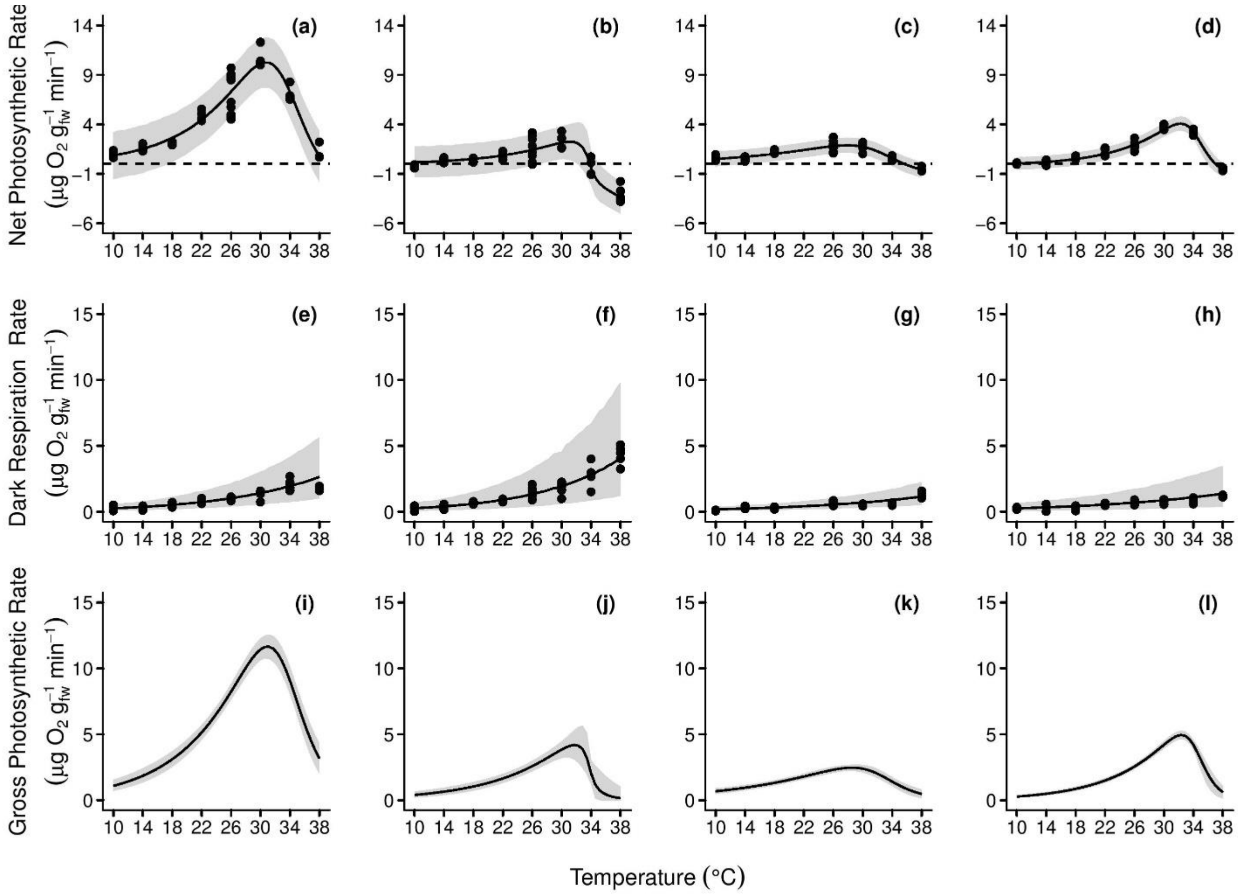


**Fig. 1** The response of the oxygenic photosynthesis and dark respiration of *Eucheuma denticulatum* (a, e, i) and *Kappaphycus striatus* (b, f, j) from Bali, Indonesia, and of brown (c, g, k) and green (d, h, l) strains of *Kappaphycus alvarezii* from Arakan, Sulawesi Utara, Indonesia. a–d: The oxygenic net photosynthesis to temperature determined at 200 μmol photons $m^{-2}$ $s^{-1}$. e–h: The dark respiration rate to temperature at 0 μmol photons $m^{-2}$ $s^{-1}$. i–l: The modeled gross photosynthetic rates. Data were derived from the model curve of net photosynthesis (a–d) and dark respiration (e–h). The dots indicate the measured rates ($n$ = 5), the lines indicate the expected value, and the shaded regions indicate the 95% Bayesian prediction interval (95% BPI) of the model.

Dark respiration was likewise affected by temperature, with rates increasing from 0.3 μg $O_2$ $g_{fw}^{-1}$ $min^{-1}$ (0.1–0.6, 95% BPI) at 10°C to 2.6 μg $O_2$ $g_{fw}^{-1}$ $min^{-1}$ (1.0–5.6, 95% BPI) at 38°C for *E. denticulatum* (Fig. 1e); from 0.3 μg $O_2$ $g_{fw}^{-1}$ $min^{-1}$ (0.1–0.7, 95% BPI) to 4.0 μg $O_2$ $g_{fw}^{-1}$

$min^{-1}$ (1.2–9.8, 95% BPI) for *K. striatus* (Fig. 1f); from 0.2 μg $O_2$ $g_{fw}^{-1}$ $min^{-1}$ (0.1–0.4, 95% BPI) to 1.1 μg $O_2$ $g_{fw}^{-1}$ $min^{-1}$ (0.5–2.2, 95% BPI) for brown *K. alvarezii* (Fig. 1g); and from 0.3 μg $O_2$ $g_{fw}^{-1}$ $min^{-1}$ (0.1–0.7, 95% BPI) to 1.4 μg $O_2$ $g_{fw}^{-1}$ $min^{-1}$ (0.4–3.4, 95% BPI) for green *K. alvarezii* (Fig. 1h). The respiration rates at the median value of temperature ($R_{24}$) for *E. denticulatum*, *K. striatus,* and brown and green *K. alvarezii* were 0.9, 1.2, 0.5, and 0.6 μg $O_2$ $g_{fw}^{-1}$ $min^{-1}$, respectively. Data from the 22°C of brown *K. alvarezii* were excluded from the analysis due to malfunction of the DO sensors during measurement.

On the basis of the *GP*–temperature curves (Fig. 1i–l) derived from simultaneous model fittings (Eq. 1 and 2) of net photosynthesis and dark respiration rates, maximum gross photosynthetic rates ($GP_{max}$) of *E. denticulatum* and *K. striatus* were estimated to be 11.7 and 4.4 μg $O_2$ $g_{fw}^{-1}$ $min^{-1}$, which occurred at 31.0 and 31.6°C, respectively. As for the brown and green *K. alvarezii*, their $GP_{max}$ (2.5 μg $O_2$ $g_{fw}^{-1}$ $min^{-1}$ for brown and 5.0 μg $O_2$ $g_{fw}^{-1}$ $min^{-1}$ for green) occurred at 28.5 and 32.4°C, respectively. Other model parameter estimates are presented in Table 1.

**Table 1** Mean and 95% Bayesian prediction intervals (95% BPI) of the parameters estimated for the gross photosynthesis–temperature model in *E. denticulatum*, *K. striatus*, and brown and green *K. alvarezii*

| | ***E. denticulatum*** | | ***K. striatus*** | | **Brown *K. alvarezii*** | | **Green *K. alvarezii*** | |
|---|---|---|---|---|---|---|---|---|
| **Parameter** | **Mean** | **95% BPI** | **Mean** | **95% BPI** | **Mean** | **95% BPI** | **Mean** | **95% BPI** |
| $GP_{max}$ | 11.7 | 10.8 – 12.6 | 4.4 | 3.3 – 5.7 | 2.5 | 2.3 – 2.7 | 5.0 | 4.6 – 5.3 |
| $H_a$ | 91 | 74 – 110 | 83 | 61 – 110 | 58 | 40 – 78 | 98 | 86 – 112 |
| $H_d$ | 392 | 319 – 489 | 1367 | 362 – 3930 | 347 | 109 – 535 | 674 | 529 – 940 |
| $T_{opt}$ | 31.0 | 30.3 – 31.6 | 31.6 | 29.9 – 33.1 | 28.5 | 27.0 – 30.1 | 32.4 | 32.1 – 32.7 |
| $E_a$ | 61 | 50 – 72 | 71 | 60 – 82 | 48 | 38 – 57 | 44 | 30 – 57 |
| $R_{24}$ | 0.9 | 0.8 – 1.1 | 1.2 | 1.0 – 1.3 | 0.5 | 0.4 – 0.6 | 0.6 | 0.5 – 0.7 |

$GP_{max}$, maximum gross photosynthesis (µg $O_2$ $g_{fw}^{-1}$ $min^{-1}$); $H_a$, activation energy for photosynthesis (kJ $mol^{-1}$); $H_d$, deactivation energy (kJ mol−1); $E_a$, activation energy for respiration (kJ $mol^{-1}$); $R_{24}$, respiration rate at median temperature (µg $O_2$ $g_{fw}^{-1}$ $min^{-1}$); $T_{opt}$, optimum temperature (°C)

### *Effect of PAR on the net photosynthesis*

*P–E* curves of *E. denticulatum, K. striatus,* and *K. alvarezii* at 26°C showed a characteristic hyperbolic shape, with an initial increase in *NP* rates and then saturating to a constant rate at high PAR (Fig. 2). No indication of photoinhibition was also observed for all carrageenophyte species up to the maximum PAR of 1000 µmol photons $m^{-2}$ $s^{-1}$.

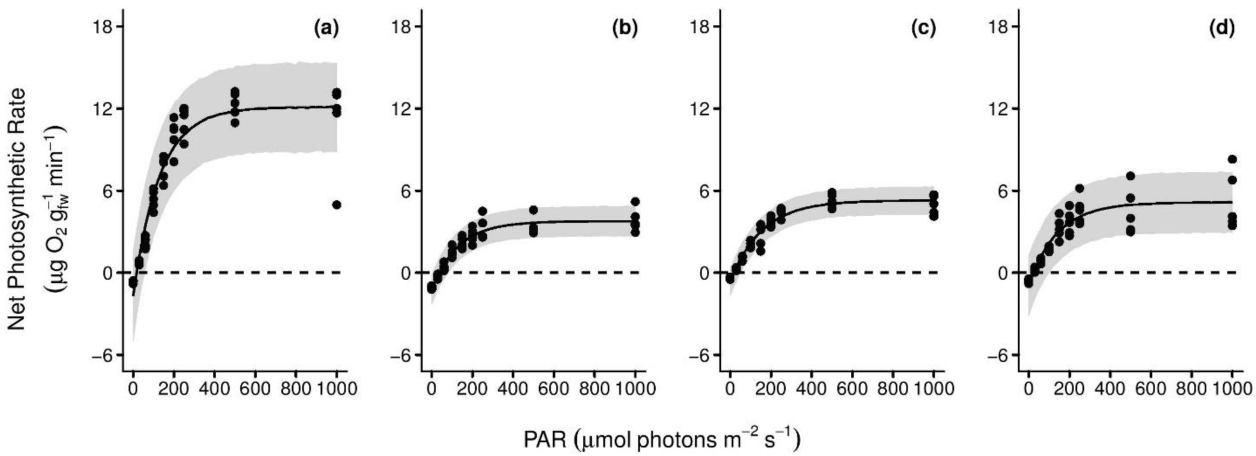


**Fig. 2** The response of the net photosynthetic rates of *E. denticulatum* (a), *K. striatus* (b), and brown (c) and green (d) *K. alvarezii* to increasing photosynthetically active radiation (PAR) measured at 26°C. The dots indicate the measured rates ($n$ = 5), the lines indicate the expected value, and the shaded regions indicate the 95% BPI of the model.

The measured *NP* rates of *E. denticulatum* and *K. striatus* gradually increased from -1.7 and -1.2 μg $O_2$ $g_{fw}^{-1}$ $min^{-1}$ (-5.0–1.6 and -2.3–0.1, 95% BPI) at 0 μmol photons $m^{-2}$ $s^{-1}$ to a high of 12.1 and 3.8 μg $O_2$ $g_{fw}^{-1}$ $min^{-1}$ (8.8–15.3 and 2.7–4.8, 95% BPI) at 1000 μmol photons $m^{-2}$ $s^{-1}$, respectively. *NP* rates of the brown and green *K. alvarezii* likewise rose from -0.6 and -0.9 μg $O_2$ $g_{fw}^{-1}$ $min^{-1}$ (-1.7–0.4 and -3.2–1.3, 95% BPI) at 0 μmol photons $m^{-2}$ $s^{-1}$ to 5.3 and 5.2 μg $O_2$ $g_{fw}^{-1}$ $min^{-1}$ (4.3–6.3 and 2.9–7.4, 95% BPI) at 1000 μmol photons $m^{-2}$ $s^{-1}$, respectively.

The parameter estimates which describe the significant features of each *P–E* curve are shown in Table 2.

**Table 2** Mean and 95% BPI of the parameters estimated for the *P–E* model in *E. denticulatum*, *K. striatus*, and brown and green *K. alvarezii*

| | ***E. denticulatum*** | | ***K. striatus*** | | **Brown *K. alvarezii*** | | **Green *K. alvarezii*** | |
|---|---|---|---|---|---|---|---|---|
| **Parameter** | **Mean** | **95% BPI** | **Mean** | **95% BPI** | **Mean** | **95% BPI** | **Mean** | **95% BPI** |
| $NP_{max}$ | 13.8 | 12.5 – 15.2 | 5.0 | 4.6 – 5.5 | 5.9 | 5.5 – 6.4 | 6.1 | 5.2 – 7.0 |
| $\alpha$ | 0.11 | 0.08 – 0.13 | 0.04 | 0.03 – 0.05 | 0.04 | 0.03 – 0.04 | 0.04 | 0.03 – 0.06 |
| $R_d$ | 1.7 | 0.6 – 2.8 | 1.3 | 0.9 – 1.6 | 0.6 | 0.3 – 1.0 | 1.0 | 0.7 – 1.7 |
| $E_c$ | 17 | 7 – 25 | 37 | 29 – 45 | 18 | 10 – 25 | 23 | 18 – 36 |
| $E_k$ | 130 | 105 – 160 | 131 | 105 – 162 | 157 | 133 – 185 | 143 | 125 – 201 |

$NP_{max}$, maximum net photosynthesis (μg $O_2$ $g_{fw}^{-1}$ $min^{-1}$); $R_d$, respiration rate (μg $O_2$ $g_{fw}^{-1}$ $min^{-1}$); $\alpha$, initial slope [μg $O_2$ $g_{fw}^{-1}$ $min^{-1}$ (μmol photons $m^{-2}$ $s^{-1}$)$^{-1}$]; $E_c$, compensation PAR (μmol photons $m^{-2}$ $s^{-1}$); $E_k$, saturation PAR (μmol photons $m^{-2}$ $s^{-1}$)

### *Effect of temperature on the maximum quantum yield ($F_v/F_m$)*

The $F_v/F_m$ of all carrageenophyte species were also observed to gradually increase from low temperatures to a peak, and then decrease with further rise in temperature (Fig. 3). Their maximum $F_v/F_m$ ranged from 0.55 to 0.65, which occurred at temperatures between 15.7 and 19.7°C. Other model parameter estimates are presented in Table 3.

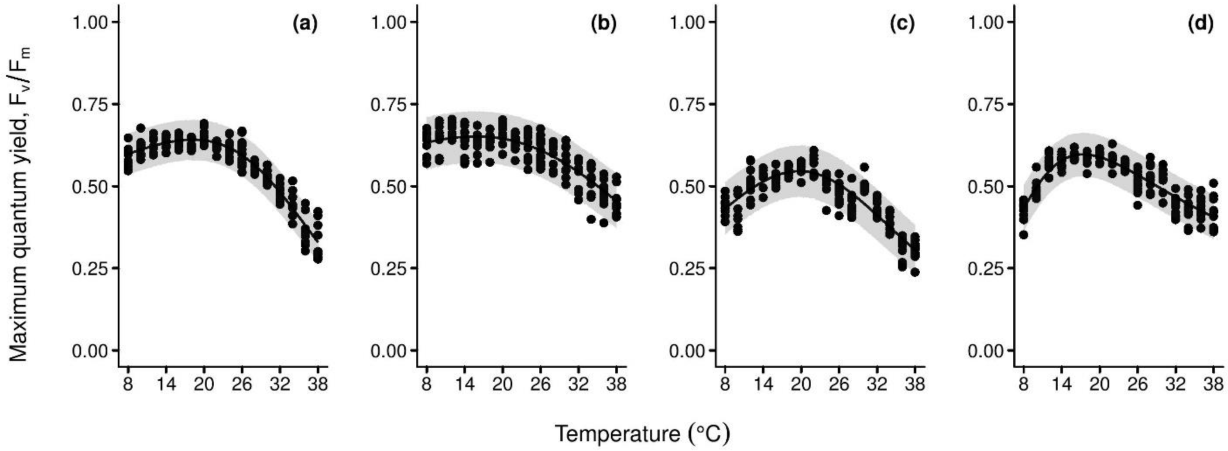


**Fig. 3** The temperature response of the maximum quantum yield ($F_v/F_m$) in *E. denticulatum* (a), *K. striatus* (b), and brown (c) and green (d) strains of *K. alvarezii*. The dots indicate the measured values ($n$ = 10), the lines indicate the expected value, and the shaded regions indicate the 95% BPI of the model.

**Table 3** Mean and 95% BPI of the parameters estimated for the $F_v/F_m$–temperature model in *E. denticulatum*, *K. striatus*, and brown and green *K. alvarezii*

| | ***E. denticulatum*** | | ***K. striatus*** | | **Brown *K. alvarezii*** | | **Green *K. alvarezii*** | |
|---|---|---|---|---|---|---|---|---|
| **Parameter** | **Mean** | **95% BPI** | **Mean** | **95% BPI** | **Mean** | **95% BPI** | **Mean** | **95% BPI** |
| $F_v/F_{m\ (max)}$ | 0.64 | 0.63 – 0.66 | 0.65 | 0.64 – 0.66 | 0.55 | 0.53 – 0.56 | 0.60 | 0.59 – 0.61 |
| $H_a$ | 9 | 6 – 14 | 10 | 4 – 21 | 35 | 22 – 51 | 119 | 92 – 147 |
| $H_d$ | 112 | 98 – 127 | 70 | 56 – 88 | 94 | 88 – 102 | 139 | 115 – 164 |
| $T_{opt}$ | 18.2 | 17.4 – 19.0 | 15.7 | 13.7 – 17.4 | 19.7 | 18.8 – 20.6 | 17.4 | 16.7 – 18.1 |

### *Effect of continuous PAR exposures on quantum yields ($F_v/F_m$, $\Phi_{PSII}$)*

The effects of continuous exposure to low (300 µmol photons m$^{-2}$ s$^{-1}$) and high (1000 µmol photons m$^{-2}$ s$^{-1}$) PAR on the quantum yields of the two color morphotypes of *K. alvarezii* were similar, with decrease in their quantum yields ($\Phi_{PSII}$) in the first hour of exposure until the sixth hour (Fig. 4). The quantum yields of brown and green *K. alvarezii* after 6 h of low PAR exposure significantly declined ($P < 0.01$) from the initial $F_v/F_m$ of 0.32 and 0.47 to $\Phi_{PSII}$ of 0.20 and 0.26, respectively. However, after the 12-h dark acclimation period, the $F_v/F_m$ recovered to 0.39 and 0.48, respectively. Similarly, $\Phi_{PSII}$ decreased throughout the 6-h exposure to high PAR, from an initial $F_v/F_m$ of 0.35 for brown *K. alvarezii* and 0.43 for green *K. alvarezii* to $\Phi_{PSII}$ values of 0.16 and 0.24, respectively. Their post-dark acclimation $F_v/F_m$ (i.e., 0.36 for brown *K. alvarezii* and 0.46 for green *K. alvarezii*) also recovered, with no significant difference from their initial values ($P = 0.637$, brown; $P = 0.106$, green).

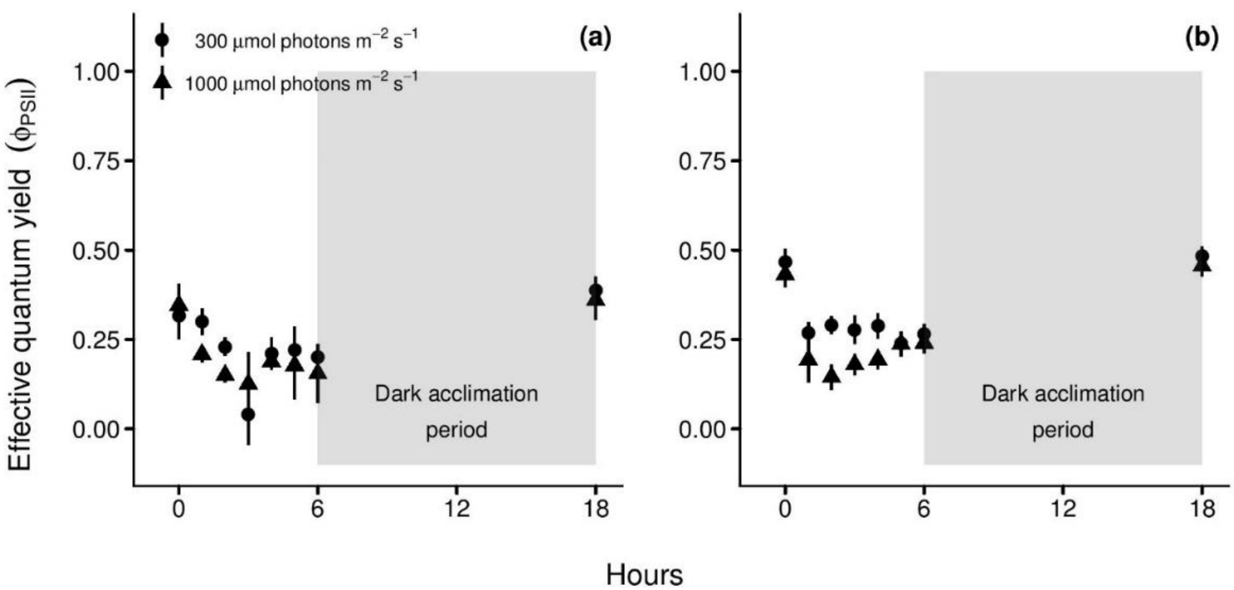


**Fig. 4** The hourly response of the effective quantum yields ($\Phi_{PSII}$) in brown (a) and green (b) strains of *K. alvarezii* to low (300 μmol photons $m^{-2}$ $s^{-1}$, circle) and high (1000 μmol photons $m^{-2}$ $s^{-1}$, triangle) PAR at 26°C. The symbols indicate the mean of actual values measured ($n = 10$), and bars indicate one standard deviation. Initial values and the values after 12-h dark acclimation were measured as $F_v/F_m$.

## Discussion

Evaluating the impact of varying environmental conditions (Aguirre von Wobeser *et al.* 2001; Granbom *et al.* 2001; Hayashi *et al.* 2011; Terada *et al.* 2016b), including the effects of biotic stress (i.e., "ice-ice disease" and epiphytic filamentous algae *Neosiphonia* sp. infestations; Ganzon-Fortes *et al.* 1993; Hurtado *et al.* 2006; Borlongan *et al.* 2011, 2016) on the physiology and production of carrageenan in *Eucheuma* and *Kappaphycus* species, has proven crucial for development of improved agricultural technologies and management protocols ensuring the sustainability of the seaweed farming industry, especially in the context of global climate change. There are approximately 16 morphotypes or commercial varieties of *Kappaphycus* (Hurtado *et al.* 2015), having distinct acclimation and adaptation capabilities relative to cultivation method or site (Trono *et al.* 2000); hence optimum conditions need to be established for each variety independently. Cultivation of *E. denticulatum* and *K. striatus* on shallow coasts of Bali beach, Indonesia employs the fixed off-bottom method; while those of *K. alvarezii* from Sulawesi Utara, Indonesia use the hanging long-line method. Regardless of cultivation method, these seaweeds are exposed to direct sunlight throughout the day.

In this study, all carrageenophyte samples did not undergo photoinhibition, as neither decline in the convexity of the *P–E* curve nor drop in quantum yield of oxygen evolution ($\alpha$) was observed up to the highest PAR of 1000 μmol photons $m^{-2}$ $s^{-1}$. Exposure to such high PAR level for 1 h under laboratory conditions may not have yet reduced the photosynthetic activity that can result into a negative $\beta$ (i.e., quantum yield of oxygenic evolution) of the cultivated macroalgae. However, the possibility of photoinhibition of photosynthetic rates under prolonged exposure to such PAR level or to even higher magnitudes, reaching as high as 2000 μmol photons $m^{-2}$ $s^{-1}$ (Collen *et al.* 1995; Terada *et al.* 2016b), in the cultivation site is inevitable, since these carrageenophytes are planted just below the sea surface, and so are exposed to direct sunlight throughout the day. A concrete manifestation that these seaweeds are under high PAR is thallus bleaching (Dawes 1981).

On one hand, a depression of the effective quantum yield ($\Phi_{PSII}$) at noon, and recovery by sunset was observed with Vietnamese-cultivated *K. alvarezii* (Terada *et al.* 2016b) and other macroalgae (Figueroa *et al*. 1997; Cabello-Pasini *et al.* 2000; Kokubu *et al.* 2015; Terada *et al.* 2016a), revealing their efficient protective response mechanism for down-regulating photosynthesis to avoid chronic photodamage at high PAR levels (Beer *et al*. 2014). In this study, continuous exposure to 1000 μmol photons $m^{-2}$ $s^{-1}$ resulted to a decline in $\Phi_{PSII}$ of brown and green *K. alvarezii* by 56 and 44%, respectively, after the 6-h exposure. Similarly, at 300 μmol photons $m^{-2}$ $s^{-1}$, $\Phi_{PSII}$ of the two color morphotypes apparently decreased from their respective initial values by 38% (brown) and 43% (green). All *K. alvarezii* samples exposed to both low and high PAR had their $\Phi_{PSII}$ returned to initial levels after a 12-h dark acclimation period, indicative of their tolerance to high PAR. Besides decline in oxygen production and quantum yield, variations in pigment composition could also constitute the photoprotective process in the natural environment, as similar pattern of daily changes in chlorophyll-a (*chl-a*) and biliprotein content was observed in *Pyropia leucosticta* (Thuret) Neefus *et* J. Brodie (as *Porphyra leucosticta*, Figueroa *et al.* 1997). Further work is required to confirm the diurnal pigment fluctuations in these carrageenophytes so as to elucidate their role, if any, in the response to PAR stress. Nevertheless, $E_k$ of all carrageenophyte samples in this study were somehow similar, and were within the range of estimated $E_k$ values of carrageenophytes from Indonesia (96–176 μmol photons $m^{-2}$ $s^{-1}$; Lideman *et al.* 2013), Vietnam (117–203 μmol photons $m^{-2}$ $s^{-1}$; Terada *et al.* 2016b), and the Philippines (103–290 μmol photons $m^{-2}$ $s^{-1}$; Borlongan *et al.* 2016). Despite the difference on how these seaweeds were planted in the sea, results showed that these seaweeds are adapted to the same PAR conditions, with low PAR requirement for oxygenic photosynthesis. Variations in growth performance of these carrageenophytes, relative to the farming method employed, can rather be attributed to nutrient availability and water movement (Glenn and Doty 1992), as these factors are also crucial for the successful cultivation of these seaweeds under natural conditions (Santelices 1999).

Likewise, temperature strongly influenced the photosynthetic activity of the four sample carrageenophytes, with peak gross photosynthetic rates of *E. denticulatum, K. striatus,* and brown and green *K. alvarezii* occurring at 31.0, 31.6, 28.5, and 32.4°C ($T_{opt}$), respectively. These optimal temperatures are within the range of temperatures where $rETR_{\max}$ of Indonesian *E. denticulatum* (23–32°C) and *Kappaphycus* sp. (22–33°C) were highest (Lideman *et al.* 2013). More importantly, they are within the scope of annual seawater temperatures recorded at mariculture sites of Indonesia, (28–34°C; Amin *et al.* 2008; World Sea Temperatures 2016), Malaysia (25–31°C; Vairappan 2006), the Philippines (28–31°C; Hurtado *et al.* 2012), and Vietnam (25–32°C, Ohno *et al.* 1996; Hung *et al.* 2009). Dark respiration of all samples increased exponentially with rise in temperature up to 38°C. Maximum gross photosynthetic rates ($GP_{max}$) varied among each other, with highest values in *E. denticulatum*, suggestive of their possible growth advantage over the other carrageenophytes under optimal conditions in commercial seaweed cultures. Moreover, the brown *K. alvarezii* had $T_{opt}$ 4°C lower than those of other cultivars, which may indicate some genetic differentiation among them. The difference in their photosynthetic responses may also be attributed to the variation in pigment composition, with reduced photosynthetic and growth efficiency in species or strains with lower pigment levels per unit biomass (Dawes 1992).

*$F_v/F_m$* of *E. denticulatum, K. striatus,* and *K. alvarezii* also corresponded with the temperature response of oxygenic evolution (gross photosynthesis) in this study, and were similar to other macroalgae (Fujimoto *et al.* 2015; Vo *et al.* 2015; Terada *et al.* 2016a, b), where $F_v/F_m$ gradually increased with rising temperature, and quickly dropped as temperatures reached their apparent threshold levels. The temperature dependence of oxygen production and $F_v/F_m$ can be attributed to the role of temperature in the oxygen-evolving complex, enzymatic reactions of carbon fixation, photophosphorylation, and electron transport during photosynthesis (Allakhverdiev *et al.* 2008; Colvard *et al.* 2014). Thermal stress at high temperatures produces reactive oxygen species (ROS), which consequently inhibit de novo synthesis of the $D_1$ protein in *PSII*, resulting in a reduction of $F_v/F_m$ and *GP* rates. Despite the similar *GP*– and $F_v/F_m$–temperature responses, their temperature optima were quite dissimilar, with apparently lower $T_{opt}$ for $F_v/F_m$ than for *GP*. The discrepancy between the two parameters is probably due to the process being observed, where oxygen evolution represents net photosynthesis, which includes the oxygen-consuming process of respiration; whereas $F_v/F_m$ reflects the efficiency of light harvesting and electron transport in *PSII* (Beer *et al.* 2014); which is only a part of several processes involved in photosynthesis. Between the two photosynthetic measurements, *GP* seemed more sensitive to temperature than $F_v/F_m$ in these carrageenophytes; and so provides a better link between seaweed productivity and the thermal environment. Nonetheless, both $F_v/F_m$ and *GP* measurements were considered significant in estimating for the lower and upper limits of temperature tolerance, rather than simply an optimum temperature range based on only one type of observation. Hence, the lower and upper limits of temperature tolerance are 18.2–31.0°C for *E. denticulatum*, 15.7–31.6°C for *K. striatus*, 19.7–28.5°C for brown *K. alvarezii*, and 17.4–32.4°C for green *K. alvarezii*. The carrageenophytes may photosynthesize and grow within such range of seawater temperature in the

cultivation site, but may likely undergo thermal inhibition and stunted growth at temperatures approaching threshold levels. Indeed, growth rates of *K. alvarezii* in culture systems dropped after prolonged periods at 30°C (Aguirre von Wobeser *et al.* 2001; Mandal *et al.* 2015). Seaweeds became fragile and had retarded growth rates when seawater temperature exceeded 33°C (Ohno *et al.* 1996). Temperatures of up to 33–35°C have also caused seaweed pigment concentrations to drop, leading to loss of photosynthetic efficiency, poor growth rates, and finally to "ice-ice" whitening and loss of biomass due to fragmentation (Ganzon-Fortes *et al.* 1993; Largo *et al.* 1995). While the seaweeds' lower limits of temperature tolerance may not be of ecological importance in tropical areas, this information is valuable when we consider cultivation sites outside the tropics, in more temperate areas. For example, seawater temperatures drop to as low as 16°C during winter along the southeastern coast of Brazil (Paula *et al.* 2002; Hayashi *et al.* 2011). Additional investigations including photosynthetic pigment determination and temperature acclimation experiments for photosynthesis and respiration (with longer time-scale) are necessary in order to provide better estimates of the optimum temperature for the cultivation of such species.

## CHAPTER 3: Effects of temperature and PAR on the photosynthesis of *Kappaphycus* sp. from Okinawa, Japan

### Introduction

Okinawa Island is one of the major islands of Japan's Ryukyu Islands, situated between mainland Japan and Taiwan in the western Pacific Ocean (26°N). Its climate is described as humid-subtropical, with a mean annual temperature of 22.3°C (Climate Data for Cities Worldwide 2016). In this coastal region, environmental conditions are strongly influenced by seasonal changes, climatic (e.g., 'El Niño' events; Tokyo Climate Center, Japan Meteorological Agency 2016) and oceanographic (e.g., *Kuroshio* current; Gerung and Ohno 1997) processes, which result in changing physiological scenarios, specifically for algae inhabiting shallow and intertidal sites. Indeed, a mixture of naturally-occurring Paleotropical / temperate edible seaweeds (e.g., *Betaphycus gelatinus* (Esper) Doty ex P.C. Silva, *Sargassum fusiforme* (Harvey) Setchell, *Monostroma nitidum* Wittrock) have been observed in the region (Yoshida 1998; Yoshida *et al.* 2010).

The native red alga *Kappaphycus* sp. (referred to as *Eucheuma striatum* sensu Yamada = "*K. striatus"* auctorum japonicorum; Yamada 1936) occurs in the Ryukyu Islands, but has never been observed in mainland Japan; thus suggesting that this species in Okinawa is at the northern limit of *Kappaphycus* distribution in the western Pacific (Yoshida 1998). Similar to *Cladosiphon okamuranus* Tokida (Chordariaceae; *Mozuku* in Japanese) and *Caulerpa lentillifera* J. Agardh (Caulerpaceae; *Umi-budou* in Japanese), this species has been harvested from natural populations in Okinawa Island and other small islands in the Ryukyu Islands by local inhabitants for regional consumption (Terada 2012), and can be observed during early spring and summer. However, it often disappears by the end of spring due to overharvesting. This necessitates appropriate management and the establishment of mariculture for this species. Indeed, this species has not been reported as commercially cultivated in Japan, although initial field trials have shown potential for the mariculture of introduced *Eucheuma* and *Kappaphycus* (origin: Philippines) in the southern region of Shikoku Island, Japan proper (Ohno *et al.* 1994; Gerung and Ohno 1997).

The successful development of commercial cultivation of this carrageenophyte on the shores of Okinawa, Japan requires a fundamental understanding of its photobiology, dependent upon careful consideration of the local climate. However, most of our knowledge on temperature and PAR response of photosynthesis is limited to cultivars from tropical environments (Lideman *et al.* 2013; Borlongan *et al.* 2016; 2017a, b; Terada *et al.* 2016b). Insight regarding the ecophysiology of *Kappaphycus* in cooler regions remains scarce, exclusive of investigations related to its introduction and successful cultivation (Bulboa and de Paula 2005; Bulboa *et al.* 2008; Hayashi *et al.* 2007; De Góes and Reis 2012). Additionally, most of the previous studies (Reis *et al.* 2011; Pang *et al.* 2012; Li *et al.* 2016) focused on cultivated strains, and knowledge of non-cultivated strains is lacking.

This study focused on the temperature and PAR requirements for photosynthesis of the native alga *Kappaphycus* sp. from Okinawa, Japan by employing methods based on PAM-chlorophyll fluorometry and dissolved oxygen sensors. Changes in the *PSII* quantum yields ($F_v/F_m$, $\Phi_{PSII}$) of *Kappaphycus* sp., as subjected to different combinations of temperature and PAR over an extended period of time were also examined to determine the influence of both environmental factors in photoinhibition and recovery of *PSII*. In many cases, the impact of any particular stressor on the physiology and performance of marine macrophytes will depend upon the presence and magnitude of additional limiting or disruptive stressors (Harley *et al.* 2012).

## Materials and Methods

### *Sample collection and stock maintenance*

*Kappaphycus* sp. was collected from Inamine, Nago City, Okinawa Prefecture, Japan (26°38’20” N, 128°3’20” E) on 29 March 2016 for oxygen evolution and PAM fluorescence measurements. Additional specimens were collected from the same site on 2 June 2016 for photoinhibition-recovery experiments. The seaweeds were attached on rocks and pebbles in a coral lagoon, at a depth of 0.5 m at low tide (1.5 m deep from mean sea level). Approximately 0.5 kg of collected algae were stored in plastic bottles (1000 mL) with seawater, and transported to the laboratory at the Faculty of Fisheries, Kagoshima University, Japan. The chloroplast-encoded *rbc*L gene of the algal sample was sequenced based on the procedure of Vo *et al.* (2014), and deposited in GenBank with the accession number (LC213034). Voucher specimens were likewise deposited in the Herbarium of Kagoshima University Museum, Kagoshima.

Samples were acclimated to laboratory conditions for 1 to 3 days prior to experimentation. During this time, *Kappaphycus* sp. was maintained in an aquarium tank (1500 L) under the following laboratory conditions: moderate aeration (*c.* 2.0 L $min^{-1}$) at 24°C, PAR of 200 μmol photons $m^{-2}$ $s^{-1}$ (14:10 light: dark cycle), salinity of 33, and pH of 8.0.

### *Underwater PAR and temperature*

Continuous measurements of underwater PAR at the actual depth of collection site were also taken using a 2π quantum data-logger (DEFI-L, JFE Advantech Co. Ltd., Hyogo, Japan) from 5:30 AM on 7 November to 7:00 PM on 8 November 2016. PAR was measured at 1 Hz and the mean values were determined every minute. Seawater temperature near the study site (Okinawa Prefectural Sea Farming Center, 15 km northwest of the study site) was obtained from the online database (J-

DOSS) of Japan Oceanographic Data Center (2017). In this institution, seawater was pumped from offshore (approx. 17,000 tons per day), and seawater temperature was measured daily at 8:00 AM. Available monthly data from 2002 to 2009 were used to compute for the mean seawater temperature.

### *Effect of temperature on photosynthesis and respiration*

Photosynthetic oxygen evolution and respiratory oxygen consumption rates of *Kappaphycus* sp. were determined at eight temperature treatments (i.e., 8, 12, 16, 20, 24, 28, 32, and 36°C), with methods similar to those described in the *P–T* experiment in chapter 2. Approximately 1.33 ± 0.31 $g_{fw}$ of algal segments were placed into each BOD bottles ($n$ = 5) containing sterile natural seawater. The samples were incubated at each experimental temperature for 30 min under a constant saturating PAR of 200 μmol photons $m^{-2}$ $s^{-1}$, before photosynthesis was monitored for an additional 30 min. This was followed by measurement of respiration rates for another 30 min in the dark.

### *Effect of PAR on oxygenic photosynthesis*

*P–E* experiment on *Kappaphycus* sp. was conducted at a fixed temperature of 24°C, under nine PAR treatments similar to those described in chapter 2. Sample segments used in this experiment were approximately 2.03 ± 0.7 $g_{fw}$. All rates were normalized the to water volume of each BOD bottle ($n$ = 5) and fresh weight of the sample.

***Effect of temperature on chlorophyll fluorescence***

The $F_v/F_m$ of the alga were measured from 8 to 38°C in 2°C increments, with a red measuring light version (at 650 nm) of the Maxi Imaging-PAM (Heinz Walz GmbH, Effeltrich, Germany), as described in chapter 2.

***Photoinhibition-recovery experiments***

The quantum yields of *Kappaphycus* sp. were measured under two PAR levels (300 and 1000 μmol photons $m^{-2}$ $s^{-1}$), and at two temperatures (18 and 28°C) with a Maxi Imaging-PAM. The two temperatures served as the minimum and maximum temperature treatments, based on the *GP*– and $F_v/F_m$–temperature results. Twenty to thirty segments (> 2 cm long) of algal sample were initially incubated overnight (12 h) at each temperature condition in the dark. Ten sections, which served as replicates, were then randomly assigned to each PAR treatment group. $F_v/F_m$ at 0 μmol photons $m^{-2}$ $s^{-1}$ ($n$ = 10 per PAR–temperature combination) were measured to provide initial values. Samples were placed in separate beakers (1000 mL) containing sterile natural seawater maintained at a specific temperature (Coolnit CL-600R, Taitec, Inc., Tokyo, Japan), and were exposed to either 300 or 1000 μmol photons $m^{-2}$ $s^{-1}$ (metal halide lamp). $\Phi_{PSII}$ ($n$ = 10 per PAR–temperature combination) were measured every hour for 6 h of continuous exposure to each PAR treatment. Following the experiment, samples were once more dark-acclimated for 12 h at their respective temperatures; and their final $F_v/F_m$ were measured to confirm the possibility of recovery.

***Statistical analyses and model fittings***

Statistical analyses were done using *R* version 3.3.3 (R Development Core Team 2017) and model fittings were carried out using rstan version 2.17.3 (Stan Development Team 2017). The parameters were obtained by fitting the relevant models (Equations 1–3; chapter 2) using Bayesian inference.

A one-way ANOVA was used to examine if chronic PAR exposures affected $\Phi_{PSII}$ for each PAR–temperature combination. Time was considered a factor with levels: 0, 6 and 18 h after the start of the experiment (i.e., initial $F_v/F_m$, $\Phi_{PSII}$ after 6 h, and the final $F_v/F_m$ after 12 h of darkness).

## Results

### *Daily change of PAR and the seasonal change of seawater temperature*

The sky conditions were somewhat uniform during the two-day PAR survey, with very little cloud cover. The time of sunrise and sunset for the two days were 6:42 AM and 5:44 PM on 7 November, and 6:43 AM and 5:43 PM on 8 November, respectively. The sunshine duration for the two days was 9.4 and 8.7 h, respectively (Japan Meteorological Agency 2016). The minute-averaged underwater PAR was highest at 935.4 μmol photons $m^{-2}$ $s^{-1}$ on 7 November 2016, 11:30 AM; and at 1193.8 μmol photons $m^{-2}$ $s^{-1}$ on 8 November 2016, 11:59 AM (Fig. 5). Hourly averages from 12:00 – 1:00 PM were 800.4 μmol photons $m^{-2}$ $s^{-1}$ (7 November) and 898.7 μmol photons $m^{-2}$ $s^{-1}$ (8 November), respectively.

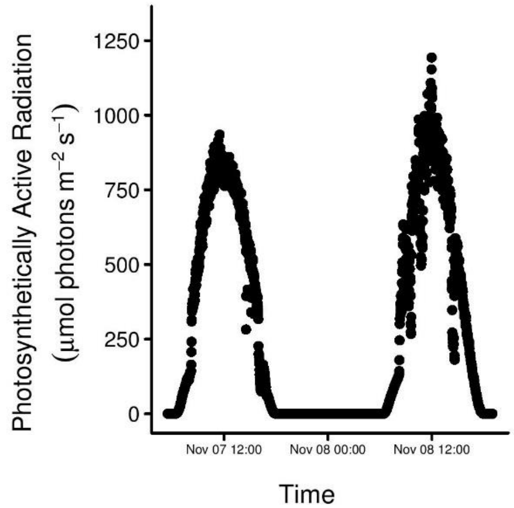


**Fig. 5** Underwater incident PAR on the *Kappaphycus* sp. habitat at Inamine, Nago, Okinawa, Japan, on 7–8 November 2016. Measurement was taken at every 1 Hz, and the mean PAR for every 60 Hz was calculated.

Mean annual seawater temperature in Okinawa is 24.5°C (Fig. 6). Minimum seawater temperature was recorded in February (20.7°C), while the maximum in August (28.7°C).

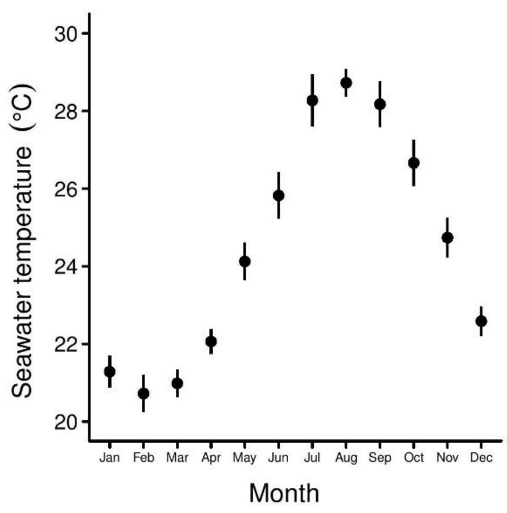


**Fig. 6** Seasonal changes of seawater temperature near the study site (Okinawa Prefectural Sea Farming Center), Motobu, Okinawa Island, Japan. The dots indicate the mean of seawater temperatures from 2002 to 2009, and bars indicate standard deviation (SD).

***Effect of temperature on photosynthesis and dark respiration rates***

Net photosynthesis of *Kappaphycus* sp. at 8°C was relatively low, with a mean rate of 0.2 μg $O_2$ $g_{fw}^{-1}$ $min^{-1}$ [(-0.6–0.9, 95% BPI]. It continuously increased between 12 and 28°C with a maximum of 3.9 μg $O_2$ $g_{fw}^{-1}$ $min^{-1}$ (3.0–4.7, 95% BPI), and subsequently decreased to a low of 1.0 μg $O_2$ $g_{fw}^{-1}$ $min^{-1}$ (0.1–1.8, 95% BPI) at 36°C (Fig. 7a).

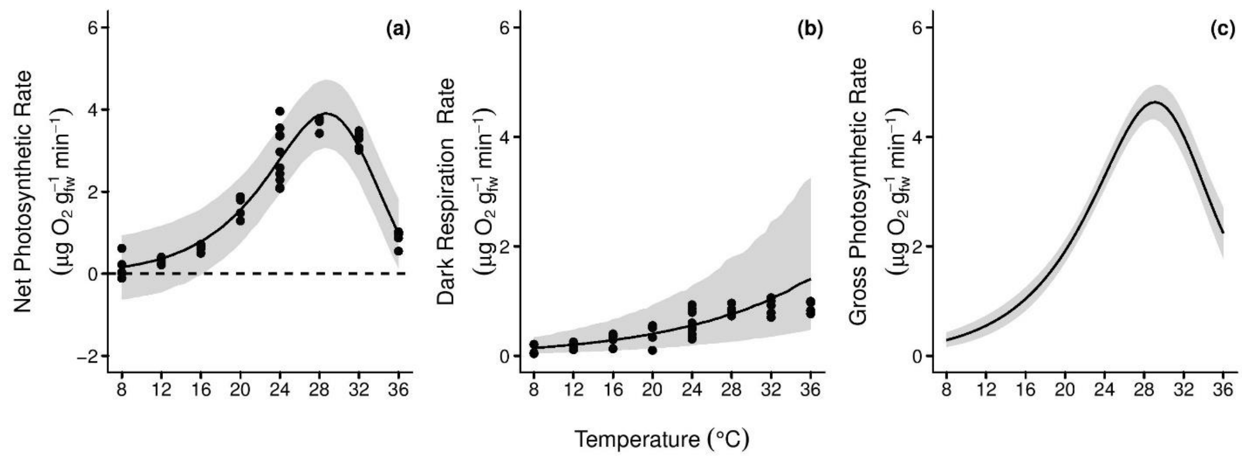


**Fig. 7** The response of the oxygenic photosynthesis and dark respiration to temperature of *Kappaphycus* sp. from Okinawa, Japan. (a) The net photosynthesis to temperature determined at 200 μmol photons $m^{-2}$ $s^{-1}$. (b) The dark respiration rate to temperature at 0 μmol photons $m^{-2}$ $s^{-1}$. (c) The modeled gross photosynthetic rates. Data were derived from the model curve of net photosynthesis (a) and dark respiration (b). The dots indicate the measured rates ($n$ = 5), the lines indicate the expected value, and the shaded regions indicate the 95% BPI of the model.

Meanwhile, dark respiration rates increased with rising temperature, from 0.1 μg $O_2$ $g_{fw}^{-1}$ $min^{-1}$ (0.05–0.3, 95% BPI) at 8°C to 1.4 μg $O_2$ $g_{fw}^{-1}$ $min^{-1}$ (0.5–3.2, 95% BPI) at 36°C (Fig. 7b). The respiration rates at the median value of temperature ($R_{22}$) for *Kappaphycus* sp. was 0.4 μg $O_2$ $g_{fw}^{-1}$ $min^{-1}$.

Simultaneous model fittings of net photosynthesis and dark respiration rates provided for estimates of gross photosynthesis rates (Fig. 7c), and model parameter values (Table 4). The optimum temperature ($T_{opt}$) of *Kappaphycus* sp. i.e., the temperature at which its maximum gross photosynthetic rate ($GP_{max}$ = 4.6 μg $O_2$ $g_{fw}^{-1}$ $min^{-1}$) would occur was 29.1°C.

**Table 4** Mean and 95% BPI of the parameters estimated for the gross photosynthesis–temperature model in *Kappaphycus* sp. from Okinawa, Japan

| Parameter | Mean | 95% BPI |
|---|---|---|
| $GP_{max}$ | 4.6 | 4.3 – 5.0 |
| $H_a$ | 111 | 90 – 138 |
| $H_d$ | 289 | 247 – 342 |
| $T_{opt}$ | 29.1 | 28.4 – 29.8 |
| $E_a$ | 59 | 46 – 72 |
| $R_{22}$ | 0.4 | 0.4 – 0.5 |

$GP_{max}$, maximum gross photosynthesis (μg $O_2$ $g_{fw}^{-1}$ $min^{-1}$); $H_a$, activation energy for photosynthesis (kJ $mol^{-1}$); $H_d$, deactivation energy (kJ mol−1); $E_a$, activation energy for respiration (kJ $mol^{-1}$); $R_{22}$, respiration rate at median temperature (μg $O_2$ $g_{fw}^{-1}$ $min^{-1}$); $T_{opt}$, optimum temperature (°C)

### *Effect of PAR on the net photosynthesis*

Increasing PAR stimulated the photosynthetic oxygen production in *Kappaphycus* sp. leading to a *P*–*E* curve (Fig. 8) from which characteristic parameters for the description of the PAR requirements were derived (Table 5). While $R_d$ was estimated to be 1.1 μg $O_2$ $g_{fw}^{-1}$ $min^{-1}$, $NP_{max}$ was 6.2 μg $O_2$ $g_{fw}^{-1}$ $min^{-1}$. *Kappaphycus* sp. had an $\alpha$ value of 0.05 μg $O_2$ $g_{fw}^{-1}$ $min^{-1}$ (μmol photons $m^{-2}$ $s^{-1}$)$^{-1}$, $E_c$ of 26 μmol photons $m^{-2}$ $s^{-1}$, and $E_k$ of 140 μmol photons $m^{-2}$ $s^{-1}$. There was no indication of photoinhibition up to the maximum PAR of 1000 μmol photons $m^{-2}$ $s^{-1}$.

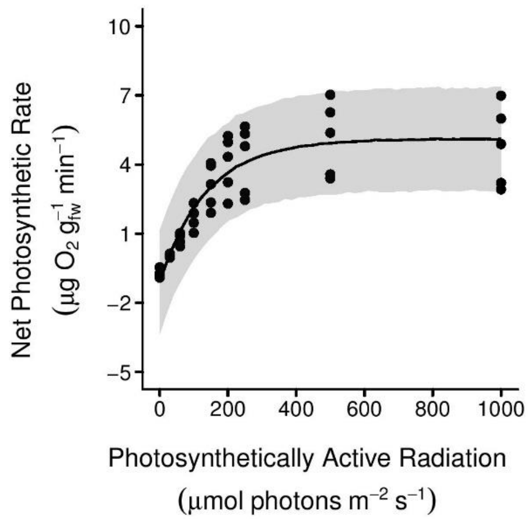


**Fig. 8** The response of the net photosynthetic rates of *Kappaphycus* sp. from Okinawa, Japan to increasing PAR measured at 24°C. The dots indicate the measured rates ($n$ = 5), the line indicates the expected value, and the shaded region indicates the 95% BPI of the model.

**Table 5** Mean and 95% BPI of the parameters estimated for the *P–E* model in *Kappaphycus* sp. from Okinawa, Japan

| Parameter | Mean | 95% BPI |
|---|---|---|
| $NP_{max}$ | 6.2 | 5.3 – 7.2 |
| $\alpha$ | 0.05 | 0.03 – 0.06 |
| $R_d$ | 1.1 | 0.4 – 1.9 |
| $E_c$ | 26 | 11 – 39 |
| $E_k$ | 140 | 98 – 192 |

$NP_{max}$, maximum net photosynthesis (µg $O_2$ $g_{fw}^{-1}$ $min^{-1}$); $R_d$, respiration rate (µg $O_2$ $g_{fw}^{-1}$ $min^{-1}$); $\alpha$, initial slope [µg $O_2$ $g_{fw}^{-1}$ $min^{-1}$ (µmol photons $m^{-2}$ $s^{-1}$)$^{-1}$]; $E_c$, compensation PAR (µmol photons $m^{-2}$ $s^{-1}$); $E_k$, saturation PAR (µmol photons $m^{-2}$ $s^{-1}$)

### ***Effect of temperature on the maximum quantum yield ($F_v/F_m$)***

The $F_v/F_m$ of *Kappaphycus sp.* remained relatively stable at temperatures between 8 and 28°C, with values ranging from 0.54 to 0.60; and decreased thereafter to a minimum of 0.21 at 38°C (Fig. 9). Parameter estimates of the model (Table 6) indicated the highest $F_v/F_m$ of 0.59 occurring at 17.4°C ($T_{opt}$).

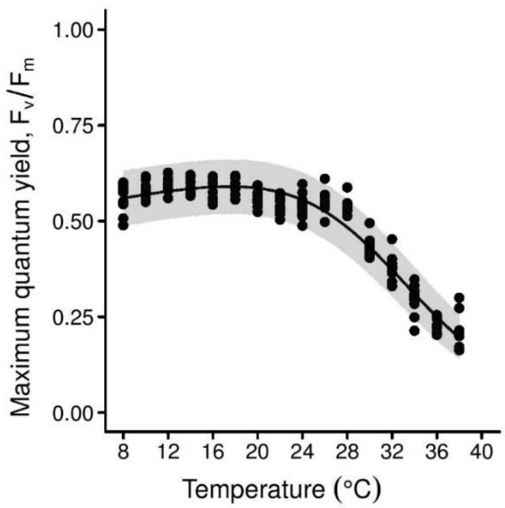


**Fig. 9** The temperature response of $F_v/F_m$ in *Kappaphycus* sp. from Okinawa, Japan. The dots indicate the measured values (*n* = 10), the lines indicate the expected value, and the shaded regions indicate the 95% BPI of the model.

**Table 6** Mean and 95% BPI of the parameters estimated for the $F_v/F_m$–temperature model in *Kappaphycus* sp. from Okinawa, Japan

| **Parameter** | **Mean** | **95% BPI** |
|---|---|---|
| $F_v/F_{m\ (max)}$ | 0.59 | 0.58 – 0.60 |
| $H_a$ | 6 | 5 – 9 |
| $H_d$ | 150 | 137 – 164 |
| $T_{opt}$ | 17.4 | 16.4 – 18.4 |

***Combined effects of temperature and PAR on the PSII quantum yields, and their potential of recovery***

The *PSII* quantum yields of *Kappaphycus* sp. in the two PAR treatments at 18 and 28°C decreased drastically in the first hour of exposure, and stabilized thereafter up to the sixth hour (Fig. 10). At 18°C, quantum yields of seaweeds after 6 h of exposure to 300 (low) and 1000 μmol photons $m^{-2}$ $s^{-1}$ (high) significantly declined ($P < 0.01$) from their initial $F_v/F_m$ of 0.51 and 0.49 to $\Phi_{PSII}$ of 0.21 and 0.15, respectively. Despite the rise in $F_v/F_m$ to 0.40 and 0.28, following 12-h dark acclimation, the values were still significantly different ($P < 0.01$) from the initial (Fig. 10a). Likewise, $\Phi_{PSII}$ of *Kappaphycus* sp. at 28°C declined throughout the 6-h exposure to both PAR treatments; from an initial $F_v/F_m$ of 0.48 to $\Phi_{PSII}$ of 0.26 at low PAR, and from 0.41 to 0.15 at high PAR. However, unlike with seaweeds at 18°C, $F_v/F_m$ of *Kappaphycus* sp. at 28°C returned to initial values after overnight acclimation ($P = 0.893$, low PAR; $P = 0.513$, high PAR; Fig. 10b).

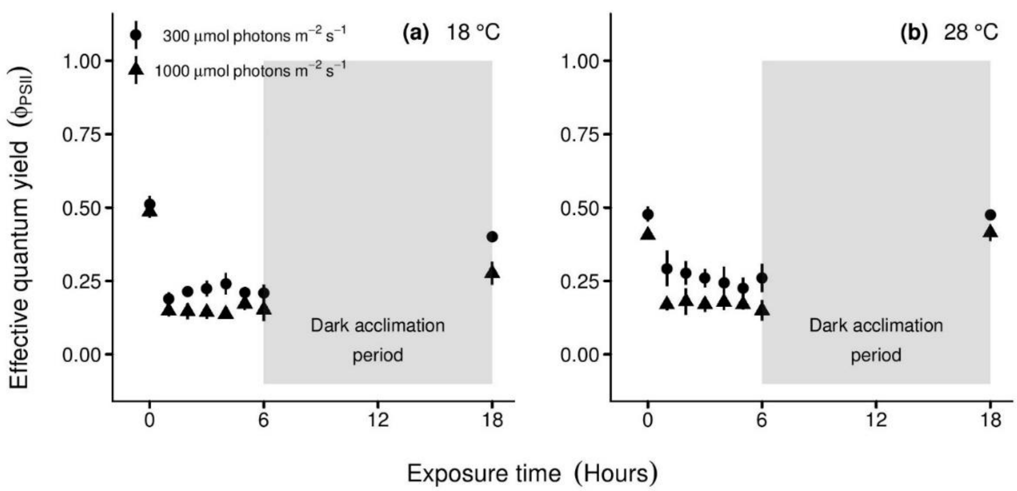


**Fig. 10** Chronological change of the *PSII* quantum yields of *Kappaphycus* sp. from Okinawa, Japan at 18°C (a) and 28°C (b). Measurements were carried out from the initial state (under dark condition, $F_v/F_m$) up to 6 h ($\Phi_{PSII}$) of continuous exposure to low (300 μmol photons $m^{-2}$ $s^{-1}$, circle) and high (1000 μmol photons $m^{-2}$ $s^{-1}$, triangle) PAR. Recovery in $F_v/F_m$ were also measured after 12 h of dark acclimation.

## Discussion

Species of *Kappaphycus* are generally distributed in tropical and subtropical coastal marine ecosystems, and they are extensively cultivated in regions near 10° latitudes (Hayashi *et al.* 2010). Despite the relatively high latitude (26° N), *Kappaphycus* sp. has been observed in the coastal waters of Okinawa, Japan over the past 80 years (as *Eucheuma striatum* sensu Yamada = *K. striatus* auct. japon.; Yamada 1936). Although this taxon had been treated as *K. striatus* in Japan for several years, there has been no phylogenetic study of Japanese species of *Kappaphycus* / *Eucheuma*; and so necessitates its taxonomic reassessment for future studies. Species identification of the algal sample is essential; as photosynthetic characteristics vary within the genus (Vo *et al.* 2015; Li *et al.* 2016; Terada *et al.* 2016c) or even within species (Borlongan *et al.* 2017b, d), which may indicate some genetic divergence. Nonetheless, algal samples in this study were regarded as *Kappaphycus* sp. Such red algae have not been observed naturally in mainland Japan, including Kyushu and Shikoku Islands; therefore, *Kappaphycus* sp. in Okinawa is regarded as one of the northernmost entities in the western Pacific (Yamada 1936; Yoshida 1998).

In this study, photosynthetic activity of *Kappaphycus* sp. was temperature-dependent at rather high temperatures, given the decline in both *GP* rates and $F_v/F_m$ after 28°C. The photophysical events of light harvesting and electron transfer may not have been strongly influenced by cold temperatures for *Kappaphycus* sp., given their consistently high $F_v/F_m$ values over the low temperature range. Such a *PSII* response contrasts with those of *K. striatum* and *K. alvarezii* from China (Li *et al.* 2016), where their $F_v/F_m$ and performance indices ($PI_{ABS}$) significantly dropped as a consequence of low temperature stress. The excess $H_2O_2$ generated by low temperature stress may have indirectly damaged the photosynthetic apparatus of the seaweeds, leading to their reduced photosynthetic activity. However, we compared our results with the previous study with caution, taking into consideration the longer period of exposure (i.e., 2 h) of algal samples to the low temperature conditions. *GP* rates of *Kappaphycus* sp. at low temperatures (8 and 12°C) were relatively low, but were stimulated by rising temperatures up to 29.1°C ($T_{opt}$); followed by an inhibition up to 36°C. Such decline in *GP* rates can be attributed to thermal damage associated with enzymes of the Calvin cycle, ATP-generating synthase and *PSII*, with oxidative stress impeding its repair process (Nishiyama *et al.* 2006; Allakhverdiev *et al.* 2008), as well as to increased respiration at elevated temperatures (Salvucci and Crafts-Brandner 2004; Fujimoto *et al*. 2015; Terada *et al*. 2016b). While dark respiration in *Kappaphycus* sp. was not detectable at 8°C and still low at 20°C, it continuously increased from 24 to 28°C. Further rise in temperature up to 36°C, however, did not affect respiratory oxygen consumption. The low respiratory activity at 36°C reduces potential cellular carbon loss; resulting in moderate net photosynthesis rates that are yet adequate for biomass gain.

A degree of variation in optimum temperatures for the two measured variables was also evident, i.e., 29.1°C for *GP* and 17.4°C for $F_v/F_m$. Nevertheless, both features depict thresholds of temperature tolerance, within which the native alga may photosynthesize efficiently. Temperature requirements for optimum photosynthesis of the Japanese *Kappaphycus* sp. (i.e., 17.4–29.1°C) were remarkably lower than those of cultivars from the Philippines (30°C; Aguirre von Wobeser *et al.* 2001), Indonesia (31–33°C; Lideman *et al.* 2013; Borlongan *et al.* 2017a, b) and Vietnam (31°C; Terada *et al.* 2016b). Moreover, the $F_v/F_m$–temperature relationship of the Japanese entity was different from those of other Paleotropical red algae (Fujimoto *et al.* 2015; Vo *et al.* 2015; Terada *et al.* 2016b, c; Borlongan *et al.* 2017a, b), that have a dome-like response to rising temperatures. The disparity in photosynthetic responses to temperature between subtropical and tropical seaweeds is primarily attributed to the difference in the temperature conditions of their respective habitats, with regions far from the equator experiencing larger variations in temperature due to seasonal changes. Seawater temperatures in Okinawa extend from 20.7°C (in February) to 28.7°C (in August), which is within the range of temperature requirement for photosynthesis of the Japanese *Kappaphycus* sp. Temperate and subtropical species have shown higher efficiencies and tolerances to a wide range of temperature (Bischoff-Bäsmann 1997; Yokoya *et al.* 1999; Terada *et al.* 2013; Graiff *et al.* 2015); hence, no drastic thermal effects on photosynthesis for these seaweeds would be expected. However, since the difference of mean monthly temperatures in Okinawa is not very high (SD = 3°C), variations in algal photosynthetic responses in summer and winter could be possible.

Given their varied photosynthetic responses when exposed to different combinations of temperature and PAR for an extended period, the Japanese *Kappaphycus* sp. exhibited marked seasonality in photosynthetic capacity. The seaweed showed inhibition of $\Phi_{PSII}$ after 6 h of continuous PAR exposure to both 300 and 1000 μmol photons $m^{-2}$ $s^{-1}$ at 18 and 28°C. The decline in $\Phi_{PSII}$ at 28°C over the 6-h period of PAR exposure was more pronounced (i.e., by 54% under 300 μmol photons $m^{-2}$ $s^{-1}$ and 36% under 1000 μmol photons $m^{-2}$ $s^{-1}$), as compared with that of PAR exposure experiments at 18°C, where $\Phi_{PSII}$ decreased approximately by 41% under 300 μmol photons $m^{-2}$ $s^{-1}$ and 31% under 1000 μmol photons $m^{-2}$ $s^{-1}$. Nevertheless, $F_v/F_m$ of seaweeds exposed to both PAR treatments at 18°C failed to recover after the 12-h dark acclimation period; while full recovery occurred at 28°C. Photoinhibition of $\Phi_{PSII}$ occurs under light exceeding their photosynthetic capacity as a regulatory mechanism to avoid photodamage (Hanelt 1996; Beer *et al.* 2004), with failure of photosynthetic recovery at sub-optimal temperatures (Roleda *et al.* 2009). The reduction in $\Phi_{PSII}$ of *Kappaphycus* sp. was due to PAR (300 or 1000 μmol photons $m^{-2}$ $s^{-1}$), which was remarkably higher than the extrapolated $E_k$ (98–192 μmol photons $m^{-2}$ $s^{-1}$). This is true, particularly for species / populations that are frequently exposed to high PAR, characterized by a decline in $\Phi_{PSII}$ at midday and a recovery phase in the afternoon, when a decrease in incident PAR to sub-inhibitory levels occurs (Figueroa *et al.* 1997; Cabello-Pasini *et al.* 2000; Terada *et al.* 2016b, c). Although in-depth studies regarding the mechanisms of photoinhibition in *Kappaphycus* sp. are needed, it is assumed that these seaweeds also have developed protective mechanisms, such as changes in *chl-a* and phycobiliproteins (Figueroa *et al.* 1997), movement of chloroplasts (Hanelt and Nultsch 1991), and synthesis of certain photoprotective substances related to the xanthophyll cycle (Schubert *et al.* 1994), so as to lessen the damaging effects of high PAR. However, the capacity of the Japanese *Kappaphycus* sp. to recover from photoinhibition was further complicated by low temperature, with post-dark acclimation $F_v/F_m$ values significantly lower than the initial. Low temperatures altered the repair of *PSII*, given that protein synthesis decreases with declining temperatures (Allakhverdiev and Murata 2004); and so prevented the seaweed's full recovery from photoinhibition. Despite the steady $F_v/F_m$ response at low temperatures and the low temperature requirement for photosynthesis of *Kappaphycus* sp. in this study, a sufficiently high ambient temperature may be necessary so that the seaweeds do not suffer from photodamage on clear, sunny days during winter.

In relation to the photosynthetic response of the Japanese *Kappaphycus* sp. to PAR, no reduction in both oxygenic evolution and quantum yield was observed up to 1000 μmol photons $m^{-2}$ $s^{-1}$. Their net photosynthesis rate at 24°C reached saturation at 140 μmol photons $m^{-2}$ $s^{-1}$ ($E_k$), which was comparable to that of the Indonesian species (Lideman *et al.* 2013; Borlongan *et al*. 2017a, b), but lower than those of Vietnamese (154 μmol photons $m^{-2}$ $s^{-1}$; Terada *et al.* 2016b) and Philippine (166 μmol photons $m^{-2}$ $s^{-1}$; Borlongan *et al.* 2016) entities. Even so, their $NP_{max}$ and $\alpha$ values matched those reported from Vietnam and Philippines; hence, they share similar photosynthetic responses to light. Japanese *Kappaphycus* sp. inhabits the upper littoral zone in reef shores, where they get exposed to direct sunlight throughout the day, with PAR levels as high as 1000 μmol photons $m^{-2}$ $s^{-1}$ on clear sunny days. Such a PAR environment is also encountered by cultivated carrageenophytes in the tropics, regardless of the farming method employed. However, *P–E* responses of *Kappaphycus* sp. may vary depending on ambient temperature, given their photochemical efficiency ($\Phi_{PSII}$, $F_v/F_m$) under prolonged PAR exposures. For example, a seasonal acclimation response, characterized by seasonal change in *P–E* parameters, enabled the temperate kelp *Ecklonia radiata* (C. Agardh) J. Agardh to remain productive and competitive throughout widely different PAR environments, varying across seasons (Fairhead and Cheshire 2004). Investigations on seasonal patterns of photosynthesis (including *P–E* experiments under low temperature conditions, and temperature acclimation experiments) and growth in the Japanese *Kappaphycus* sp. are necessary to elucidate the capacity of such native alga to maintain optimal photosynthetic performance across a range of environmental conditions. Such studies would further strengthen its observed incidence throughout the year (Terada 2012).

Nevertheless, this study revealed how temperature, rather than PAR, plays a structuring role in the distribution of species of *Kappaphycus* across latitudes. The northern distributional limit of this species endemic in Okinawa, Japan is probably set by low winter temperatures.

Furthermore, commercial cultivation of this native alga in Okinawa is possible, but will probably be futile in the northern part of Japan, due to low seawater temperatures in winter (< 18°C). It may be necessary to modify the conventional *Kappaphycus* farming techniques so as to suit the culture of this species to the subtropical waters of Japan.

# CHAPTER 4: Effects of temperature and PAR on the photosynthesis of two life history stages of *Costaria costata* and *Alaria crassifolia*

## Introduction

*Costaria costata* (C. Agardh) Saunders is a subarctic kelp species that populates the low intertidal and upper subtidal waters of the North Pacific (Druehl 1970), including the coasts of the United States (Abbott and Hollenberg 1976; Lindeberg and Lindstrom 2010), Canada (Starko and Martone 2016), Russia (Tokida 1954; Titlyanov and Titlyanov 2012), Korea (Cho 2010; Boo and Ko 2012), and Japan (Yoshida 1998; Kawashima 2012). In Japan, this species is distributed in Hokkaido Island and the Pacific coast of northern Honshu Island, which are affected by the cold *Oyashio* current (Kurile current; Kawashima 1989; Yoshida 1998; Kumura *et al.* 2006).

Likewise, *Alaria crassifolia* Kjellman is distributed in the southwestern region of Hokkaido and the Pacific coast of northern Honshu Islands, Japan. Among the five naturally-occurring species of *Alaria* in Japan, this alga is found in the lowest latitude of the northwestern Pacific (Notoya and Asuke 1984; Kawashima 1989; Yoshida *et al.* 2010). The southern limit of distribution of such subarctic kelp species in this region is perhaps due in part by seawater temperatures of over 20°C in summer (Niihara *et al*. 1987; Japan Oceanographic Data Center 2017). These species are also harvested from natural populations in Hokkaido and Aomori Prefectures for regional consumption (Niihara *et al.* 1987; Tokuda *et al.* 1987); however, production is quite limited (Kirihara 2007) due to the expansion of cultivation of *U. pinnatifida*. Cultivation trials of *C. costata* in Aomori (by the Aomori Prefectural Fisheries Research Center Aquaculture Institute; Kirihara 2007), and of *A. crassifolia* in Hakodate, Hokkaido (Fisheries Research Department, Hokkaido Research Organization, 2018) were successful; yet culture methods remain to be optimized, which requires a detailed understanding of their photobiology, especially with regards to the alternation of generations.

As in the other species of Laminariales, the life cycle of *C. costata* and *A. crassifolia* exhibits an alternation of heteromorphic stages, consisting of a macroscopic diploid sporophyte stage and a microscopic haploid gametophyte stage (Kawashima 1989; Nakahara 1993). In Japan, *C. costata* sporophytes mostly disappear from the habitat following their maturation in summer (May – August). Young sporophytes then reappear in early winter (November), growing rapidly and forming dense communities with other kelp species from spring to early summer (April to August; Kawashima 2012). As for *A. crassifolia*, maturation of zoosporangia in sporophylls in the adult (≥ 2 year-old) sporophyte was observed from late summer to early winter (August – December; Niihara *et al.* 1987). Young sporophytes emerge in early spring, and grow slowly from spring to summer of the following year as juvenile (1-year old) individuals. Growth is suppressed during the summer and early autumn, and resumes in winter. Population of this species can be found throughout the year, with steady recruitment of new individuals in the kelp community (Niihara *et al.* 1987; Nakahara 1993).

The purpose of this study was to examine the photosynthetic responses of *C. costata* and *A. crassifolia* to temperature and PAR gradients, based on $F_v/F_m$, oxygenic photosynthesis and respiration measurements. Specifically, it aimed to compare the light harvesting efficiency, in terms of $F_v/F_m$ and quantum yield of oxygen evolution ($\alpha$) in response to increasing temperature and PAR, in the two different life history stages of *C. costata* and *A. crassifolia*. The ability of these species to recover from photoinhibition after continuous exposures to different combinations of temperature and PAR was also evaluated for each stage.

## Materials and Methods

### *Collection of sporophytes*

Mature sporophytes of *C. costata* (SPO; *c.* 10 individuals on each date) were collected from a study site facing Uchiura Bay at Charatsunai Beach (old site of the Muroran Marine Station, Hokkaido University; 42°18'20" N, 140°59'20" E), Muroran City, Hokkaido Island, Japan at a depth of 3 m by SCUBA diving on 7 July 2015 for oxygen evolution and chlorophyll fluorescence measurements, and on 12 July 2016 for photoinhibition-recovery experiments.

Adult sporophytes of *A. crassifolia* (blade length: > 40 cm long; 10 individuals on each date) were also collected from the same site at a depth of 2 m on 12 July 2016 for $F_v/F_m$ and *P–T* experiments, and on 10 July 2017 for *P–E* and photoinhibition-recovery experiments. Whereas fertile sporophylls from at least ten different individuals of *A. crassifolia* were collected from another study site facing Uchiura Bay at Usujiri (Usujiri Fisheries Station, Hokkaido University; 41°56'10" N, 140°57'0" E), Hakodate City, Hokkaido Island on 13 December 2016 for sporulation and gametophyte culture.

Samples were transported to the laboratory at the Faculty of Fisheries, Kagoshima University (via Muroran Marine Station, Hokkaido University), in a cooler at 16°C, which was approximately the same temperature as *in situ* on the sampling dates.

The sporophytes were maintained for 1 to 3 days prior to photosynthesis experiments in an aquarium tank (1,500 L) at salinity of 33, pH of 8.0, seawater temperature of 16°C, and at PAR of 200 μmol photons $m^{-2}$ $s^{-1}$ (14:10 h light: dark cycle). Moderate aeration (*c.* 2.0 L $min^{-1}$) was also provided to maintain saturated conditions of dissolved oxygen.

### *Isolation and cultivation of gametophytes from zoospores*

Gametophytes (GAM) of *C. costata* and *A. crassifolia* were isolated from spores using the procedure from Watanabe *et al.* (2014b) with few modifications. Sori from mature sporophylls were cut, rinsed with sterile natural seawater, wiped with tissue paper, and stored overnight in a dark moist chamber at 10°C. Zoospores were released by immersing the sporophylls in sterile natural seawater at room temperature (20°C) for 30 min. Zoospore suspensions were then inoculated in 9 cm diameter Petri dishes with *c.* 20 mL Provasoli's enriched seawater with iodine (PESI; Tatewaki 1966), and incubated under the following culture conditions: 12°C, 30 μmol photons $m^{-2}$ $s^{-1}$, and 12:12 h (L: D) photoperiod. After 3 weeks of culture, male and female gametophytes showed clear sexual dimorphism; they were then separated with a Pasteur pipette, using an optical microscope (SMZ1500; Nikon, Tokyo, Japan). This prevented the mature female gametophytes from getting fertilized. Male and female gametophytes were maintained in separate cultures for 24–28 additional weeks; during which they form 2–3-mm hemiglobular tufts of filaments at the bottom of the Petri dish. The culture medium was changed every two weeks. Given the long culture period of the gametophytes, photosynthesis experiments were carried out later (*c.* 28 weeks) than for the sporophytes. Male and female gametophyte cultures were pooled on the day of photosynthesis experiments to obtain the appropriate replicate requirements.

### *Effect of temperature on photosynthesis and respiration*

*C. costata* SPO (0.99 ± 0.09 $g_{fw}$) and GAM (0.13 ± 0.02 $g_{fw}$) were examined under eight temperature treatments (8, 12, 16, 20, 24, 28, 32, and 36°C), at PAR of 500 μmol photons $m^{-2}$ $s^{-1}$ for SPO, and 100 μmol photons $m^{-2}$ $s^{-1}$ for GAM, respectively. Such PAR treatments were assigned based on their respective saturation PAR ($E_k$) estimated from $P$–$E$ curves.

*A. crassifolia* SPO and GAM were subjected to the same temperature treatments, at PAR of 200 μmol photons $m^{-2}$ $s^{-1}$. Approximately 0.60 ± 0.19 $g_{fw}$ of sporophyte blades (from the 10 collected individuals), and 0.06 ± 0.01 $g_{fw}$ of gametophytes were used for each temperature treatment ($n$ = 5). Methods for the *P–T* experiment were described in detail in chapter 2.

### *Effect of PAR on oxygenic photosynthesis*

*P–E* experiments on *C. costata* SPO and GAM were carried out under nine PAR treatments similar to those described in chapter 2, at a fixed temperature based on their respective pre-incubation temperatures (i.e., 16°C for SPO and 12°C for GAM). *C. costata* SPO and GAM were approximately 1.01 ± 0.10 and 0.09 ± 0.02 $g_{fw}$, respectively.

As for *A. crassifolia*, *P–E* experiments were conducted at 8, 16, and 20°C, respectively. The three temperature treatments were assigned based on the mean seawater temperatures near the collection site (Muroran / Hakodate) in early winter (December – January), in the dominant season of the seaweed (June – July), and in summer (August – September; Niihara *et al.* 1987; Japan Oceanographic Data Center 2017). Randomly selected sections (*c.* 2 cm long, 1 cm wide) of sporophyte blades (from the 10 collected individuals) and tufts of gametophytes were approximately 0.14 ± 0.02 and 0.05 ± 0.01 $g_{fw}$, respectively. Prior to the experiment, samples were acclimated overnight (12 h) with sterile natural seawater in the incubator at each temperature treatment.

### *Effect of temperature on chlorophyll fluorescence*

The $F_v/F_m$ of both life history stages of *C. costata* and *A. crassifolia* were measured at various temperatures between 8 and 36°C in 2°C intervals, with a red measuring light version (at 650 nm) of Maxi Imaging-PAM (Heinz Walz GmbH, Effeltrich, Germany), following the methods described in chapter 2. Randomly selected sections (*c.* 2 cm long, 1 cm wide; $n$ = 10) of sporophyte blades and tufts of gametophyte filaments on culture plates ($n$ = 10) were subjected to each experimental temperature.

***Photoinhibition-recovery experiments***

The effects of continuous PAR exposures on the quantum yields of *C. costata* SPO and GAM was investigated under two PAR levels (100 and 1000 μmol photons $m^{-2}$ $s^{-1}$) at 12°C. Whereas those of *A. crassifolia* SPO and GAM were studied at two PAR levels (200 and 1000 μmol photons $m^{-2}$ $s^{-1}$), and at two temperatures (8 and 20°C).

Sections (*c.* 2 cm long, 1 cm wide) of sporophyte blades and tufts of gametophytes were prepared to provide 10 replicates for each PAR–temperature treatment group. Samples were initially incubated at each temperature condition overnight (12 h) in the dark prior to photoinhibition-recovery experiments. Continuous PAR exposures were carried out for 6 h, with measurement of $\Phi_{PSII}$ ($n$ = 10) every hour. After which, samples were once again placed under dark conditions at their respective temperatures for 12 h in *C. costata*, and for 6 h in *A. crassifolia*; and their final $F_v/F_m$ were measured to assess photosynthetic recovery. Temperature and PAR controls used were the same as described in chapters 2 and 3.

***Statistical analyses and model fittings***

Model fittings and determination of parameters for *GP*– and $F_v/F_m$–temperature, and *P–E* models of *C. costata* and *A. crassifolia* were carried out using a Bayesian approach, with appropriate prior probability distributions assigned to the parameters. Model equations used for the respective photosynthesis response models were described in chapter 2.

A one-way ANOVA was used to examine if continuous PAR exposures affected $\Phi_{PSII}$ for each PAR–temperature treatment. Time was considered a factor with levels: 0, 6 and 12 h (for *A. crassifolia*) or 18 h (for *C. costata*) after the start of the experiment (i.e., initial $F_v/F_m$, $\Phi_{PSII}$ after 6 h, and the final $F_v/F_m$ after 6 or 12 h of darkness).

Statistical analyses were done using *R* version 3.3.3 (R Development Core Team 2017) and model fittings were carried out using rstan version 2.17.3 (Stan Development Team 2017).

## Results

### *Effect of temperature on photosynthesis and dark respiration rates*

*NP* rates of *C. costata* SPO and GAM were stable at low temperatures, with a slight increase up to 24°C, and a decrease thereafter (Fig. 11a). Their respiration rates increased from 0.9 µg $O_2$ $g_{fw}^{-1}$ $min^{-1}$ (0.6–1.4, 95% BPI) at 8°C to 4.7 µg $O_2$ $g_{fw}^{-1}$ $min^{-1}$ (2.9–7.4, 95% BPI) at 36°C for SPO, and from 0.2 µg $O_2$ $g_{fw}^{-1}$ $min^{-1}$ (0.04–0.5, 95% BPI) to 7.7 µg $O_2$ $g_{fw}^{-1}$ $min^{-1}$ (1.8–22.0, 95% BPI) for GAM ((Fig. 11c), respectively. Maximum gross photosynthetic rate ($GP_{max}$) of SPO was estimated to be 8.8 µg $O_2$ $g_{fw}^{-1}$ $min^{-1}$ at 22.1°C ($T_{opt}$; Fig. 11e). Whereas for GAM, $GP_{max}$ was 3.6 µg $O_2$ $g_{fw}^{-1}$ $min^{-1}$, which occurred at 21.7°C.

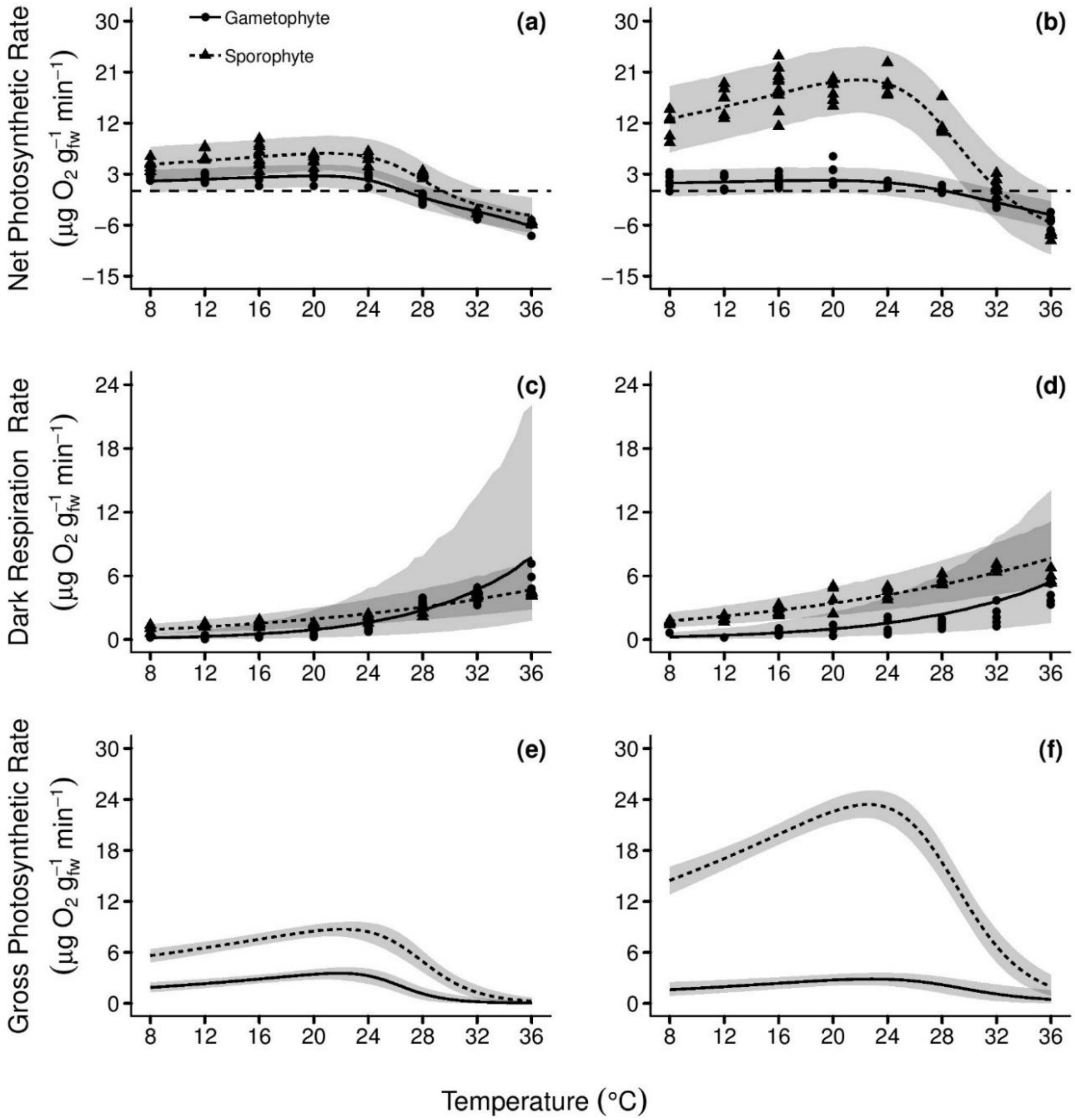


**Fig. 11** The response of the oxygenic photosynthesis and dark respiration to temperature of *Costaria costata* (a, c, e) and *Alaria crassifolia* (b, d, f). (a, b) The net photosynthesis to temperature determined at 500 μmol photons $m^{-2}\ s^{-1}$ for *C. costata* sporophyte (SPO), at 100 μmol photons $m^{-2}\ s^{-1}$ for *C. costata* gametophyte (GAM), and at 200 μmol photons $m^{-2}\ s^{-1}$ for *A. crassifolia* SPO and GAM. (c, d) The dark respiration rate to temperature at 0 μmol photons $m^{-2}\ s^{-1}$. (e, f) The modeled gross photosynthetic rates. Data were derived from the model curve of net photosynthesis (a, b) and dark respiration (c, d). The symbols indicate the measured rates ($n$ = 5), the lines indicate the expected value, and the shaded regions indicate the 95% BPI of the model.

As for *A. crassifolia*, *NP* rates of SPO increased from 12.7 μg $O_2$ $g_{fw}^{-1}$ $min^{-1}$ (6.8–18.5, 95% BPI) at 8°C to 18.9 μg $O_2$ $g_{fw}^{-1}$ $min^{-1}$ (13.0–24.7, 95% BPI) at 24°C, then decreased to -5.6 μg $O_2$ $g_{fw}^{-1}$ $min^{-1}$ (-11.1–0.02, 95% BPI) at 36°C (Fig. 11b). *NP* rates of GAM were stable between 8 and 16°C, slightly increased at 20°C, and gradually decreased at higher temperatures. Respiration rates increased from 1.8 μg $O_2$ $g_{fw}^{-1}$ $min^{-1}$ (1.2–2.5, 95% BPI) at 8°C to 7.7 μg $O_2$ $g_{fw}^{-1}$ $min^{-1}$ (5.2–11.1, 95% BPI) at 36°C for SPO, and from 0.3 μg $O_2$ $g_{fw}^{-1}$ $min^{-1}$ (0.1–0.7, 95% BPI) to 5.5 μg $O_2$ $g_{fw}^{-1}$ $min^{-1}$ (1.6–14.0, 95% BPI) for GAM, respectively (Fig. 11d). Their $GP_{max}$ (23.5 μg $O_2$ $g_{fw}^{-1}$ $min^{-1}$ for SPO and 3.0 μg $O_2$ $g_{fw}^{-1}$ $min^{-1}$ for GAM) occurred at 22.6 and 22.7°C, respectively ($T_{opt}$; Fig. 11f). Other model parameter estimates are presented in Table 7.

**Table 7** Mean and 95% BPI of the parameters estimated for the gross photosynthesis–temperature model in *Costaria costata* and *Alaria crassifolia* sporophyte (SPO) and gametophyte (GAM)

| | ***Costaria costata*** | | | | ***Alaria crassifolia*** | | | |
|---|---|---|---|---|---|---|---|---|
| | **SPO** | | **GAM** | | **SPO** | | **GAM** | |
| **Parameter** | **Mean** | **95% BPI** | **Mean** | **95% BPI** | **Mean** | **95% BPI** | **Mean** | **95% BPI** |
| $GP_{max}$ | 8.8 | 8.0 – 9.7 | 3.6 | 3.0 – 4.3 | 23.5 | 22.0 – 25.1 | 3.0 | 2.3 – 3.7 |
| $H_a$ | 26 | 18 – 35 | 37 | 22 – 56 | 28 | 20 – 38 | 37 | 16 – 68 |
| $H_d$ | 377 | 260 – 516 | 468 | 245 – 712 | 308 | 236 – 388 | 284 | 111 – 506 |
| $T_{opt}$ | 22.1 | 20.1 – 23.8 | 21.7 | 18.8 – 23.7 | 22.6 | 21.2 – 23.8 | 22.7 | 16.9 – 26.8 |
| $E_a$ | 41 | 36 – 47 | 99 | 89 – 110 | 38 | 33 – 42 | 79 | 64 – 95 |
| $R_{22}$ | 2.1 | 2.0 – 2.3 | 1.0 | 0.9 – 1.2 | 3.7 | 3.6 – 4.0 | 1.1 | 0.9 – 1.3 |

$GP_{max}$, maximum gross photosynthesis (μg $O_2$ $g_{fw}^{-1}$ $min^{-1}$); $H_a$, activation energy for photosynthesis (kJ $mol^{-1}$); $H_d$, deactivation energy (kJ mol−1); $E_a$, activation energy for respiration (kJ $mol^{-1}$); $R_{22}$, respiration rate at median temperature (μg $O_2$ $g_{fw}^{-1}$ $min^{-1}$); $T_{opt}$, optimum temperature (°C)

***Effect of PAR on the net photosynthesis of C. costata***

*P–E* curves in the two life history stages of *C. costata* differed (Fig. 12). The rise in *NP* rates of SPO at 16°C was gradual, from -0.2 µg $O_2$ $g_{fw}^{-1}$ $min^{-1}$ [-2.3–1.8, 95% BPI] at 0 µmol photons $m^{-2}$ $s^{-1}$ to 6.3 µg $O_2$ $g_{fw}^{-1}$ $min^{-1}$ (4.1–8.5, 95% BPI) at 1000 µmol photons $m^{-2}$ $s^{-1}$ (Fig. 12a). In GAM, *NP* rates at 12°C quickly increased from -0.1 (-3.1–2.8, 95% BPI) to 6.0 µg $O_2$ $g_{fw}^{-1}$ $min^{-1}$ (2.9–8.9, 95% BPI) at 1000 µmol photons $m^{-2}$ $s^{-1}$ (Fig. 12b). Thus, the initial slope ($\alpha$) of GAM (0.14 µg $O_2$ $g_{fw}^{-1}$ $min^{-1}$ (µmol photons $m^{-2}$ $s^{-1}$) $^{-1}$) was higher than that of SPO (0.03 µg $O_2$ $g_{fw}^{-1}$ $min^{-1}$ (µmol photons $m^{-2}$ $s^{-1}$) $^{-1}$. Whereas their $NP_{max}$ rates were similar (i.e., 6.7 µg $O_2$ $g_{fw}^{-1}$ $min^{-1}$ for SPO and 6.1 µg $O_2$ $g_{fw}^{-1}$ $min^{-1}$ for GAM). In effect, SPO had higher $E_c$ and $E_k$ than GAM. Other model parameter estimates are presented in Table 8.

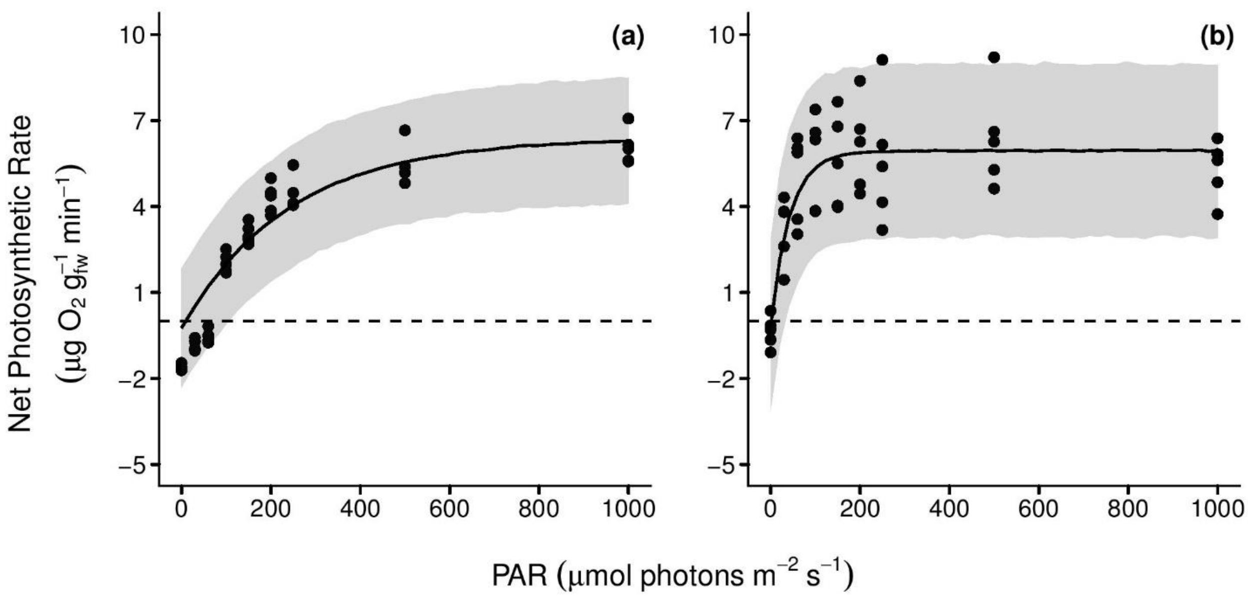


**Fig. 12** The response of the net photosynthetic rates of *C. costata* SPO (a) and GAM (b) to increasing PAR. Net photosynthesis measurements were carried out 16°C for SPO, and at 12°C for GAM, respectively. The dots indicate the measured rates ($n$ = 5), the lines indicate the expected value, and the shaded regions indicate the 95% BPI of the model.

**Table 8** Mean and 95% BPI of *P–E* parameters of *C. costata* SPO at 16°C, and GAM at 12°C

| | SPO | | GAM | |
|---|---|---|---|---|
| **Parameter** | **Mean** | **95% BPI** | **Mean** | **95% BPI** |
| $NP_{max}$ | 6.7 | 5.8 – 7.6 | 6.1 | 5.5 – 6.7 |
| $\alpha$ | 0.03 | 0.02 – 0.03 | 0.14 | 0.10 – 0.19 |
| $R_d$ | 0.3 | 0.1 – 0.4 | 0.1 | 0.01 – 0.3 |
| $E_c$ | 9 | 3 – 16 | 1 | 0 – 2 |
| $E_k$ | 243 | 180 – 326 | 44 | 30 – 63 |

$NP_{max}$, maximum net photosynthesis (μg $O_2$ $g_{fw}^{-1}$ $min^{-1}$); $R_d$, respiration rate (μg $O_2$ $g_{fw}^{-1}$ $min^{-1}$); $\alpha$, initial slope [μg $O_2$ $g_{fw}^{-1}$ $min^{-1}$ (μmol photons $m^{-2}$ $s^{-1}$)$^{-1}$]; $E_c$, compensation PAR (μmol photons $m^{-2}$ $s^{-1}$); $E_k$, saturation PAR (μmol photons $m^{-2}$ $s^{-1}$)

### *Effect of PAR on the net photosynthesis of A. crassifolia at three different temperatures*

*P–E* curves at 8, 16, and 20°C in the two life history stages of *A. crassifolia* showed increases in *NP* rates as PAR levels rise until saturation, with no indication of photoinhibition up to 1000 μmol photons $m^{-2}$ $s^{-1}$ (Fig. 13). *NP* rates of SPO were consistently higher than those of GAM on all temperature treatments. Measured *NP* rates of GAM were also widely spread out (Fig. 13b, d, f), which may have limited the robustness of the best fit.

Nonetheless, the parameter estimates derived from each *P–E* curve are shown in Table 9. The $NP_{max}$ of SPO at 8, 16 and 20°C were 24.6, 40.9 and 43.9 μg $O_2$ $g_{fw}^{-1}$ $min^{-1}$, respectively. Whereas for the gametophyte, $NP_{max}$ at the same order of temperature were 3.6, 7.7 and 4.5 μg $O_2$ $g_{fw}^{-1}$ $min^{-1}$. Initial slopes ($\alpha$) of the curve of SPO were similar among temperature treatments, which likewise fall within the 95% BPI for $\alpha$ of GAM. In effect, SPO had higher $E_c$ and $E_k$ than GAM.

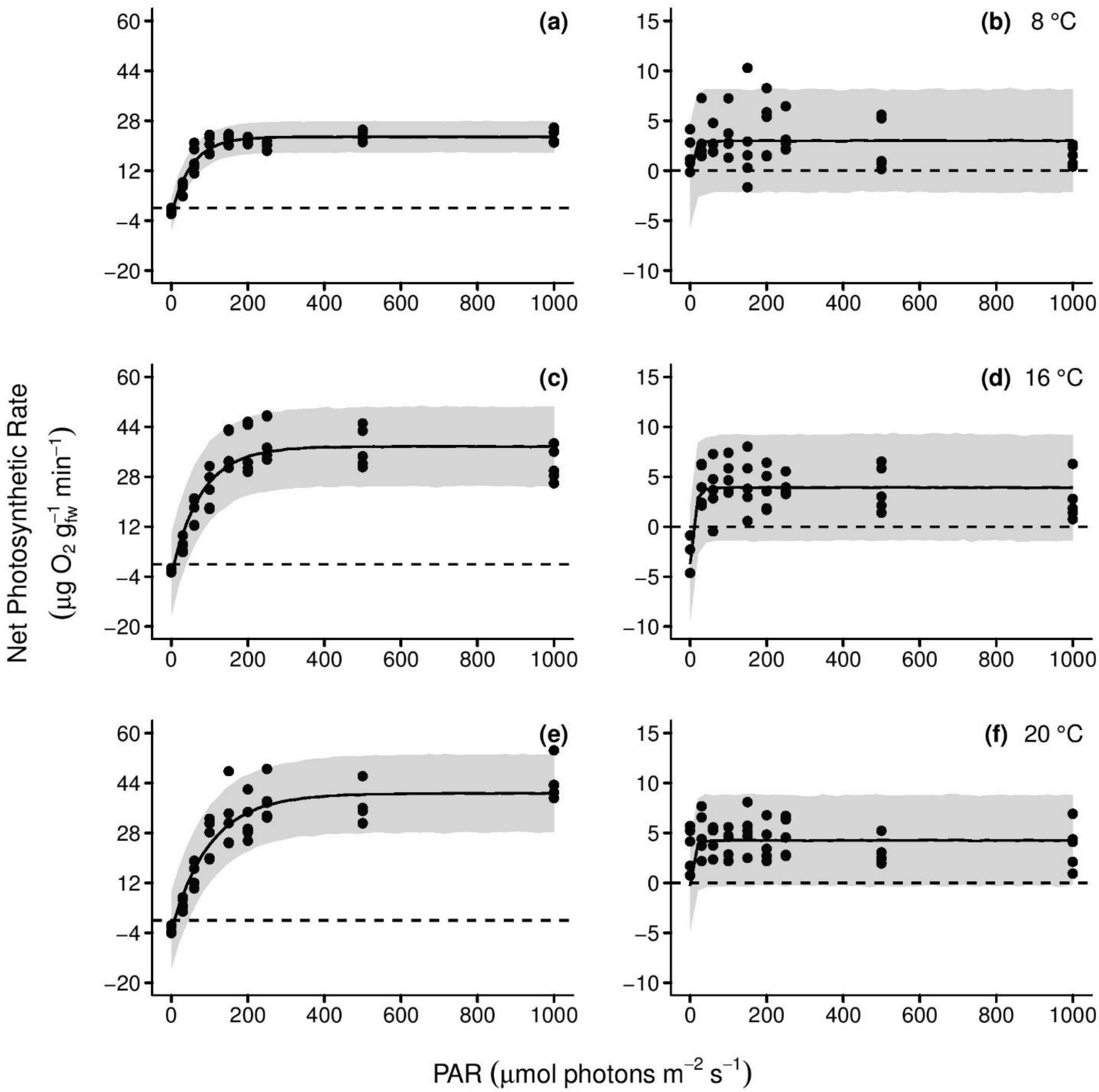


**Fig. 13** The response of the net photosynthetic rates of *A. crassifolia* SPO (a, c, e) and GAM (b, d, f) to increasing PAR at 8°C (a, b), 16°C (c, d), and 20°C (e, f). The dots indicate the measured rates ($n$ = 5), the lines indicate the expected value, and the shaded regions indicate the 95% BPI of the model.

**Table 9** Mean and 95% BPI of *P–E* parameters of *A. crassifolia* SPO and GAM at 8, 16, and 20°C

| | **SPO** | | | | | | **GAM** | | | | | |
|---|---|---|---|---|---|---|---|---|---|---|---|---|
| | **8°C** | | **16°C** | | **20°C** | | **8°C** | | **16°C** | | **20°C** | |
| **Parameter** | **Mean** | **95% BPI** | **Mean** | **95% BPI** | **Mean** | **95% BPI** | **Mean** | **95% BPI** | **Mean** | **95% BPI** | **Mean** | **95% BPI** |
| $NP_{max}$ | 24.6 | 22.8 – 26.5 | 40.9 | 36.9 – 45.0 | 43.9 | 39.6 – 48.2 | 3.6 | 2.5 – 5.0 | 7.7 | 5.5 – 9.8 | 4.5 | 3.7 – 5.5 |
| $\alpha$ | 0.5 | 0.4 – 0.6 | 0.5 | 0.4 – 0.7 | 0.4 | 0.3 – 0.6 | 0.7 | 0.1 – 1.6 | 0.9 | 0.4 – 1.6 | 0.8 | 0.2 – 1.6 |
| $R_d$ | 1.8 | 0.2 – 3.5 | 3.2 | 0.5 – 6.1 | 3.1 | 0.6 – 6.1 | 0.6 | 0 – 1.7 | 3.7 | 1.8 – 5.7 | 0.3 | 0 – 1.0 |
| $E_c$ | 4 | 1 – 7 | 6 | 1 – 11 | 7 | 1 – 14 | 1 | 0 – 6 | 7 | 2 – 14 | 0 | 0 – 2 |
| $E_k$ | 53 | 44 – 64 | 79 | 61 – 99 | 103 | 78 – 132 | 8 | 2 – 26 | 10 | 4 – 21 | 7 | 3 – 19 |

$NP_{max}$, maximum net photosynthesis (µg $O_2$ $g_{fw}^{-1}$ $min^{-1}$); $R_d$, respiration rate (µg $O_2$ $g_{fw}^{-1}$ $min^{-1}$); $\alpha$, initial slope [µg $O_2$ $g_{fw}^{-1}$ $min^{-1}$ (µmol photons $m^{-2}$ $s^{-1}$)$^{-1}$]; $E_c$, compensation PAR (µmol photons $m^{-2}$ $s^{-1}$); $E_k$, saturation PAR (µmol photons $m^{-2}$ $s^{-1}$)

### ***Effect of temperature on the maximum quantum yield ($F_v/F_m$)***

The $F_v/F_m$ responses to temperature of the two life history stages of *C. costata* and *A. crassifolia* were relatively stable at low temperatures, but decreased with rising temperature (Fig. 14). Parameter estimates indicated the maximum $F_v/F_m$ of *C. costata* SPO and GAM to be 0.73 and 0.69, which occurred at 14.9 and 14.0°C, respectively ($T_{opt}$; Table 10). As for *A. crassifolia*, maximum $F_v/F_m$ of SPO (0.71) occurred at 20.1°C, while that of GAM (0.51) occurred at 15.8°C. Other model parameter estimates are presented in Table 10.

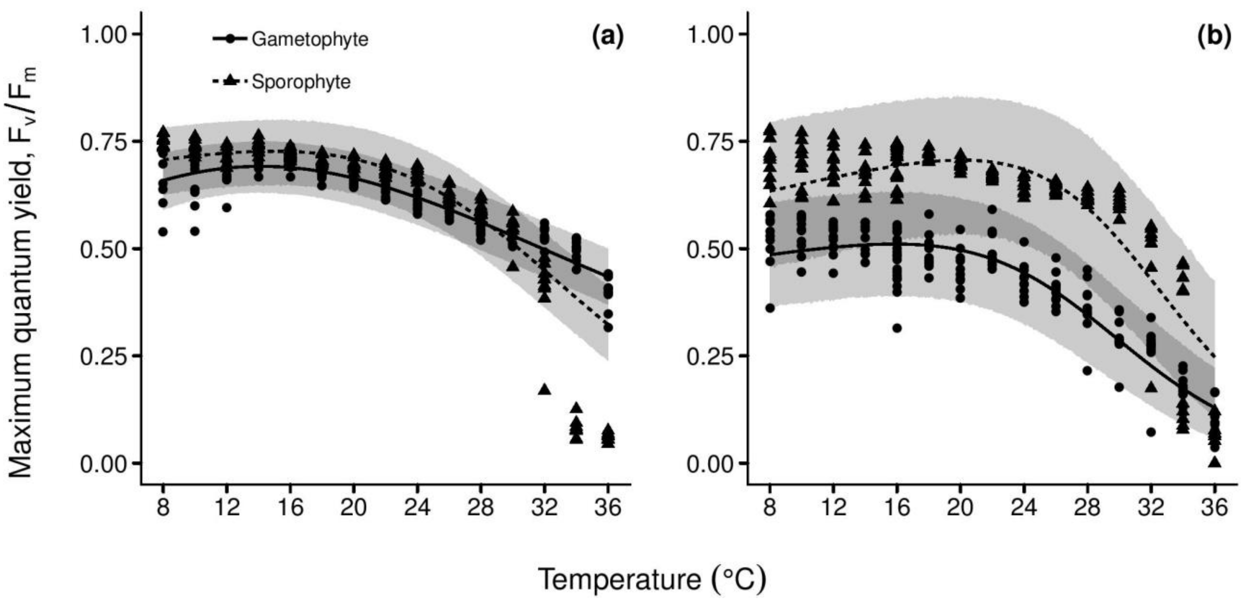


**Fig. 14** The temperature response of $F_v/F_m$ in the two life history stages of *C. costata* (a) and *A. crassifolia* (b). The symbols indicate the measured values ($n$ = 10), the lines indicate the expected value, and the shaded regions indicate the 95% BPI of the model.

**Table 10** Mean and 95% BPI of the parameters estimated for the $F_v/F_m$–temperature model in the two life history stages of *C. costata* and *A. crassifolia*

| | ***Costaria costata*** | | | | ***Alaria crassifolia*** | | | |
|---|---|---|---|---|---|---|---|---|
| | **SPO** | | **GAM** | | **SPO** | | **GAM** | |
| **Parameter** | **Mean** | **95% BPI** | **Mean** | **95% BPI** | **Mean** | **95% BPI** | **Mean** | **95% BPI** |
| $F_v/F_{m\ (max)}$ | 0.73 | 0.72 – 0.74 | 0.69 | 0.68 – 0.70 | 0.71 | 0.69 – 0.73 | 0.51 | 0.50 – 0.53 |
| $H_a$ | 6 | 4 – 10 | 33 | 9 – 73 | 9 | 6 – 12 | 8 | 6 – 12 |
| $H_d$ | 124 | 102 – 146 | 73 | 63 – 98 | 190 | 147 – 238 | 163 | 141 – 186 |
| $T_{opt}$ | 14.9 | 13.5 – 16.2 | 14.0 | 12.2 – 15.1 | 20.1 | 18.2 – 21.8 | 15.8 | 14.0 – 17.5 |

***Effect of continuous PAR exposures on quantum yields ($F_v/F_m$, $\Phi_{PSII}$) of C. costata***

Quantum yields of *C. costata* SPO and GAM for up to 6 h of exposure to low (100 μmol photons $m^{-2}$ $s^{-1}$) and high PAR (1000 μmol photons $m^{-2}$ $s^{-1}$) showed decreasing $\Phi_{PSII}$ at 12°C (Fig. 15). From initial $F_v/F_m$ of 0.69, $\Phi_{PSII}$ of SPO exposed to low and high PAR significantly declined ($P <$ 0.01) to 0.61 and 0.28, respectively (Fig. 15a). As for GAM, its quantum yields decreased ($P <$ 0.01) from initial $F_v/F_m$ of 0.65 to 0.36 (under low PAR) and 0.12 (under high PAR; Fig. 15b). Analysis of variance within each life history stage showed PAR-dependent recovery from photoinhibition of quantum yields. The final $F_v/F_m$ after 12 h of dark acclimation were restored to 0.67 for SPO under low PAR ($P$ = 0.428); while that of SPO under high PAR increased to 0.51, and yet was significantly different ($P$ < 0.01) from its value before PAR exposure. Post-dark acclimation $F_v/F_m$ of low (0.62) and high PAR-treated (0.37) GAM were likewise significantly different ($P$ < 0.1) from their respective initial values.

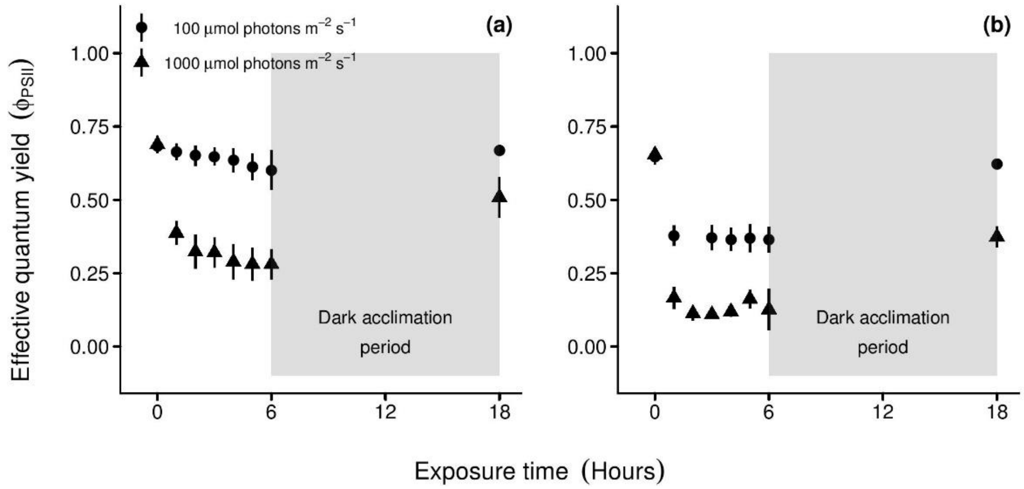


**Fig. 15** The hourly response of the effective quantum yields ($\Phi_{PSII}$) in *C. costata* SPO (a) and GAM (b) to low (100 µmol photons m$^{-2}$ s$^{-1}$, circle) and high (1000 µmol photons m$^{-2}$ s$^{-1}$, triangle) PAR at 12°C. The symbols indicate the mean of actual values measured ($n$ = 10), and bars indicate one standard deviation. Initial values and the values after 12-h dark acclimation were measured as $F_v/F_m$.

***Combined effects of temperature and PAR on the PSII quantum yields of A. crassifolia, and their potential of recovery***

Responses of the $\Phi_{PSII}$ in the two life history stages of *A. crassifolia* over the 6-h exposures to low (200 µmol photons m$^{-2}$ s$^{-1}$) and high (1,000 µmol photons m$^{-2}$ s$^{-1}$) PAR at 8 and 20°C were similar, with apparent drops from their initial $F_v/F_m$ (Fig. 16). However, recovery of their $F_v/F_m$ after a 6-hour dark acclimation phase were different from each PAR–temperature treatment.

At 8°C, quantum yields of SPO after 6 h of exposure to low and high PAR significantly decreased ($P < 0.01$) from initial $F_v/F_m$ of 0.75 to $\Phi_{PSII}$ of 0.57 and 0.26, respectively (Fig. 16a). As for GAM, its quantum yields decreased ($P < 0.01$) from 0.43 to 0.16 under low PAR, and from 0.49 to 0.08 under high PAR (Fig. 16b). Despite the rise in their respective post-dark acclimation $F_v/F_m$, values were still significantly different ($P < 0.01$) from initial (Fig. 16a, b).

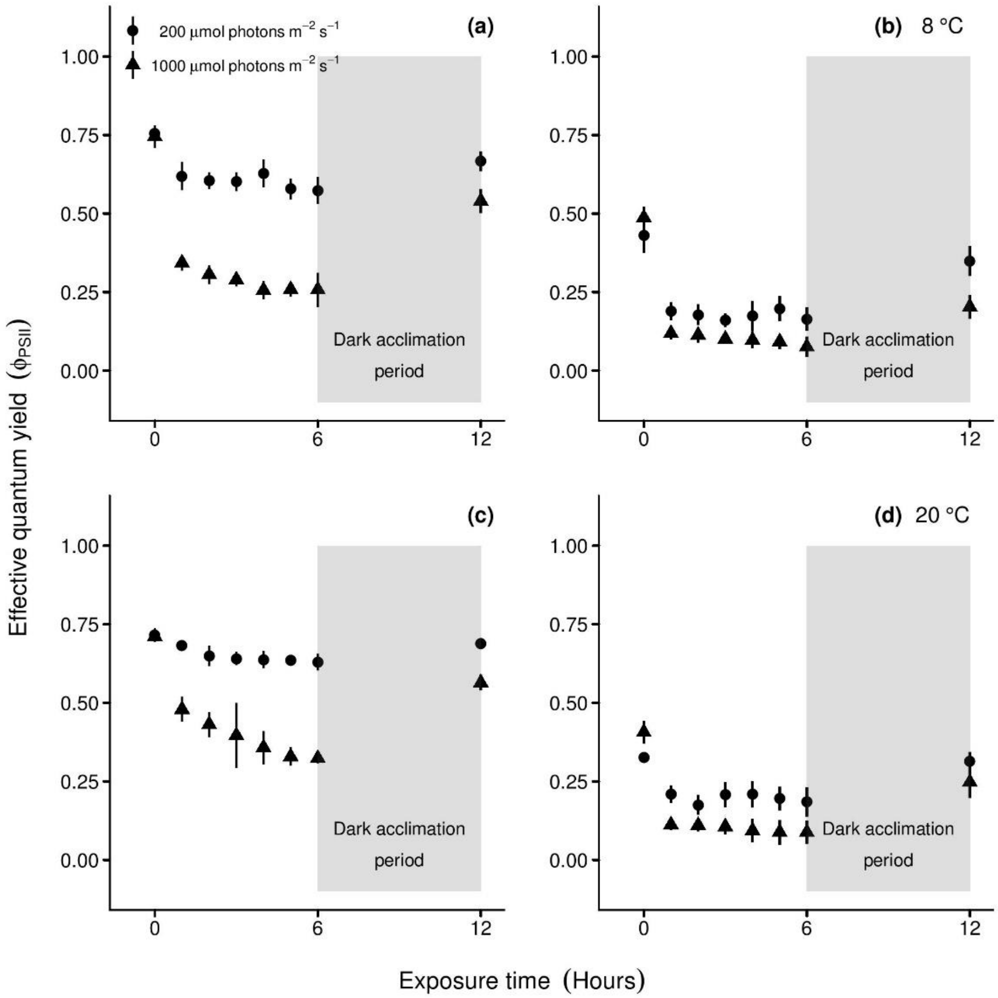


**Fig. 16** Chronological change of the *PSII* quantum yields of *A. crassifolia* SPO (a, c) and GAM (b, d) at 8°C (a, b) and 20°C (c, d). Measurements were carried out from the initial state (under dark condition, $F_v/F_m$) up to 6 h ($\Phi_{PSII}$) of continuous exposure to low (200 µmol photons m$^{-2}$ s$^{-1}$, circle) and high (1000 µmol photons m$^{-2}$ s$^{-1}$, triangle) PAR. Recovery in $F_v/F_m$ were also measured after 6 h of dark acclimation.

At 20°C, $\Phi_{PSII}$ of SPO declined ($P < 0.01$) from initial $F_v/F_m$ of 0.71 to $\Phi_{PSII}$ of 0.63 under low PAR, and 0.32 under high PAR (Fig. 16c). $\Phi_{PSII}$ of GAM under low and high PAR also decreased from 0.33 to 0.18, and 0.41 to 0.09, respectively (Fig. 16d). After overnight dark acclimation, only $F_v/F_m$ of GAM exposed to low PAR were restored to initial values ($P = 0.23$; Fig. 16d).

## Discussion

Photosynthetic characteristics of both *C. costata* and *A. crassifolia* varied in the two life history stages, with PAR as the principal environmental factor. The differential *P–E* curves, particularly the higher *NP* rates, $E_c$ and $E_k$ of the sporophyte as compared to the gametophyte, revealed the higher photosynthetic activity and adaptation to high PAR of the macroscopic stage. The difference in photosynthetic responses between the two life stages is related to the differences in their morphology and PAR exposures within the subtidal zone (Reed and Foster 1984; Hanelt *et al.* 1997). The lower $E_k$ of the gametophyte reflects shade adaptation compared to the adult stage, and is probably related to the chlorophyll antenna size and the number of chloroplasts present in the microscopic stage (Roleda *et al.* 2009). Mature sporophytes have fully-developed thalli and long blades that get exposed to higher light regimes than the early life history stages that settle on shaded crevices under algal canopies.

The compensation PAR for photosynthesis of *C. costata* and *A. crassifolia* sporophyte is minimal ($E_c$ = 4–9 μmol photons $m^{-2}$ $s^{-1}$), which agrees with the minimum PAR requirement of kelp species (i.e., 0.81 mol photons $m^{-2}$ $d^{-1}$ or ~9.38 μmol photons $m^{-2}$ $s^{-1}$; Gattuso *et al.* 2006). Saturation PAR of *A. crassifolia* SPO at 8–20°C ($E_k$ = 53–103 μmol photons $m^{-2}$ $s^{-1}$) could also be considered low and typical for shade-adapted plants (Germann 1989; Spalding *et al.* 2003). However, $E_k$ of *C. costata* SPO at 16°C (i.e., 243 μmol photons $m^{-2}$ $s^{-1}$) was higher than that of *A. crassifolia* and other subtidal species (Serisawa *et al*. 2001; Watanabe *et al*. 2014a; Terada *et al*. 2016a), owing to its low $NP_{max}$ and *α*. *C. costata* GAM also had higher $E_k$ (44 μmol photons $m^{-2}$ $s^{-1}$) than *A. crassifolia* GAM (i.e., 7–10 μmol photons $m^{-2}$ $s^{-1}$). *P–E* responses of kelps may vary depending on ambient temperature, as observed in *Ecklonia cava* Kjellman (Serisawa *et al*. 2001) and *Ecklonia radiata* (C. Agardh) J. Agardh (Fairhead and Cheshire 2004) that exhibited seasonal acclimation responses (i.e., seasonal change in *P–E* parameters). Such variations are the result of processes that are involved in the photoacclimation and thermal acclimation of the photosynthetic apparatus (Falkowski and Raven 2007). The increase in nutrient levels in the water column during winter may also enhance the photosynthetic capacity of seaweeds. Kelps accumulate nitrogen reserves during winter, as higher nitrogen levels are often correlated with the lowest temperatures, to maintain growth during nutrient limitation in summer (Kerrison *et al.* 2015). More detailed studies are yet to be done, including the effect of nutrient levels on the seasonal photosynthesis of these two kelp species under *in situ* PAR and temperature conditions.

The *P–E* curves also showed no significant reduction in oxygenic evolution and quantum yield up to 1000 μmol photons $m^{-2}$ $s^{-1}$ for both life stages of *C. costata* and *A. crassifolia*. However, time-series measurements of $\Phi_{PSII}$ revealed PAR dose-dependent (as a function of exposure time) photoinhibition of *C. costata* and *A. crassifolia*, with more pronounced declines at high PAR (54–81% for SPO; 78–84% for GAM) than at low PAR (12–24% for SPO; 43–62% for GAM). Previous studies also showed PAR and/ or UVR dose-dependent decrease in the *PSII* photochemical efficiency of seaweeds (Roleda *et al.* 2010; Borlongan *et al.* 2017b, c; Terada *et al.* 2018), with greater reductions in optimum quantum yields on vegetative tissues of *Saccharina latissima* (Linnaeus) Lane *et al.* [as *Laminaria saccharina* (Linnaeus) Lamouroux] under PAR (20 μmol photons $m^{-2}$ $s^{-1}$) and PAR + UVR treatments (Holzinger *et al.* 2011). Sensitivity to photoinhibition also differed between the two stages, where the gametophyte expressed greater declines in $\Phi_{PSII}$ (43–84%). Such down regulation of photosynthetic activity may suggest an activated photoprotective mechanism, known as dynamic photoinhibition (Hanelt *et al.* 1997; Beer *et al.* 2014). This transient phenomenon has been described *in situ* in several seaweeds, with depression in *PSII* quantum yields following high PAR exposures, and a quick reversal of the process as PAR levels decrease (Delebecq *et al*. 2011; Terada *et al*. 2016a, b, 2018). Among brown algae, such photoprotective process involves the xanthophyll cycle through the completely reversible enzymatic-mediated conversion of violaxanthin into antheraxanthin and zeaxanthin in the light harvesting complex of *PSII* (Gévaert *et al.* 2002; Delebecq *et al.* 2011). However, despite the increase in post-dark acclimation $F_v/F_m$ of *C. costata* and *A. crassifolia* previously exposed to 1000 μmol photons m$^{-2}$ s$^{-1}$ (by 43–66% for SPO; 63–81% for GAM), values were still significantly different from their initial. Therefore, full recovery of photosynthesis for these samples has not been reached, indicative of chronic photoinhibition (Beer *et al.* 2014). Maximum incident PAR on the kelp community [*Saccharina longissima* (Miyabe) Lane *et al*.; as *Laminaria longissima* Miyabe] at 3-m depth in the eastern part of Hokkaido Island was about 207–467 μmol photons m$^{-2}$ s$^{-1}$ (Sakanishi and Iizumi 2001). Meanwhile, incident PAR on the community floor, where the gametophytes are settled, and which often fluctuates by shading of dense sporophytes and continuous wave motion, was close to 0 μmol photons m$^{-2}$ s$^{-1}$. While photoinhibition will probably not occur on the microscopic stage in their habitat, the sporophytes may be more at risk due to high PAR exposures in the field. Indeed, post-dark acclimation $F_v/F_m$ of *A. crassifolia* SPO failed to recover from chronic photoinhibition following exposure to low PAR (200 μmol photons m$^{-2}$ s$^{-1}$) at 8°C, suggesting the possibility of the seaweed to suffer from photodamage during winter. Low temperature limitation of enzymes for repair of *PSII* (Allakhverdiev and Murata 2004) may have led to such results, as also observed in *S. latissima* that had higher recovery rates at 18–22°C than at 12°C (Bruhn and Gerard 1996). Low seawater temperatures during winter (8°C in January as opposed to 14°C in May) slowed the xanthophyll cycle in *S. latissima*, resulting in its weak recovery (Gévaert *et al.* 2002). Also in Arctic *S. latissima*, UV damage of the photosynthetic $D_1$ protein was less severe at 12°C than at 2°C (Heinrich *et al.* 2015), suggesting that increased temperature could also mitigate the damaging effects of UVR, thus improving their tolerance (Navarro *et al.* 2016). Full recovery from photoinhibition of the Japanese *Kappaphycus* sp. (Borlongan *et al.* 2017c), *Sargassum patens* C. Agardh (Terada *et al.* 2018), *Cladosiphon okamuranus* Tokida, and *Cladosiphon umezakii* Ajisaka (Fukumoto *et al*. 2018a, b) was likewise constrained by low temperature, suggesting the influence of both low winter temperatures and PAR in establishing the northern distributional limits of these species in the western Pacific.

As for the temperature response in *C. costata* and *A. crassifolia*, both of their life history stages were relatively less sensitive to low temperature, given their stable $F_v/F_m$ between 8 and 20°C. $F_v/F_m$ maxima occurred at 14.9–20.1°C in SPO, and at 14.0–15.8°C in GAM, respectively. Whereas maximum gross photosynthesis ($GP_{max}$) was reached at 22.1–22.6°C in SPO, and at 21.7–22.7°C in GAM (regardless of the different experimental PAR provided to the two life history stages or species). $F_v/F_m$ and $GP$ rates of the two life history stages subsequently declined above 24°C. The same photosynthetic response was reported on *S. latissima* sporophytes, unaffected by low temperature up to 22°C (Bruhn and Gerard 1996). Culture experiments on *C. costata* likewise showed broad tolerance to temperatures ranging from 5 to 25°C; with gametophytes growing best at 15°C, and juvenile sporophytes at 10°C (Fu *et al*. 2010).

The combined results of oxygen evolution and $F_v/F_m$ measurements on *C. costata* and *A. crassifolia* revealed the overlapping temperature optima for photosynthesis of their heteromorphic life history stages (i.e., 14.9–22.6°C for SPO and 14.0–22.7°C for GAM). While such temperatures correspond to the growth and maturation periods of these two kelp species in Japan (April to August; Niihara *et al.* 1987; Kawashima 2012), they are likely close to the upper limit for thermal inhibition, as photosynthesis of both stages were inhibited above 24°C. Summertime seawater temperatures in southwestern part of Hokkaido (Muroran / Hakodate, Hokkaido

Prefecture) and the Pacific coast (Yamada Bay, Iwate Prefecture) of northeastern Honshu Islands, Japan may reach a high of 20–22°C (Niihara *et al.* 1987; Japan Oceanographic Data Center 2017), which is close to their physiological limit. This perhaps explains the observed erosion of kelp blades (Niihara *et al.* 1987; Kawashima 2012), and even the disappearance of *C. costata* sporophytes during summer in this region. Similar observations have been made for sporophytes of *Alaria esculenta* (Linnaeus) Greville by Fredersdorf *et al.* (2009), wherein temperatures over 20°C were lethal to sporophytes, which correspond to the northerly distribution pattern of this Arctic kelp species with a southern limit close to the 20°C isotherm of maximum sea temperature (Widdowson 1971). Decline of kelp forests all over the world has been reported as well, and this was related to the increase in seawater temperature through global warming (Kirihara *et al.* 2006; Suzuki *et al.* 2008; Müller *et al.* 2009; Voerman *et al.* 2013). Another potential factor contributing to kelp erosion and die-back in summer is the level of nutrients, particularly nitrogen, in the water column. Nitrogen deficiency negatively affected recruitment, growth and survival of juvenile sporophytes of *U. pinnatifida*, *E. cava* and *Saccharina* spp. by reducing their tolerance to high seawater temperatures (Agatsuma *et al.* 2014; Gao *et al.* 2013; 2016). Shifts in the distribution patterns of these kelp species are assumed, in consequence to changes brought about by global climate change. The southern limit of distribution of *C. costata* and *A. crassifolia* in the northwestern Pacific will likely shift further north if seawater temperatures remain high because of continuous global warming. Further research on physiological responses to interactions between two or more environmental stress factors is recommended, especially with regard to ecological aspects and in the context of global climate change.

## CHAPTER 5: General Discussion and Conclusion

Seaweeds are often subjected to highly variable underwater light climate and temperature regimes, especially for species that occur across latitudinal temperature gradients. During evolution, their metabolism (including photosynthesis) has adapted to these strongly changing conditions in their habitat (Hanelt *et al.* 2003), which allows them to survive and remain competitive.

In this study, all carrageenophytes samples from Indonesia, as well as the native *Kappaphycus* sp. from Okinawa, Japan shared similar *P–E* responses, with $E_k$ values ranging from 130 to 157 μmol photons m$^{-2}$ s$^{-1}$. Neither photoinhibition (in terms of oxygen production) nor photodamage of *PSII* (characterized by failure of recovery in $F_v/F_m$ following high PAR stress) was observed at the highest experimental PAR of 1000 μmol photons m$^{-2}$ s$^{-1}$ for these species, suggesting their photosynthetic tolerance to high PAR. These seaweeds were planted just below the sea surface, or were found in the upper sublittoral zone in reef shores; hence, they are exposed to direct sunlight throughout the day, with PAR levels that could reach as high as 2000 μmol photons m$^{-2}$ s$^{-1}$ during noon (Collen *et al.* 1995; Terada *et al.* 2016b). On one hand, kelp species *C. costata* and *A. crassifolia* had minimal $E_c$ (4–9 μmol photons m$^{-2}$ s$^{-1}$) and $E_k$ values (53–103 μmol photons m$^{-2}$ s$^{-1}$), typical for arctic and subarctic kelps in the subtidal zone (Germann 1989; Kühl *et al.* 2001; Borum *et al.* 2002; Spalding *et al.* 2003; Gattuso *et al.* 2006; Gómez *et al.* 2011; Terada *et al.* 2016a). They also seemed to be more sensitive to chronic photoinhibition, as compared to the intertidal carrageenophytes in this study, as shown by their more pronounced declines in $\Phi_{PSII}$ and incomplete recovery in $F_v/F_m$ following PAR stress. Several studies have shown that intertidal species are more resistant to PAR stress than subtidal species (Hanelt *et al.* 1997; Karsten *et al.* 2001; Figueroa *et al.* 2003; Marquardt *et al.* 2010). Larger depressions in variable fluorescence and slower or less pronounced recovery were observed in the green alga

*Halimeda tuna* (Ellis & Solander) Lamouroux from 5-m depth than from 0-m depth (Häder *et al.* 1996), as well as in the red alga *Chondrus crispus* Stackhouse (Sagert *et al.* 1997) from the lower shore. The deep-water ecotype of *S. pacifica* was also more sensitive to high PAR as revealed by its relatively lower net photosynthetic rates and greater declines in $\Phi_{PSII}$ after continuous PAR exposure, in contrast to the shallow-water ecotype occurring at depths of 5 m. (Borlongan *et al.* 2017d). Additionally, the deep-water ecotype had higher $\alpha$ (light use efficiency), suggesting that their photosynthetic apparatus has adapted to maximizing light capture rather than photoprotection. A depression of $\Phi_{PSII}$ at noon, and recovery by sunset was observed with Vietnamese-cultivated *K. alvarezii* (Terada *et al.* 2016b) and other intertidal seaweeds (Figueroa *et al*. 1997; Cabello-Pasini *et al.* 2000; Kokubu *et al.* 2015; Terada *et al.* 2016a), revealing their efficient protective response mechanism for down-regulating photosynthesis to avoid chronic photodamage at high PAR levels. They are able to decrease the energy pressure on photosynthesis by harmless thermal energy dissipation and/or by decrease of the absorption cross section through chloroplast displacement or shrinking (Hanelt and Nultsch 1991; Schubert *et al.* 2006). The up-regulation of antioxidants and antioxidant enzymes are also strategies to protect *PSII* repair against reactive oxygen species during high PAR and temperature stress (Gao *et al.* 2018; Yuan *et al.* 2018). In contrast, the inability of *Ecklonia radicosa* (Kjellman) Okamura sporophytes to fully recover overnight from high PAR exposure provided a physiological evidence of the influence of PAR in restricting the upper limits of vertical distribution of this species in the intertidal zone (Terada *et al.* 2016a). Besides photosynthetic and chlorophyll fluorescence parameters, pigment composition also showed depth-dependent differences. *Chondrus crispus* from the lower shore had higher phycoerythrin content, parallel to the increased light use efficiency of photosynthesis (Sagert *et al.* 1997). The sublittoral kelp *S. latissima* were also shown to hold large amounts of *chl-c*, in response to the low PAR environment during winter, while an accumulation of pigments involved in the xanthophyll cycle was observed on these seaweeds to minimize photoinhibition during the strong irradiance periods of spring (Gévaert *et al.* 2002). The subtidal *Ulva rotundata* Bliding had higher contents of *chl-a*, *chl-b,* and carotenoids than the sun-adapted *Ulva olivascens* (= *Umbraulva dangeardii* Wynne et Furnari), which resulted in higher $\alpha$ and lower $E_k$ (Figueroa *et al.* 2003). We did not assess the pigment concentrations of the seaweeds in this study; nonetheless a concrete manifestation that seaweeds are under high PAR stress is thallus bleaching (Dawes 1981; Kobayashi and Fujita 2014; Endo *et al.* 2017). Therefore, the depth distribution of kelps and carrageenophytes in coastal waters, and their appropriate depth range for cultivation depend not only on the lower PAR limit which allows biomass production to the minimal energy input, but also on their respective tolerance to the high PAR conditions near the water surface.

A similar morpho-functional variation has been demonstrated between gametophytes and sporophytes of *C. costata* and *A. crassifolia*. The adult sporophytes of these kelp species are characterized by higher *NP* rates, $E_c$ and $E_k$ than the microscopic gametophytes. Growth of gametophytes is favored at low PAR owing to their filamentous organization, high assimilatory pigment content per biomass, high area/ volume ratio and a low proportion of non-photosynthetic tissue (Hanelt *et al.* 2003; Roleda *et al.* 2009). Similarly, sensitivity of photosynthesis to high PAR is dependent on the life history stage as shown for *C. costata* and *A. crassifolia* in this study, as well as for *S. latissima* (Hanelt *et al.* 1997), *C. okamuranus* (Fukumoto *et al.* 2018a), and *C. umezakii* (Fukumoto *et al.* 2018b). These morpho-functional differences are regarded as a fundamental feature of the life strategy of these species.

The temperature gradient caused by latitudinal variation and water current is a driving factor in biogeographical distributions of macroalgae. In this study, a considerable adaptation to temperature was observed especially on the carrageenophytes from Indonesia. Their temperature optima for photosynthesis (28–32°C) were in the same range as that for growth of species in the tropics (Ohno *et al.* 1996; Hung *et al.* 2009; Hurtado *et al.* 2012; Lideman *et al.* 2013, Terada *et al.* 2016b), which reflect their exposure to such relatively high temperatures over long geological periods. They also seemed to have limited scope for acclimation relative to the temperate species, presumably due to reduced environmental variability in tropical habitats (Padilla-Gamino and Carpenter 2007; Borlongan *et al.* 2017a, b, c). In comparison, the subarctic kelps *C. costata* and *A. crassifolia* from Hokkaido, Japan showed broad tolerance to temperature ranging from 14 to 23°C. This can be attributed to the larger variations in seawater temperature in this coastal region, as strongly influenced by seasonal changes, as well as by the cold *Oyashio* current flowing down from the east coast of Hokkaido, and by the warm *Tsugaru* current (a branch of the *Tsushima* current) that flows through the Tsugaru Strait and passes along the eastern coast of Honshu. They are likewise strongly adapted to the ambient temperature regimes in their habitat, as their temperature optima for photosynthesis are in parallel with the seawater temperatures during the peak of growth and reproductive maturation of these species in Japan (Niihara *et al.* 1987; Kawashima 2012). Although seaweeds are generally well adapted to their thermal environment, they nevertheless experience temperatures in nature that are sufficiently high or low to result in disruptive stress in the form of cellular and subcellular damage (Davison 1991; Eggert *et al.* 2012). For instance, the decline in $F_v/F_m$ and *NP* rates, as well as the poor photoinhibition-recovery response to high PAR of *C. costata* and *A. crassifolia* at temperatures above 24°C signify deactivation of photosynthesis. Such a response can be attributed to thermal damage of enzymes of the Calvin cycle, ATP-generating synthase and *PSII*, structural rearrangements in the thylakoid membranes, and/or to accumulation of hydrogen peroxide that inhibit de novo synthesis of $D_1$

protein in *PSII* (Nishiyama *et al.* 2006; Allakhverdiev et al. 2008; Takahashi & Murata 2008; Roleda 2009). Such damage may consequently lead to slow growth, delayed development, or mortality. Much remains to be learned regarding temperature dependence of the key physiological processes that control growth, reproduction and survival across the full range of temperatures experienced by an individual in its lifetime.

Increase in seawater temperature through global warming will lead to changes in the geographic distribution of seaweeds. For instance, the southern distributional limit of *C. costata* and *A. crassifolia* in the northwestern Pacific will likely shift further north, as abscission of senescent blades of *Saccharina* species occurred at high seawater temperature and low nutrient levels (Gao *et al.* 2015, 2017). Drastic population declines and even local extinctions have been documented at the warm (lower latitude) end of species' biogeographic ranges during periods of warming (e.g., Serisawa *et al.* 2004; Kawashima 2012). Range retraction at low latitudes of these subarctic kelp species may be offset by expansion into higher latitudes of warm-temperate species (*e.g.*, *U. pinnatifida*, *E. radicosa*, *S. patens*).

A deeper understanding of the extent to which seaweeds (whether in population- or species-level) will acclimatize or adapt to environmental change is crucial for predicting future change in seaweed-dominated systems. We also highlight the importance of a better integration of the physiological techniques (PAM fluorometry and photorespirometry) in an ecological context, and the need for additional ecophysiological studies relating to impacts of multiple environmental stressors to provide a more complete account of the responses of macroalgal communities to global stressors.

# REFERENCES


Abbott IA, Hollenberg GJ (1976) Marine algae of California. Stanford University Press, California. 827 pp.

Adnan H, Porse H (1987) Culture of *Eucheuma cottonii and Eucheuma spinosum* in Indonesia. Proc Int Seaweed Symp 12: 355–358.

Agatsuma Y, Endo H, Yoshida S, Ikemori C, Takeuchi Y, Fujishima H, Nakajima K, Sano M, Kanezaki N, Imai H, Yamamoto N, Kanahama H, Matsubara T, Takahashi S, Isogai T, Taniguchi K (2014) Enhancement of *Saccharina* kelp production by nutrient supply in the Sea of Japan off southwestern Hokkaido, Japan. J Appl Phycol 26: 1845–1852.

Aguirre von Wobeser E, Figueroa F, Cabello-Pasini A (2001) Photosynthesis and growth of the red and green morphotypes of *Kappaphycus alvarezii* (Rhodophyta) from the Philippines. Mar Biol 138: 679–686.

Alexandrov GA, Yamagata Y (2007) A peaked function for modeling temperature dependence of plant productivity. Ecol Model 200: 189–192.

Allakhverdiev S, Murata N (2004) Environmental stress inhibits the synthesis de novo of proteins involved in the photodamage-repair cycle of Photosystem II in *Synechocystis* sp. PCC 6803. Biochim Biophys Acta 1657: 23–32.

Allakhverdiev S, Kreslavski V, Klimov V, Los D, Carpentier R, Mohanty P (2008) Heat stress: an overview of molecular responses in photosynthesis. Photosynth Res 98: 541–550.

Amin M, Rumayar TP, Femmi NF, Keemur D, Suwitra IK (2008) The assessment of seaweed (*Eucheuma cottonii*) growing practice of different systems and planting seasons in Bangkep Regency Central Sulawesi. Indonesian J Agricul Sci 1:132–139.

Beer S, Björk M, Beardall J (2014) Photosynthesis in the Marine Environment. Wiley and Sons, Iowa.

Bischoff-Bäsmann B, Bartsch I, Xia B, Wiencke C (1997) Temperature responses of macroalgae from the tropical island Hainan (P.R. China). Phycol Res 45: 91–104.

Bixler HJ, Porse H (2011) A decade of change in the seaweed hydrocolloids industry. J Appl Phycol 23: 321–335.

Boo SM, Ko YD (2012) Marine plants from Korea. Junghaeng-Sa, Seoul.  233 pp. (in Korean).

Borlongan IA, Tibubos KR, Yunque DAT, Hurtado AQ, Critchley AT (2011) Impact of AMPEP on the growth and occurrence of epiphytic *Neosiphonia* infestation on two varieties of commercially cultivated *Kappaphycus alvarezii* grown at different depths in the Philippines. J Appl Phycol 23: 615–621.

Borlongan IA, Luhan MRJ, Padilla PIP, Hurtado AQ (2016) Photosynthetic responses of '*Neosiphonia* sp. epiphyte-infected' and healthy *Kappaphycus alvarezii* (Rhodophyta) to irradiance, salinity and pH variations. J Appl Phycol 28: 2891–2902.

Borlongan IA, Gerung GS, Kawaguchi S, Nishihara GN, Terada R (2017a) Thermal and PAR effects on the photosynthesis of *Eucheuma denticulatum* and *Kappaphycus striatus* (so-called *Sacol* strain) cultivated in shallow bottom of Bali, Indonesia. J Appl Phycol 29: 395–404.

Borlongan IAG, Gerung GS, Nishihara GN, Terada R (2017b) Light and temperature effects on photosynthetic activity of *Eucheuma denticulatum* and *Kappaphycus alvarezii* (brown and green color morphotypes) from Sulawesi Utara, Indonesia. Phycol Res 65: 69–79.

Borlongan IA, Nishihara GN, Shimada S, Terada R (2017c) Effects of temperature and PAR on the photosynthesis of *Kappaphycus* sp. (Solieriaceae, Rhodophyta) from Okinawa, Japan, at the northern limit of native *Kappaphycus* distribution in the western Pacific. Phycologia 56: 444–453.

Borlongan IA, Nishihara GN, Shimada S, Terada R (2017d) Photosynthetic performance of the red alga *Solieria pacifica* (Solieriaceae) from two different depths in the sublittoral waters of Kagoshima, Japan. J Appl Phycol 29: 3077–3088.

Borum J, Pedersen MF, Krause-Jensen D, Christensen PB, Nielsen K (2002) Biomass, photosynthesis and growth of *Laminaria saccharina* in a high-arctic fjord, NE Greenland. *Mar Biol* 141: 11–19.

Bruhn J, Gerard VA (1996) Photoinhibition and recovery of the kelp *Laminaria saccharina* at optimal and superoptimal temperatures. Mar Biol 125: 639–648.

Bulboa CR, Paula EJ (2005) Introduction of non-native species of *Kappaphycus* (Rhodophyta, Gigartinales) in subtropical waters: comparative analysis of growth rates of *Kappaphycus alvarezii* and *Kappaphycus striatum in vitro* and in the sea in south-eastern Brazil. Phycol Res 53: 183–188.

Bulboa C, Paula EJ, Chow F (2008) Germination and survival of tetraspores of *Kappaphycus alvarezii* var. *alvarezii* (Solieriaceae, Rhodophyta) introduced in subtropical waters of Brazil. Phycol Res 56: 39–45.

Cabello-Pasini A, Aguirre von Wobeser E, Figueroa FL (2000) Effect of solar radiation on photoinhibition of marine macrophytes in culture systems. J Photochem Photobiol 57: 167–178.

Cho GY (2010) Laminariales. In: Anonymous (Ed.) Algal flora of Korea, vol 2, National Institute of Biological Resources, Incheon, pp. 175–196.

Climate Data for Cities Worldwide. 2016. Climate Data for Cities Worldwide. http://en.climate-data.org/.

Collen J, Mtolera M, Abrahamsson K, Semesi A, Pedersen M (1995) Farming and Physiology of the Red Algae *Eucheuma*: Growing Commercial Importance in East Africa. Ambio 24 (7): 497–501.

Colombo-Pallota MF, Rodríguez-Román A, Iglesias-Prieto R (2010) Calcification in bleached and unbleached *Montastraea faveolata*: evaluating the role of oxygen and glycerol. Coral Reefs 29: 899–907.

Colvard NB, Carrington E, Helmuth B (2014) Temperature-dependent photosynthesis in the intertidal alga *Fucus gardneri* and sensitivity to ongoing climate change. J Exp Mar Biol Ecol 458: 6–12.

Cosgrove J, Borowitzka MA (2011) Chlorophyll fluorescence terminology: an introduction. In: Suggett DJ, Prášil O, Borowitzka MA (Eds.) Chlorophyll a fluorescence in aquatic sciences, methods and developments. Developments in Applied Phycology, vol 4. Springer SBM, Dordrecht, pp. 1–17.

Davison IR (1991) Environmental effects on algal photosynthesis: Temperature. J Phycol 27: 2–8.

Dawes CJ (1981) Marine Botany. Wiley and Sons, New York.

Dawes CJ (1992) Irradiance Acclimation of the Cultured Philippine Seaweeds, *Kappaphycus alvarezii* and *Eucheuma denticulatum.* Bot Mar 35: 189–195.

De Góes H, Reis R (2012) Temporal variation of the growth, carrageenan yield and quality of *Kappaphycus alvarezii* (Rhodophyta, Gigartinales) cultivated at Sepetiba bay, southeastern Brazilian coast. J Appl Phycol 24: 173–180.

Delebecq G, Davoult D, Menu D, Janquin MA, Mignié A, Dauvin JC, Gévaert F (2011) In situ photosynthetic performance of *Laminaria digitata* (Phaeophyceae) during spring tides in Northern Brittany. Cah Biol Mar 52: 405–414.

Doty MS (1973) Farming the red seaweed, *Eucheuma*, for carrageenans. Micronesica 9: 59–73.

Druehl LD (1970) The pattern of Laminariales distribution in the northeast Pacific. Phycologia 9: 237–247.

Eggert A (2012) Seaweed responses to temperature. In: Wiencke C, Bischof K (Eds.) Seaweed biology. Springer, Berlin, pp 47–66.

Endo H, Okumura Y, Sato Y, Agatsuma Y (2017) Interactive effects of nutrient availability, temperature, and irradiance on photosynthetic pigments and color of the brown alga *Undaria pinnatifida*. J Appl Phycol 29:1683–1693.

Enriquez S, Borowitzka MA (2011) The use of the fluorescence signal in studies of seagrass and macroalgae. In: Suggett DJ, Prášil O, Borowitzka MA (Eds.) Chlorophyll a fluorescence in aquatic sciences: methods and developments. Developments in Applied Phycology 4. Springer, Dordrecht, pp. 187–208.

Fairhead VA, Cheshire AC (2004) Seasonal and depth related variation in the photosynthesis-irradiance response of *Ecklonia radiata* (Phaeophyta, Laminariales) at West Island, South Australia. Mar Biol 145: 415–426.

Falkowski PG, Raven JA (2007) Aquatic photosynthesis, 2nd ed. Princeton University Press, New Jersey.

Figueroa FL, Salles S, Aguilera J, Jiménez C, Mercado J, Viñegla B, Flores-Moya A, Altmirano M (1997) Effects of solar radiation on photoinhibition and pigmentation in the red alga *Porphyra leucosticte*. Mar Ecol Prog Ser 151:81–90.

Figueroa F, Conde-Alvarez R, Gomez I (2003) Relations between electron transport rates determined by pulse amplitude modulated chlorophyll fluorescence and oxygen evolution in macroalgae under different light conditions. Photosynth Res 75:259–275.

Fisheries Research Department, Hokkaido Research Organization. 2018. URL: http://www.fishexp.hro.or.jp/shidousyo/top/topic/suihoku/h19-06/h19-06.htm (in Japanese).

Fredersdorf J, Müller R, Becker S, Wiencke C, Bischof K (2009) Interactive effects of radiation, temperature and salinity on different life history stages of the Arctic kelp *Alaria esculenta* (Phaeophyceae). Oecologia 160: 483–492.

Fu G, Liu J, Wang G, Yao J, Wang X, Duan D (2010) Early development of *Costaria costata* (C. Agardh) Saunders and cultivation trials. Chi J Oceanol Limnol 28: 731–737.

Fujimoto M, Nishihara GN, Prathep A, Terada R (2015) The effect of irradiance and temperature on the photosynthesis of an agarophyte, *Gelidiella acerosa* (Gelidiales, Rhodophyta), from Krabi, Thailand. J Appl Phycol 27: 1235–1242.

Fukumoto R, Borlongan IA, Nishihara GN, Endo H, Terada R (2018a) The photosynthetic responses to PAR and temperature including chilling-light stress on the heteromorphic life history stages of a brown alga, *Cladosiphon okamuranus* (Chordariaceae) from Ryukyu Islands, Japan. Phycol Res 66: 209–217.

Fukumoto R, Borlongan IA, Nishihara GN, Endo H, Terada R (2018b) Effect of photosynthetically active radiation and temperature on the photosynthesis of two heteromorphic life history stages of a temperate edible brown alga, *Cladosiphon umezakii* (Chordariaceae, Ectocarpales), from Japan. J Appl Phycol doi: 10.1007/s10811-018-1655-3.

Gantt E (1990) Pigmentation and photoacclimation. In: Cole KM, Sheath KG (Eds.) Biology of the red algae. Cambridge University Press, Cambridge, pp 203–221.

Ganzon-Fortes ET, Azanza-Corrales R, Aliaza TT (1993) Comparison of photosynthetic responses of healthy and diseased *Kappaphycus alvarezii* (Doty) Doty using P vs. I curve. Bot Mar 36: 503–506.

Gao X, Endo H, Taniguchi K, Agatsuma Y (2013) Combined effects of seawater temperature and nutrient condition on growth and survival of juvenile sporophytes of the kelp *Undaria pinnatifida* (Laminariales; Phaeophyta) cultivated in northern Honshu, Japan. J Appl Phycol 25: 269–275.

Gao X, Endo H, Agatsuma Y (2015) Effect of increased seawater temperature on biomass, growth, and maturation of *Saccharina japonica* near its southern limit in northern Japan. J Appl Phycol 27: 1263–1270.

Gao X, Endo H, Nagaki M, Agatsuma Y (2016) Growth and survival of juvenile sporophytes of the kelp *Ecklonia cava* in response to different nitrogen and temperature regimes. Fish Sci 82: 623–629.

Gao X, Endo H, Nagaki M, Agatsuma Y (2017) Interactive effects of nutrient availability and temperature on growth and survival of different size classes of *Saccharina japonica* (Laminariales, Phaeophyceae). Phycologia 56: 253–260.

Gao G, Shi Q, Xu Z, Xu J, Campbell DA, Wu H (2018) Global warming interacts with ocean acidification to alter *PSII* function and protection in the diatom *Thalassiosira weissflogii*. Environ Exp Bot 147: 95–103.

Gattuso JP, Gentili B, Duarte CM, Kleypas JA, Middelburg JJ, Antoine D (2006) Light availability in the coastal ocean: impact on the distribution of benthic photosynthetic organisms and their contribution to primary production. Biogeosciences 3: 489–513.

Germann I (1989) Aspects of carbon metabolism in relation to autumnal blade abscission in the kelp *Pleurophycus gardneri* (Phaeophyceae, Laminariales). Mar Ecol Prog Ser 54: 179–188.

Gerung GS, Ohno M (1997) Growth rates of *Eucheuma denticulatum* (Burman) Collins et Harvey and *Kappaphycus striatum* (Schmitz) Doty under different conditions in warm waters of Southern Japan. J Appl Phycol 9: 413–415.

Gévaert F, Creach A, Davoult D, Holl AC, Seuront L, Lemoine Y (2002) Photoinhibition and seasonal photosynthetic performance of the seaweed *Laminaria saccharina* during a simulated tidal cycle: chlorophyll fluorescence measurements and pigment analysis. Plant Cell Environ 25:859–872.

Glenn EP, Doty MS (1992) Water motion affects the growth rates of *Kappaphycus alvarezii* and related seaweeds. Aquaculture 108: 233–246.

Gómez I, Wulff A, Roleda M, Huovinen P, Karsten U, Quartino ML, Dunton K, Wiencke C (2011) Light and temperature demands of marine benthic microalgae and seaweeds in polar regions. In: Wiencke C. (Ed.) Biology of Polar Benthic Algae. Walter de Gruyter GmbH, Berlin, pp. 195–220.

Graiff A, Liesner D, Karsten U, Bartsch I (2015) Temperature tolerance of western Baltic Sea *Fucus vesiculosus* - growth, photosynthesis and survival. J Exp Mar Biol Ecol 471: 8–16.

Granbom M, Pedersen M, Kadel P, Lüning K (2001) Circadian rhythm of photosynthetic oxygen evolution in *Kappaphycus alvarezii* (Rhodophyta): dependence on light quantity and quality. J Phycol 37: 1020–1025.

Häder DP, Lebert M, Mercado J, Aguilera J, Salles S, Flores-Moya S, Jiméz C, Figueroa FL (1996) Photosynthetic oxygen production and PAM fluorescence in the brown alga *Padina pavonica* measured in the field under solar radiation. Mar Biol 127: 61–66.

Hanelt D (1996) Photoinhibition ofphotosynthesis in marine macroalgae. Sci Mar 60:243–248.

Hanelt D, Nultsch W (1991) The role of chromatophore arrangement in protecting the chromatophores of the brown alga *Dictyota dichotoma* against photodamage. J Plant Physiol 138: 470–475.

Hanelt D, Huppertz K, Nultsch W (1992) Photoinhibition of photosynthesis and its recovery in red algae. Bot Acta 105: 278–284.

Hanelt D (1996) Photoinhibition of photosynthesis in marine macroalgae. Sci Mar 60: 243–248.

Hanelt D, Wiencke C, Karsten U, Nultsch W (1997) Photoinhibition and recovery after high light stress in different developmental and life-history stages of *Laminaria saccharina* (Phaeophyta). J Phycol 33: 387–395.

Hanelt D, Wiencke C, Bischof K. (2003) Photosynthesis in marine macroalgae. In: Larkum, AW, Douglas SE, Raven JA (Eds.) Photosynthesis in algae. Kluwer Academic Publishers, Dordrecht, The Netherlands, pp. 413–435.

Harley CDG, Anderson KM, Demes KW, Jorve JP, Kordas RL, Coyle TA, Graham MH (2012) Effects of climate change on global sea- weed communities. J Phycol 48:1064–1078.

Hayashi L, Paula EJD, Chow F (2007) Growth rate and carrageenan analyses in four strains of *Kappaphycus alvarezii* (Rhodophyta, Gigartinales) farmed in the subtropical waters of São Paulo State, Brazil. J Appl Phycol 19: 393–399.

Hayashi L, Hurtado AQ, Msuya FE, Bleicher-Lhonneur G, Critchley AT (2010) A review of *Kappaphycus* farming: prospects and constraints. In: Seckbach J, Einav R, Israel A (Eds.) Seaweeds and their role in globally changing environments. Springer, Dordrecht, pp. 251–283.

Hayashi L, Faria GSM, Nunes BG, Zitta CS, Scariot LA, Rover T, Felix MRL, Bouzon Z (2011) Effects of salinity on the growth rate, carrageenan yield, and cellular structure of *Kappaphycus alvarezii* (Rhodophyta, Gigartinales) cultured in vitro. J Appl Phycol 23(3): 439–447.

Hayashi L, Bulboa C, Kradolfer P, Soriano G, Robledo D (2013) Cultivation of red seaweeds: a Latin American perspective. J Appl Phycol 26: 719–727.

Heinrich S, Valentin K, Frickenhaus S, Wiencke C (2015) Temperature and light interactively modulate gene expression in *Saccharina latissima* (Phaeophyceae). J Phycol 51: 93–108.

Henley WJ (1993) Measurement and interpretation of photosynthetic light-response curves in algae in the context of photo inhibition and diel changes. J Phycol 29: 729−39.

Holzinger A, Di Piazza L, Lütz C, Roleda MY (2011) Sporogenic and vegetative tissues of *Saccharina latissima* (Laminariales, Phaeophyceae) exhibit distinctive sensitivity to experimentally enhanced ultraviolet radiation: photosynthetically active radiation ratio. Phycol Res 59: 221–235.

Hung LD, Hori K, Nang HQ, Kha T, Hoa LT (2009) Seasonal changes in growth rate, carrageenan yield and lectin content in the red alga *Kappaphycus alvarezii* cultivated in Camranh Bay, Vietnam. J Appl Phycol 21: 265–272.

Hurtado AQ, Critchley AT, Bleicher-Lhonneur G (2006). Occurrence of *Polysiphonia* epiphytes in *Kappaphycus* farms at Calaguas Is., Camarines Norte, Philippines. J Appl Phycol 18: 301–306.

Hurtado, AQ, Joe M, Sanares RC, Fan D, Prithiviraj B, Critchley AT (2012) Investigation of the application of Acadian Marine Plant Extract Powder (AMPEP) to enhance the growth, phenolic content, free radical scavenging, and iron chelating activities of *Kappaphycus* Doty (Solieriaceae, Gigartinales, Rhodophyta). J. Appl. Phycol. 24: 601–611.

Hurtado AQ, Gerung GS, Yasir S, Critchley AT (2014a) Cultivation of tropical red seaweeds in the BIMP-EAGA region. J Appl Phycol 26: 707–718.

Hurtado AQ, Reis RP, Loureiro RR, Critchley AT (2014b) *Kappaphycus* (Rhodophyta) Cultivation: Problems and the Impacts of Acadian Marine Plant Extract Powder. In: Pereira and Neto (Eds.) Marine Algae: Biodiversity, Taxonomy, Environmental Assessment, and Biotechnology. CRC Press, pp. 251−299.

Hurtado AQ, Neish IC, Critchley AT (2015) Developments in production technology of *Kappaphycus* in the Philippines: more than four decades of farming. J Appl Phycol 27: 1945–1961.

Japan Meteorological Agency 2016. URL: http://www.data.jma.go.jp/obd/stats/etrn/index.php (in Japanese).

Japan Oceanographic Data Center 2017. JODC Data On-line Service System. URL: http://www.jodc.go.jp/jodcweb/JDOSS/index_j.html (in Japanese).

Jassby AD, Platt T (1976) Mathematical formulation of the relationship between photosynthesis and light for phytoplankton. Limnol Oceanogr 21: 540–547.

Jørgensen SE, Svirezhev YM (2004) Towards a Thermodynamic Theory for Ecological Systems. Elsevier, Amsterdam, 366 pp.

Karsten U, Bischof K, Wiencke C (2001) Photosynthetic performance of arctic macroalgae after transplantation from deep to shallow waters. Oecologia 127:11–20.

Kawashima S (1989) An illustrated book of Japanese Laminariales. Kitanihon-Kaiyo Center, Sapporo (in Japanese).

Kawashima S (2012) Morphology and taxonomy of the Laminariaceous algae in cold water area of Japan. Seibutsu-Kenkyusha, Tokyo. 545 pp (in Japanese).

Kerrison PD, Stanley MS, Edwards, MD, Black KD, Hughes AD (2015) The cultivation of European kelp for bioenergy: Site and species selection. Biomass Bioenergy 80: 229–242.

Khambhaty Y, Mody K, Gandhi MR, Thampy S, Maiti P, Brahmbhatt H, Eswaran K, Ghosh PK (2012) *Kappaphycus alvarezii* as a source of bioethanol. Bioresour Technol 100(1): 180–185.

Kirihara S, Nakamura T, Kon N, Fujita D, Notoya M (2006) Recent fluctuations in distribution and biomass of cold and warm temperature species of Laminarialean algae at Cape Ohma, northern Honshu, Japan. J Appl Phycol 18: 521–527.

Kirihara S (2007) Cultivation technique of *Costaria costata*. Newsl Aomori Pref Fish Res Cen Aquacult Inst 108: 5–6 (in Japanese).

Kobayashi M, Fujita D (2014) Can thallus color of red algae be used as an environmental indicator in shallow waters? J Appl Phycol 26:1123– 1131.

Kokubu S, Nishihara GN, Watanabe Y, Tsuchiya Y, Amano Y, Terada R (2015) The effect of irradiance and temperature on the photosynthesis of a native brown alga, *Sargassum fusiforme* (Fucales) from Kagoshima, Japan. Phycologia 54: 235–247.

Krishnan M, Narayanakumar R (2013) Social and economic dimensions of carrageenan seaweed farming in India. In Valderrama D, Cai J, Hishamunda N, Ridler N (Eds.) Social and economic dimensions of carrageenan seaweed farming, Fish Aqua Tech Paper 580. FAO, Rome, p 163–185.

Kronen M (2013) Social and economic dimensions of carrageenan seaweed farming in Solomon Islands. In Valderrama D, Cai J, Hishamunda N, Ridler N (Eds.) Social and economic dimensions of carrageenan seaweed farming, Fish Aqua Tech Paper 580. FAO, Rome, p 163–185.

Kühl M, Glud RN, Borum J, Roberts R, Rysgaard S (2001) Photosynthetic performance of surface-associated algae below sea ice as measured with a pulse-amplitude-modulated (PAM) fluorometer and $O_2$ microsensors. *Mar Ecol Prog Ser* 223: 1–14.

Kumura T, Yasui H, Mizuta H (2006) Nutrient requirement for zoospore formation in two alariaceous plants *Undaria pinnatifida* (Harvey) Suringar and *Alaria crassifolia* Kjellman (Phaeophyceae: Laminariales). Fish Sci 72: 860–869.

Largo DB, Fukami K, Nishijima T (1995) Occasional bacteria promoting ice-ice disease in the carrageenan-producing red algae *Kappaphycus alvarezii* and *Eucheuma denticulatum* (Solieriaceae, Gigartinales, Rhodophyta). J Appl Phycol 7: 545–554.

Li H, Liu J, Zhang L, Pang T (2016) Antioxidant responses and photosynthetic behaviors of *Kappaphycus alvarezii* and *Kappaphycus striatum* (Rhodophyta, Solieriaceae) during low temperature stress. Bot Stud 57: 21 doi: 10.1186/s40529-016-0136-8.

Lideman, Nishihara GN, Noro T, Terada R (2013) Effect of temperature and light on the photosynthesis as measured by chlorophyll fluorescence of cultured *Eucheuma denticulatum* and *Kappaphycus* sp. (Sumba strain) from Indonesia. J Appl Phycol 25:399–406.

Lindeberg MR, Lindstrom SC (2010) Field guide to seaweeds of Alaska. University of Alaska Fairbanks, Alaska Sea Grant College Program. 188 pp.

Lobban CS, Harrison PJ (1994) Seaweed Ecology and Physiology. Cambridge University Press. Cambridge. 366p.

Luxton DM (1993) Aspects of the farming and processing of *Kappaphycus* and *Eucheuma* in Indonesia. Hydrobiologia 260/261: 365–371.

Mandal SK, Ajay G, Monisha N, Malarvizhi J, Temkar G, Mantri VA (2015) Differential response of varying temperature and salinity regimes on nutrient uptake of drifting fragments of *Kappaphycus alvarezii*: implication on survival and growth. J Appl Phycol 27: 1571–81.

Marquardt R, Schubert H, Varela DA, Huovinen P, Henríquez L, Buschmann AH (2010) Light acclimation strategies of three commercially important red algal species. Aquaculture 299:140–148.

McHugh DJ (2003) A guide to the seaweed industry, FAO Fisheries technical paper – T441. FAO, Rome.

Meinita MD, Hong YK, Jeong GT (2012) Detoxification of acidic catalyzed hydrolysate of *Kappaphycus alvarezii* (cottonii). Bioprocess Biosyst Eng 35: 93–98.

Msuya FE, Porter M (2014) Impact of environmental changes on farmed seaweed and farmers: the case of Songo Island, Tanzania. J Appl Phycol 26: 2135–2141.

Müller R, Laepple T, Bartsch I, Wiencke C (2009) Impact of oceanic warming on the distribution of seaweeds in polar and cold-temperate waters. Bot Mar 52: 617–638.

Murata N, Takahashi S, Nishiyama Y, Allakherdiev SI (2007) Photoinhibition of photosystem II under environmental stress. Biochim Biophys Acta 1767: 414–421.

Nakahara H (1993) *Alaria crassifolia*. In: Hori T (Ed.). An illustrated atlas of the life history of algae, vol 2, brown and red algae. Uchida Rokakuho Publishing, Tokyo, pp. 134–135 (in Japanese).

Navarro NP, Huovinen P, Gómez I (2016) Stress tolerance of Antarctic macroalgae in the early life stages. Eur J Phycol 51: 71–82.

Neish IC (2013) Social and economic dimensions of carrageenan seaweed farming in Indonesia. In: Valderrama D, Cai J, Hishamunda N, Ridler N (Eds.) Social and economic dimensions of carrageenan seaweed farming. Fish Aqua Tech Paper 580. FAO, Rome, p 61–89.

Niihara Y, Kudo A, Oono K, Tanaka S (1987) An ecology of *Alaria crassifolia* Kjellman at Esan, southern Hokkaido. Sci Rep Hokkaido Fish Res Inst 29: 37–49. (in Japanese with English summary).

Nishiyama Y, Allakhverdiev SI, Murata N (2006) A new paradigm for the action of reactive oxygen species in the photoinhibition of photosystem II. Biochim Biophys Acta 1757: 742–749.

Notoya M, Asuke M (1984) Distribution of Laminariales plants along the coast of Aomori Prefecture. Sci Rep Aquacult Cen Aomori Pref. 3: 15–18. (in Japanese with English summary).

Ohno M, Largo DB, Ikumoto T (1994) Growth rate, carrageenan yield and gel properties of cultured kappa-carrageenan producing red alga *Kappaphycus alvarezii* (Doty) Doty in the subtropical waters of Shikoku, Japan. J Appl Phycol 6: 1–5.

Ohno M, Nang HQ, Hirase S (1996) Cultivation and carrageenan yield and quality of *Kappaphycus alvarezii* in the waters of Vietnam. J Appl Phycol 8: 431–437.

Padilla-Gamino JL, Carpenter RC (2007) Thermal ecophysiology of *Laurencia pacifica* and *Laurencia nidifica* (Ceramiales, Rhodophyta) from tropical and warm-temperate regions. J Phycol 43: 686–92.

Pang T, Liu J, Liu Q, Zhang L, Lin W (2012) Impacts of glyphosate on photosynthetic behaviours in *Kappaphycus alvarezii* and *Neosiphonia savatieri* detected by JIP-test. J Appl Phycol 24: 467–473.

Paula EJ, Pereira RTL, Ohno M (2002) Growth rates of carrageenophyte *Kappaphycus alvarezii* (Rhodophyta, Gigartinales) introduced in subtropical waters of São Paulo State, Brazil. Phycol Res 50: 1–9.

Platt T, Gallegos CL, Harrison WG (1980) Photoinhibition of photosynthesis in natural assemblages of marine phytoplankton. J Mar Res 38: 687–701.

R Development Core Team (2017) R: a language and environment for statistical computing. R Foundation for Statistical Computing, Vienna, Austria. ISBN 3-900051-07-0. URL: http://www.R-project.org.

Reed DC, Foster MS (1984) The effects of canopy shading on algal recruitment and growth in a giant kelp forest. Ecology 65: 937–948.

Reis MO, Necchi O, Colepicolo P, Barros MP (2011) Co-stressors chilling and high light increase photooxidative stress in diuron-treated red alga *Kappaphycus alvarezii* but with lower involvement of $H_2O_2$. Pestic Biochem Physiol 99: 7–15.

Renger G, Schreiber U (1986) Practical applications of fluorometric methods to algae and higher plant research. In: Govindjee, Amesz J, Fork DD (Eds.) Light emission by plants and bacteria. Academic Press, Orlando.

Roleda MY, Campana GL, Wiencke C, Hanelt D, Quartino ML, Wulff A (2009) Sensitivity of Antarctic *Urospora penicilliformis* (Ulotrichales, Chlorophyta) to ultraviolet radiation is life-stage dependent. J Phycol 45: 600–609.

Roleda MY, Lütz-Meindl U, Wiencke C, Lütz C (2010) Physiological, biochemical, and ultrastructural responses of the green macroalga *Urospora penicilliformis* from Arctic Spitsbergen to UV radiation. Protoplasma 243: 105–116.

Sagert S, Forster RM, Feuerpfeil P, Schubert H (1997) Daily course of photosynthesis and photoinhibition in *Chondrus crispus* (Rhodophyta) from different shore levels. Eur J Phycol 32:363–371.

Sakanishi Y, Iizumi H (2001) Photosynthetic responses to light in summer sporophytes of cold water species of Laminariales from the eastern coast of Hokkaido. Jpn J Phycol 49: 1–6 (in Japanese with English Summary).

Salvucci ME, Crafts-Brandner SJ (2004) Relationship between the heat tolerance of photosynthesis and the thermal stability of rubisco activase in plants from contrasting thermal environments. Plant Physiol 134: 1460–1470.

Santelices B (1999) A conceptual framework for marine agronomy. Hydrobiologia 398/399:15–23.

Schmidt EC, Maraschin M, Bouzon ZL (2010a) Effects of UVB radiation on the carrageenophyte *Kappaphycus alvarezii* (Rhodophyta, Gigartinales): changes in ultrastructure, growth, and photosynthetic pigments. Hydrobiologia 649: 171–182.

Schmidt EC, Nunes BG, Maraschin M, Bouzon Z (2010b) Effect of ultraviolet-B radiation on growth, photosynthetic pigments, and cell biology of *Kappaphycus alvarezii* (Rhodophyta, Gigartinales) macroalgae brown strain. Photosynthetica 48: 161–172.

Schubert H, Kroon BMA, Matthijs HCP (1994) In vivo manipulation of the xanthophylls cycle and the role of zeaxanthin in the protection against photodamage in the green alga *Chlorella pyrenoidosa*. J Biol Chem 269: 7267–7272.

Schubert H, Gerbersdorf S, Titlyanov E, Titlyanova T, Granbom M, Pape C, Lüning, K (2004) Circadian rhythm of photosynthesis in *Kappaphycus alvarezii* (Rhodophyta): independence of the cell cycle and possible photosynthetic clock targets. Eur J Phycol 39: 423–430.

Schubert H, Anderson M, Snoeijs P (2006) Relationship between photosynthesis and non-photochemical quenching of chlorophyll fluorescence in two red algae with different carotenoid compositions. Mar Biol 149: 1003–1013.

Serisawa Y, Yokohama Y, Aruga Y, Tanaka J (2001) Photosynthesis and respiration in bladelet of *Ecklonia cava* Kjellman (Laminariales, Phaeophyta) in two localities with different temperature conditions. Phycol Res 49: 1–11.

Serisawa Y, Imoto Z, Ishikawa T, Ohno M (2004) Decline of the *Ecklonia cava* population associated with increased seawater temperatures in Tosa Bay, southern Japan. Fish. Sci. 70:189–91.

Spalding H, Foster M, Heine J (2003) Composition, distribution, and abundance of deep-water (>30m) macroalgae in central California. J Phycol 39: 273–284.

Stan Development Team (2017) Stan: A C++ Library for Probability and Sampling, Version 2.17.3. URL: http://mc-stan.org.

Starko S, Martone PT (2016) Evidence of an evolutionary-developmental trade-off between drag avoidance and tolerance strategies in wave-swept intertidal kelps (Laminariales, Phaeophyceae). J Phycol 52: 54–63.

Steneck RS, Graham, MH, Bourque BJ, Corbett D, Erlandson JM, Estes JA, Tegner MJ (2002) Kelp forest ecosystems: biodiversity, stability, resilience and future. Environ Conserv 29: 436–59.

Suzuki S, Furuya K, Kawai T, Takeuchi I (2008) Effect of seawater temperature on the productivity of *Laminaria japonica* in the Uwa Sea, southern Japan. J Appl Phycol 20: 833–844.

Tait LW, Hawes I, Schiel DR (2017) Integration of chlorophyll-a fluorescence and photorespirometry techniques to understand production dynamics in macroalgal communities. J. Phycol 53: 476–485.

Takahashi S, Murata N (2008) How do environmental stresses accelerate photoinhibition? Trends Plant Sci 13: 178–82.

Tatewaki M (1966) Formation of a crustose sporophyte with unilocular sporangia in *Scytosiphon lomentaria*. Phycologia 6: 62–66.

Terada R (2012) *Eucheuma* and *Kappaphycus*. In: Watanabe S. (Ed.) Handbook of Algae: Their diversity and utilization. NTS, Tokyo, pp. 621–624 (in Japanese).

Terada R, Inoue S, Nishihara GN (2013) The effect of light and temperature on the growth and photosynthesis of *Gracilariopsis chorda* (Gracilariales, Rhodophtya) from geographically separated locations of Japan. J Appl Phycol 25: 1863–1872.

Terada R, Shikada S, Watanabe Y, Nakazaki Y, Matsumoto K, Kozono J, Saino N, Nishihara GN (2016a) Effect of PAR and temperature on the photosynthesis of the Japanese alga, *Ecklonia radicosa* (Laminariales), based on field and laboratory measurements. Phycologia 55: 178–186.

Terada R, Vo TD, Nishihara GN, Shioya K, Shimada S, Kawaguchi S (2016b) The effect of irradiance and temperature on the photosynthesis and growth of a cultivated red alga *Kappaphycus alvarezii* (Solieriaceae) from Vietnam, based on in situ and in vitro measurements. J Appl Phycol 28: 457–467.

Terada R, Vo TD, Nishihara GN, Matsumoto K, Kokubu S, Watanabe Y, Kawaguchi S (2016c). The effect of photosynthetically active radiation and temperature on the photosynthesis of two Vietnamese species of *Sargassum*, *S. mcclurei* and *S. oligocystum*, based on the field and laboratory measurements. Phycol Res 64: 230–240.

Terada R, Matsumoto K, Borlongan IA, Watanabe Y, Nishihara GN, Endo H, Shimada S (2018) The combined effects of PAR and temperature including the chilling-light stress on the photosynthesis of a temperate brown alga, *Sargassum patens* (Fucales), based on field and laboratory measurements. J Appl Phycol 30: 1893–1904.

Thornley JHM, Johnson IR (2000) Plant and Crop Modelling: A mathematical approach to plant and crop physiology. Blackburn Press, Caldwell, New Jersey, 669 pp.

Titlyanov EA, Titlyanov TV (2012) Marine plants of the Asian Pacific Region countries, their use and cultivation. Dalnauka & A.V. Zhirmunsky Institute of Marine Biology, Far East Branch of the Russian Academy of Sciences, Vladivostok. 376 pp.

Tokida J (1954) The marine algae of southern Saghalien. Mem Fac Fish Hokkaido Univ 1: 1–264.

Tokuda H, Ohno M, Ogawa H (1987) The resources and cultivation of seaweeds. Midori-shobo, Tokyo (in Japanese).

Trono GC, Lluisima AO, Montaño MNE (2000) Primer on Farming and Strain Selection of Kappaphycus and Eucheuma in the Philippines. PCAMRD, UNDP and UP MSI, 33p.

Vairappan CS (2006) Seasonal occurrences of epiphytic algae on the commercially cultivated red alga *Kappaphycus alvarezii* (Solieriaceae, Gigartinales, Rhodophyta). J Appl Phycol 18: 611–617.

Vásquez JA, Zuñiga S, Tala F, Piaget N, Rodriguez DC, Vega JMA (2014) Economic evaluation of kelp forest in northern Chile: values of good and service of the ecosystem. J Appl Phycol 26: 1081–1088.

Vásquez-Elizondo RM, Enríquez S (2016) Coralline algal physiology is more adversely affected by elevated temperature than reduced pH. Sci Rep 6: 19030 doi: 10.1038/srep19030.

Vo TD, Nishihara GN, Shimada S, Watanabe Y, Fujimoto M, Kawaguchi S, Terada R (2014) Taxonomic identity and the effect of temperature and irradiance on the photosynthesis of an indoor tank-cultured red alga *Agardhiella subulata* from Japan. Fish Sci 80: 281–292.

Vo TD, Nishihara GN, Kitamura Y, Shimada S, Kawaguchi S, Terada R (2015) The effect of irradiance and temperature on the photosynthesis of *Hydropuntia edulis* and *Hydropuntia eucheumatoides* (Gracilariaceae, Rhodophyta) from Vietnam. Phycologia 54: 24–31.

Voerman SE, Llera E, Rico JM (2013) Climate driven changes in subtidal kelp forest communities in NW Spain. Mar Environ Res 90: 119–127.

Watanabe Y, Nishihara GN, Tokunaga S, Terada R (2014a) Effect of irradiance and temperature on the photosynthesis of a cultivated red alga, *Pyropia tenera* (= *Porphyra tenera*), at the southern limit of distribution in Japan. Phycol Res 62: 187–196.

Watanabe Y, Nishihara GN, Tokunaga S, Terada R (2014b) The effect of irradiance and temperature responses and the phenology of a native alga, *Undaria pinnatifida* (Laminariales), at the southern limit of its natural distribution in Japan. J Appl Phycol 26: 2405–2415.

Watanabe Y, Yamada H, Takayuki M, Yoshio K, Nishihara GN, Terada R (2016) Photosynthetic responses of *Pyropia yezoensis* f. *narawaensis* (Bangiales, Rhodophyta) to a thermal and PAR gradient vary with the life-history stage. Phycologia 55: 665–672.

Webb WL, Newton M, Starr D (1974) Carbon dioxide exchange of *Alnus rubra*: a mathematical model. Oecologia 17: 281–291.

Widdowson TB (1971) A taxonomic revision of the genus *Alaria* Greville. Syesis 4: 11–49.

World Sea Temperatures (2016) World sea temperature. URL: http://www.seatemperature.org.

Yamada Y (1936) Species of *Eucheuma* from Ryukyu and Formosa. Scientific papers of Institute of Algological Research, Hokkaido University 1: 119–134.

Yokoya NS, Kakita H, Obika H, Kitamura T (1999) Effects of environmental factors and plant growth regulators on growth of the red alga *Gracilaria vermiculophylla* from Shikoku Island, Japan. Hydrobiologia 398: 339–347.

Yoshida T (1998) Marine Algae of Japan. Uchida Rokakuho Publishing Co., Ltd., Tokyo, 1222 pp (in Japanese).

Yoshida T, Suzuki M, Yoshinaga K (2010) Checklist of marine algae of Japan (revised in 2015). Jpn J Phycol 63: 129–189 (in Japanese).

Yuan W, Gao G, Shi Q, Xu Z, Wu H (2018) Combined effects of ocean acidification and warming on physiological response of the diatom *Thalassiosira pseudonana* to light challenges. Mar Environ Res 135: 63–69.

Zemke-White L, Ohno M (1999) World seaweed utilization: An end of-century summary. J Appl Phycol 11: 369–376.

## ACKNOWLEDGMENTS

This research study would not have been possible without the help and assistance of several people to whom I would like to express my heartfelt gratitude:

To my academic adviser, **Dr. Ryuta Terada,** Vice Dean of The United Graduate School of Agricultural Sciences (UGSAS), Kagoshima University, and co-advisers, **Dr. Gregory N. Nishihara** of Nagasaki University and **Dr. Hikaru Endo** of the Faculty of Fisheries, Kagoshima University, for their untiring support and encouragement during my study in Japan. I also appreciate their generosity in sharing their expertise and knowledge in seaweed research.

To my thesis committee members, **Dr. Hiroyuki Motomura** of Kagoshima University Museum and **Dr. Tomoko Yamamoto** of the Faculty of Fisheries, Kagoshima University, for their insightful comments and suggestions to improve this thesis.

To **Dr. Grevo S. Gerung** of Sam Ratulangi University, Indonesia, **Dr. Shigeo Kawaguchi** of Kyushu University, and **Dr. Satoshi Shimada** of Ochanomizu University, **Dr. Taizo Motomura** and **Dr. Chikako Nagasato** of Muroran Marine Station, Hokkaido University, and **Dr. Chikara Kawagoe,** Kyowa Concrete Co. Ltd., Hakodate, who also contributed on field and laboratory works.

To the **Japanese Ministry of Education, Culture, Sports, Science and Technology (MEXT),** for the scholarship awarded to undertake my doctoral degree.

A special notice of thanks to my beloved **parents, family and friends**, for the support in all its forms, may it have been mentally, emotionally, and financially.

Finally, to **God Our Father,** without whose inspiration and divine providence, this thesis will never be put into completion and become a reality.